JUSTUS-LIEBIG-
UNIVERSITÄT
GIESSEN

Microenvironmental Th9 and Th17 lymphocytes induce epithelial-mesenchymal transition in lung cancer cells thereby promoting metastatic spreading

Inauguraldissertation
zur Erlangung des Grades eines Doktors der Humanbiologie
des Fachbereichs Medizin
der Justus-Liebig-Universität Gießen

vorgelegt von Ylia Maria Salazar Montano
aus Margarita Insel, Venezuela

Giessen, 2019

Aus dem Max-Planck-Institut für Herz und Lungenforschung unter der Leitung von Prof. Dr. Werner Seeger, Campus Kerckhoff der Justus-Liebig-Universität Gießen und ihres Fachbereiches Medizin

Gutachter: PD Dr. Rajkumar Savai

Gutachter: Prof. Dr. Dammann

Tag der Disputation: 9.12.2019

Table of contents

1. Introduction 1

1.1 Lung Cancer 1

1.1.1 Statistics 1

1.1.3 Pathogenesis 3

1.1.4 Risk factors 4

1.2 Lung Cancer Treatment 6

1.3 The Tumor Microenvironment 8

1.3.1 Cellular components of the tumor microenvironment 8

1.4 T cells 12

1.4.1 T cell development 12

1.4.2 T cell activation 14

1.4.3 CD8 T cells 15

1.4.4 CD4 T cells 16

1.4.5 Th1 cells 17

1.4.6 Th2 cells 18

1.4.7 T regulatory cells (Tregs) 18

1.5 Th9 cells 19

1.5.1 Development and function 19

1.5.2 Interleukin-9 20

1.5.3 Th9 cells in tumor biology 20

1.6 Th17 cells 21

1.6.1 Development and function 21

1.6.2 Interleukin-17 cytokine family 22

1.6.3 Th17 cells in tumor biology 23

1.7 Epithelial-Mesenchymal Transition in cancer progression 24

2. Aim of the Research 27

3. Materials and Methods 28

3.1 Experimental Procedures *in vitro* 28

3.1.1 Human and mouse lung cancer cell lines 28

3.1.2 Primary human cancer cells 28

3.1.3 Immunocytochemistry 28

3.1.4 Migration Assays 29

3.1.5 Proliferation Assays 30
3.1.6 RNA isolation, cDNA synthesis, real-time PCR 30
3.1.7 Human and mouse cell stimulations 33
3.1.8 Flow cytometry 33
3.1.9 Cell sorting 34
3.1.10 Leukocyte isolation from PBMCs 34
3.1.11 Murine $CD4^+$ T cell preparation 35
3.1.12 Generation of specific T helper subtypes 36
3.1.13 In vitro Co-culture model 37
3.1.14 Enzyme-linked immunosorbent assay 38
3.1.15 Cytokine array 38
3.1.16 RNA sequencing 39

3.2. Experimental Procedures *in vivo* 40
3.2.1 Opal staining 40
3.2.2 Syngeneic subcutaneous model of lung cancer 42
3.2.3 Syngeneic metastatic model of lung cancer 42
3.2.4 Tumor digestion for FACS analysis 43
3.2.5 Histology 43

3.3 Statistical Analysis 44

4. Results 45

4.1 Lymphocyte CM induces an EMT Transition in cancer cells 45
4.1.1 Stimulation with Lymphocyte CM alters protein and mRNA expression levels of epithelial and mesenchymal markers 45
4.1.2 Effect of Lymphocyte CM on migration and proliferation of human lung cancer cells 48
4.1.3 Effect of Lymphocyte CM on EMT marker expression, proliferation and migration of primary lung cancer cells 49
4.1.4 Incubation of cancer cells with PMA-activated lymphocytes prompts secretion of cytokines IL-9 and IL-17 50
4.1.4 Effect of CM on human lung cancer cells is not TGF-β dependent and involves phosphorylation of ERK1/2 52

4.2 Immunostaining of Th9 and Th17 markers allows for simultaneous detection of T cells in human lung cancer samples 53
4.2.1 Staining of Th9 and Th17 cells in human tumor samples 53
4.2.2 Th9 and Th17 are located in the stromal area of tumors and a low Th/$CD4^+$ ratio correlates with better survival 54

4.3 Th9 and Th17 CM induces EMT and migration in mouse lung cancer cells 55

4.3.1 Mouse Th9 and Th17 CM decreases expression of the mesenchymal marker ZO2 and increases migration of lung cancer cells 55
4.3.2 Th9 and Th17 Co-culture CM strongly induces EMT marker expression and increases migration of mouse lung cancer cells 57

4.4 Co-culturing of LLC1 cells with Th9 or Th17 cells alters their gene expression profile 58

4.5 Co-injection of tumor cells and/or Th9/Th17 cells promotes lung cancer growth and metastasis 62

4.5.1 Co-injection of LLC1 with Th9 cells significantly increases tumor size whereas co-injection with Th17 cells correlated with elevated incidence of metastatic nodules to the lung 62
4.5.2 Intravenous co-injection of LLC1 with both Th9 and Th17 cells significantly increased lung metastasis in mice 64

4.6 IL–9 and IL–17 induce EMT in human tumor cells while their neutralization decreases lung cancer metastasis 66

4.6.1 Stimulation of human lung cancer cells with IL-9 induces an EMT phenotype characterized by increased migration 66
4.6.2 Stimulation of human lung cancer cells with IL-17 isotypes A and F induces an EMT phenotype 68
4.6.3 Depletion of IL-9 and IL-17 results in decreased lung cancer metastasis in mice 71

5. Discussion 73

5.1 Lymphocyte CM prompted an Epithelial-Mesenchymal transition in human lung cancer cells 73

5.2 Co-culture of lymphocytes and cancer cells triggers secretion of a wide array of pro-inflammatory cytokines 74

5.3 Th9 cells and IL-9 in tumor progression and metastasis 75

5.4 Th17 cells and Il-17 in tumor progression and metastasis 77

5.5 Effect on LLC1 cells from Co-culture with Th9 and Th17 cells is characterized by the upregulation of common transcription factors associated with EMT and tumor progression 79

5.6 Conclusion 80

5.7 Outlook 81

6. Summary 82

7. Zussamenfassung **83**

8. References **85**

9. Appendix **102**

10. Statement of authenticity **105**

11. Acknowledgments **106**

List of figures

Figure 1. Distribution of cancer mortality in Germany 2
Figure 2. Characteristics of histological lung cancer subtypes 3
Figure 3. The tumour microenvironment 8
Figure 4. T cell receptor complex. 13
Figure 5. T cell activation 15
Figure 6. CD4 T helper cell differentiation and lineages 17
Figure 7. IL-17 cytokine family and their ligand-receptor structural features 22
Figure 8. Epithelial-mesenchymal transition 24
Figure 9. Scheme of cancer-immune cell Co-culture 37
Figure 10. Cytokine array template coordinates 38
Figure 11. Opal Multiplex staining protocol 41
Figure 12. Stimulation of cancer cells with Lymphocyte CM induces loss of epithelial markers and upregulation of mesenchymal markers 46
Figure 13. mRNA expression profile of EMT markers after stimulation with CM 47
Figure 14. CM enhances the migration of cancer cells 48
Figure 15. Stimulation of primary cancer cells with Lymphocyte-CM results in increased migration and proliferation 49
Figure 16. Cytokine profile of CM 50
Figure 17. Elevated levels of cytokines IL-9, IL-17A and F were observed in PMA and CD3 activated Co-Culture CM 51
Figure 18. EMT-inducing changes of the CM are not TGF-β dependent and are characterized by ERK1/2 phosphorylation 52
Figure 19. Opal seven-colour multiplex analysis of human lung tumor TMA samples 53
Figure 20. $CD4^+$ T cells are more abundant in the stromal area of tumors and their presence is associated with decreased survival 54
Figure 21. Generation of specific T helper cell subpopulations, Th9 and Th17 55
Figure 22. Th9 and Th17 CM induce a decrease in epithelial markers and potentiate migration of mouse cancer cells 56
Figure 23. Th9 and Th17 Co-Culture CM induces deregulation of EMT markers and potentiates migration of mouse cancer cells 57
Figure 24. Deregulation of tumor cell gene profile after direct Co-culture with Th9 or Th17 cells 58
Figure 25. Signaling pathways upregulated after direct Co-culture with Th9 or Th17 cells 59
Figure 26. Co-culture of LLC1 cells with Th9 induces the upregulation of genes related to immune cell activation and inflammation 60

Figure 27. Co-culture of LLC1 cells with Th17 induces the upregulation of genes related to immune cell activation, inflammation and metastatic phenotype 61
Figure 28. Co-injection of LLC1 cells with Th9 and Th17 cells leads to increased tumor growth and metastasis in vivo 62
Figure 29. Tumor stroma of mice co-injected with T cells is characterized by an EMT protein profile and upregulation of MMPs 63
Figure 30. Co-injection of Th9 and Th17 cells leads to increased metastasis *in vivo* 65
Figure 31. Stimulation with IL-9 results in an EMT-like phenotype in tumor cells 67
Figure 32. Stimulation with IL-17A results in an EMT-like phenotype in tumor cells 69
Figure 33. Stimulation with IL-17F results in an EMT- like phenotype in tumor cells 70
Figure 34. Treatment with neutralizing antibodies against IL-9 and IL-17 reduces lung tumor metastasis *in vivo* 72
Figure 35. Summary figure with proposed players in the pro-metastatic and EMT-inducing effect of Th9 and Th17 cells in lung cancer 81

List of tables

Table 1. Summary of available lung cancer treatments according to stage 6
Table 2. Antibodies used for Immunofluorescence and Immunocytochemistry 29
Table 3. DNase treatment summary 30
Table 4. Master mix for cDNA synthesis 31
Table 5. Reaction mixture for qPCR 31
Table 6. qPCR reaction conditions 32
Table 7. Primer sequence list 32
Table 8. Antibodies used for FACS sorting and analysis 34
Table 9. $CD4^+$ T cell isolation antibody cocktail 35
Table 10. T cell differentiation culture conditions 36
Table 11. Patient Information 40
Table 12. Primary antibodies used for Opal staining 41
Table 13. Human qPCR Primer accession numbers 102
Table 14. Antibodies 103
Table 15. Buffers for cell biology 104

List of abbreviations

α-SMA	α-smooth muscle actin
ALK	Anaplastic lymphoma tyrosine kinase
AML	Acute myeloid leukemia
ANOVA	One-way analysis of variance
APC	Antigen presenting cells
ATII	Alveolar type II cells
bFGF	Basic fibroblast growth factor
BMC	Bone marrow-derived cells
BrdU	Bromdesoxyuridin
BSS	Balanced salt solution
CAF	Cancer-associated fibroblasts
CDF	Colony stimulating factors
CGH	Comparative genomic hybridization
CM	Conditioned media
CNS	Central nervous system
CSF	Colony stimulating factors
CTL	Cytotoxic T lymphocyte
CTLA-8	Cytotoxic T Lymphocyte-Associated Antigen 8
DC	Dendritic cells
DMSO	Dimethylsulfoxide
DN	Double negative
DP	Double positive
EAE	Experimental autoimmune encephalomyelitis
ECM	Extracellular matrix
EGFR	Epidermal growth factor receptor
ELISA	Enzyme-linked immunosorbent assay
EMT	Epithelial mesenchymal transition
EMT-ATF	EMT-associated transcription factors
ETS	Environmental tobacco smoke
FCS	Fetal calf serum
Flt3	Fms-like tyrosine kinase 3
FOXP3	Forkhead box P3
FSP-1	Fibroblast specific protein-1
GM-CSF	Granulocyte macrophage colony-stimulating factor

GSEA	Gene Set enrichment analysis
HGF	Hepatocyte growth factor
HPRT	Hypoxanthine phosphoribosyltransferase1
HSC	Hematopoietic stem cells
IFN	Interferons
IFN-γ	Interferon-gamma
IGF	Insulin-like growth factors
KRAS	Kirsten rat sarcoma viral oncogene
LCC	Large-cell carcinoma
MAPK	Mitogen-activated protein kinase
MCP	Monocyte chemoattractant proteins
MHC	Major histocompatibility complex
NF-κB	Nuclear factor κB
NFAT	Nuclear factor of activated T cells
NK	Natural Killer cells
NSCLC	Non-small cell lung cancer
PBMC	Peripheral blood mononuclear cell
PD-L1	Programmed death-ligand 1
PDGFR	Platelet-derived growth factor receptor
PKC	Protein Kinase C
PMA	Phorbol 12-Myristate 13-Acetate
SCC	Squamous cell carcinoma
SCLC	Small cell lung cancer
SPF	Specific-pathogen-free
STAT	Signal transducer and activator of transcription
TAM	Tumor associated macrophages
TAP	Transporter associated with antigen processing
TCR	T cell receptor
Tfh	Follicular helper T cells
TGF-β	Transforming growth factor beta
Th	T helper cells
TIDC	Tumor infiltrating DC
TIL	Tumor infiltrating Lymphocytes
TKI	Tyrosine kinase inhibitor
TMA	Tissue microarrays
TME	Tumor microenvironment
TNF-α	Tumor necrosis factor alpha

Tregs	T regulatory cells
iTregs	Inducible Tregs
nTregs	Naturally arising Tregs
VEGF	Vascular endothelial growth factor
ZO2	Zonula occludens-2

1. Introduction

1.1 Lung Cancer

Lung cancer begins with the uncontrolled growth of cells in the lung and can manifest through persistent cough, breathlessness, chest and/or shoulder pain, and in some cases, blood in the sputum. Cancer that starts in the lung is considered primary lung cancer and can spread to the lymph nodes, brain, and liver. Tumors that have a start in other parts of the body and spread to the lung are regarded as secondary or metastatic cancer of the lung (Shapley et al. 2010; Hamilton and Sharp 2004).

1.1.1 Statistics

Lung cancer is the leading cause of cancer deaths in men and the second in women worldwide and is one of the few cancers with a strong environmental exposure definitively linked to risk. Lung cancer incidence is much higher than other cancer types and accounts for up to 19% of all cancer deaths (Torre, Siegel, and Jemal 2016). There are more deaths as a result of lung cancer than from colon, breast, and prostate cancer combined (Hensing et al. 2014).

Despite a large number of investigations being dedicated to the development of new therapies, the 5-year survival rate for lung cancer patients remains low, ranging between 4 and 17% (Hirsch et al. 2017). Differences in incidence, survival, and deaths caused by lung cancer vary according to world region, lifestyle, gender, and age. The highest incidence and mortality rate occur in central and eastern Europe and North America. As with many other cancer types, lung cancer frequency increases with age, probably due to accumulation of mutational changes and/or environmental hazards. The challenge when treating lung cancer is that most cases are detected at an advanced or late stage of the disease and therapy often encounters chemoresistance (Torre, Siegel, and Jemal 2016).

Regarding lung cancer mortality in Germany, statistics reveal that 24.4% of cancer deaths in men can be attributed to this tumor type *(Figure 1)*. Additionally for women, lung cancer is responsible for 15.3% of cancer deaths, exceeded only by breast cancer (Kaatsch et al. 2018).

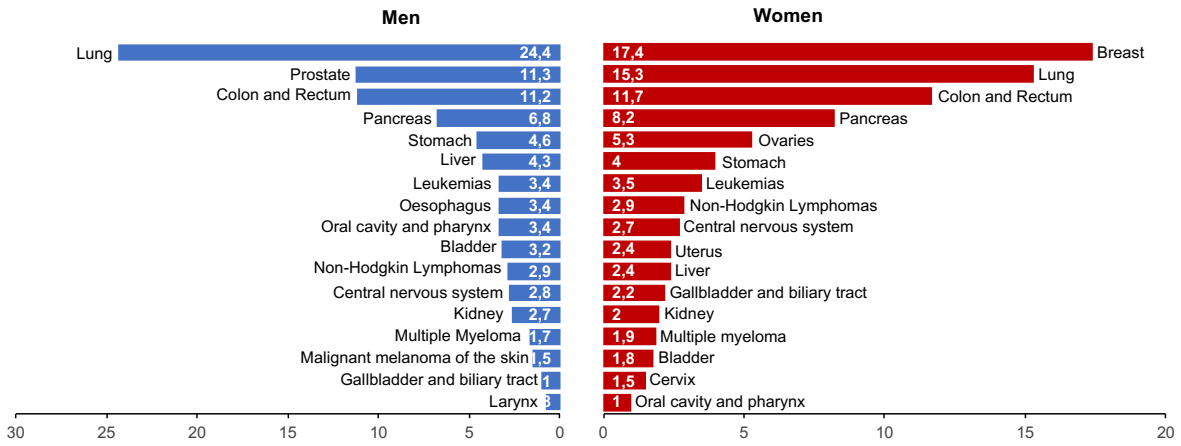

Figure 1. Distribution of cancer mortality in Germany. Lung, prostate, and colon cancer have the highest mortality in percentage amongst men in Germany. Whereas, breast, lung, and colon cancer occupy the top of the list for women (Adapted from the publications by Kaatsch et al. 2018 and Ferlay et al. 2018).

On the basis of histological features, lung cancer is classified into two types, non-small cell lung cancer (NSCLC) and small cell lung cancer (SCLC) (*Figure 2*); they mainly differ in their response to therapy and metastatic spreading. SCLC arises from neuroendocrine cells and is considered the most aggressive form of lung cancer (Sutherland and Berns 2010).

NSCLC was later further subdivided into adenocarcinoma, squamous cell carcinoma (SCC), and large-cell carcinoma (LCC). Adenocarcinoma represents almost 48% of all lung cancers and develops in distal airways. SCC accounts for 30% of all lung cancers and develops mostly as central lung tumors; however, in some cases, it can be found in the periphery of the lung. Some of the morphological features of SCC are intercellular bridging, squamous pearl formation, and individual cell keratinization (Travis 2011).

Last, LCC accounts for less than 5% of all lung cancers and is found mostly in the lung periphery, frequently appearing as large necrotic tumors. Histologically, the tumor consists of sheets and nests of large polyclonal cells with vesicular nuclei and prominent nucleoli (Travis, Brambilla, and Riely 2013).

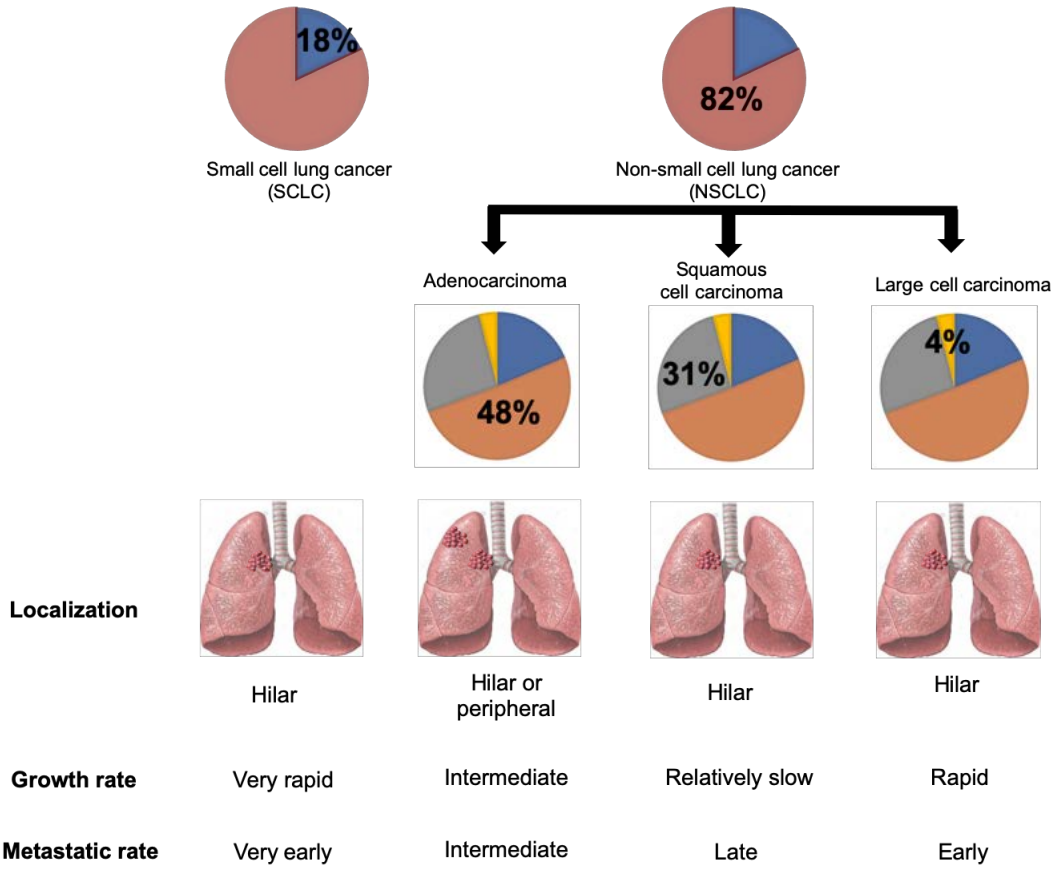

Figure 2. Characteristics of histological lung cancer subtypes. Summary of lung cancer subtypes including incidence percentage, localization, growth and metastatic rate. Cancer subtypes: SCLC and NSCLC. The latter can be subdivided into SCC, LCC and adenocarcinoma which accounts for almost 50% of all lung cancer cases (Adapted from Travis, 2011 and Travis, Brambilla & Riely, 2013).

In addition to classical histopathological features used to classify lung tumor types, the increase in data on the molecular characteristics of tumor samples resected from patients has allowed studies to incorporate genomic information into cancer classification, especially for metastatic cancers of unknown primary origin. One example of this strategy has been the association of EGFR mutations and ALK gene rearrangements exclusively with adenocarcinomas (Shames and Wistuba 2014).

1.1.3 Pathogenesis

According to accumulating evidence, malignant tumors form as a result of progressive pathological changes referred to as preneoplastic or premalignant lesions, a theory referred to as, “Airway field of injury”. This hypothesis postulates that exposure to carcinogens for example cigarette smoke, elicits a common molecular response throughout the respiratory tract. Progression from a field of injury to preneoplasia and lung malignancy is not fully understood, although elucidating the mechanisms at play in this process would provide early markers in lung cancer detection and chemoprevention (Kadara et al. 2016).

Development of tumors from lesions is a multistep process involving hyperplasia, squamous metaplasia, squamous dysplasia, and carcinoma *in situ*; changes which occur in the large airways preceding invasive lung squamous cell carcinomas (Wistuba and Gazdar 2006). Advancement of the lung malignant phenotype seems to be both a result of a stepwise sequence-specific molecular pathogenesis as well as a consequence of the accumulation of genetic and epigenetic abnormalities (Kadara et al. 2016).

Specifically, for adenocarcinomas, two molecular pathways seem to have a pivotal effect in its development: for cancers linked to tobacco consumption, the Kras (Kirsten rat sarcoma viral oncogene) pathway; and for non-smokers, the EGFR pathway (Mounawar et al. 2007; Rudin et al. 2009). Previous studies have estimated that 50-60% of patients with adenocarcinoma present mutations of either the proto-oncogene Kras or EGFR/ALK gene rearrangements (Imielinski, Berger et al. 2012).

Currently, information on the genetic component in lung cancer is utilized for the selection of new therapies specifically targeting some of the effects of these mutations, as well as to shape a more comprehensive scheme for the classification of lung tumors. Although DNA damage plays an important role in the development of lung cancer, the progression of the disease is supported and at times promoted by the tumor microenvironment, eventually resulting in the metastatic spread of cancer cells from primary tumor sites. The molecular mechanisms responsible for the intravasation of tumor cells and subsequent extravasation at distant sites are not completely understood and require further investigation (Imielinski et al. 2012; Hensing et al. 2014).

1.1.4 Risk factors

Lung cancer is a heterogeneous and complex disease; however, genetic and environmental factors that can influence the risk of developing lung cancer have been identified. Smoking has been well established as a major risk, with smokers being 10-20 times more likely to develop lung cancer than non-smokers. Repeated exposure to tobacco smoke and the more than 60 carcinogens contained in cigarettes during long periods of time can result in DNA damage that disrupts normal cellular growth and the regulation of cellular processes (Hensing et al. 2014).

Location of tumors within the lung can also be related to smoking. Primary cancers associated with smoking often develop in the central airway (SCLC and SCC), and those not associated with smoking develop in the peripheral airways (adenocarcinoma). Furthermore, lung cancers have dramatically different molecular profiles in smokers versus non-smokers (Sutherland and Berns 2010; Wistuba et al. 2000).

Another risk factor is environmental tobacco smoke (ETS), also referred to as second-hand smoke, which accounts for up to 3,000 of lung cancer cases. Additionally, exposure to

smoke and carcinogens as an occupational hazard, for example, exposure to fumes, ionizing radiation or chemicals such as asbestos, can double a person's risk of developing lung cancer (Al-Zoughool et al. 2013).

Lung cancer can still develop even in the absence of risk factors, suggesting a genetic component that accounts for cases of lung cancer in non-smokers (Smolle and Pichler 2019). Several registry-based studies have linked a family history of lung cancer with increased risk (Cote et al. 2012; Lissowska et al. 2010).

Specifically, for SCC comparative genomic hybridization (CGH) array analysis identified 15 genes within altered regions in non-smoker patients, also reported in the Cancer Gene Census. One of these genes, GAB2 was frequently amplified in non-smokers patients and moreover with the use of immunohistochemistry, the protein product of this gene was found to be significantly upregulated in non-smokers patients (Park et al. 2017).

Recent studies have also highlighted the role of genes related to metabolic syndrome in the development of adenocarcinoma. According to a study by Zhang et. al., after analyzing the pattern of adiponectin quantitative trait loci (QTLs) in association with gene expression correlations researchers concluded that genes related to metabolic syndrome contribute to cancer formation (Zhang et al. 2013). Another study using genome wide association linked expression of EGFR, VTL1A, TNFRSF10C, C3ORF21, and hyper-methylation of TNFSF10C, BHLHB5 with lung adenocarcinoma formation and pathways related to metabolic syndrome (Okazaki, Ishikawa, and Sohara 2014).

Other non-genetic factors such as diet and alcohol intake have been linked with cancer development. A vegetable and fruit-rich diet may exert a protective effect against lung cancer, while alcohol intake due to its association with tobacco use has been challenging to investigate. Studies with added adjustments for smoking related to alcohol intake have nonetheless suggested an increased risk (Bandera, Freudenheim, and Vena 2001; Garcia Lavandeira et al. 2018). Additionally, patients suffering from chronic inflammation as a result of infection or other pulmonary diseases, such as chronic obstructive pulmonary disease and tuberculosis, are at a greater risk of developing lung cancer. Inflammatory processes underlying such conditions are accompanied by cytokine secretion and recruitment of immune cells, creating a cellular microenvironment that favors angiogenesis and generation of genetic mutations (Durham and Adcock 2015; Cukic 2017).

1.2 Lung Cancer Treatment

Treatment of lung cancer patients is linked to disease stage (*Table 1*), with patients in early stages undergoing tumor resection followed by traditional chemotherapy. For patients in more advanced stages, typically treatment with cisplatin-based regimens is administered. Chemotherapy alongside radiation is common practice for highly aggressive tumors with a metastatic tendency, as is the case for SCLC.

Stage	Tumor Localization	Treatment Options
Stage Ia-Ib	Limited to the lung	Surgical resection
Stage IIa-IIb	Spread to local lymph nodes	Surgical resection
Stage IIIa	Spread to regional lymph nodes in trachea	Chemotherapy followed by radiation or surgery
Stage IIIb	Spread to contra lateral lymph nodes	Combination: chemotherapy+radiation
Stage IV	Metastasis to other organs	Chemotherapy or palliative care

Table 1. Summary of available lung cancer treatments according to stage. (Adapted from Wakelee, Kelly, and Edelman 2014).

- Surgery

Tumor resection in the lung can be done by four different procedures: wedge resection, lobectomy, pneumonectomy and sleeve resection. They differ in the amount of tissue removed, which ranges from the tumor surrounded by normal tissue to the entire lung including part of the bronchus. Patients will generally undergo chemotherapy or radiation therapy after surgery as adjuvant therapy to lower the risk of recurrence (Reveliotis et al. 2014).

- Radiation

Radiation therapy uses high-energy X-rays or other types of radiation to eliminate cancer cells and can be administered externally by high energy beams aimed at the location of the tumor or delivered internally to the tumor site through catheters. For tumors in the airways, radiation is given directly to the tumor through an endoscope. In some cases, depending on disease stage and age, radiation can be used to reduce tumor size before resection or to sensitize tumor cells prior to chemotherapy (Baskar et al. 2012).

Current therapy standard for patients with stage IIa-b NSCLC includes six weeks of thoracic radiotherapy coupled with doublet chemotherapy using either cisplatin or carboplatin and an additional drug. Multicenter trials have reported a median survival time for patients of two years (Hirsch et al. 2017).

- Chemotherapy

The goal of chemotherapy is to disrupt basic cellular processes such as proliferation, angiogenesis and metastasis. Chemotherapy can be administered systemically or locally to the tumor area. For patients with NSCLC, platinum-based chemotherapy is a standard treatment, with common drugs such as cisplatin or carboplatin being administered to patients. Both drugs can have severe side effects and studies have shown that this traditional approach to treatment leads to a modest improvement, with only an excess on median survival of 2 months for patients suffering from stage III NSCLC (Breathnach et al. 2001).

- Targeted therapies

Almost 70% of patients with lung cancer are diagnosed at an advanced stage, at which point traditional therapies have unspecific and modest effects on cancer progression. Novel and targeted therapies based on well-known genetic mutations present in a large number of lung cancers have been developed, such as EGFR tyrosine kinase inhibitors (TKI) or p53 mutations. An example of successful targeted therapy has been the administration of gefitinib and erlotinib in the early 2000s. These drugs are TKIs enhancing patient survival when compared to patients treated only with traditional chemotherapy. Other targeted therapy drugs are aimed at hindering angiogenesis such as the monoclonal antibodies, bevacizumab and ramucirumab, that target either VEGF or its receptor and have improved patient survival in clinical trials (Forde and Ettinger 2013).

- Immunotherapy

Another novel source of therapy targets the tumor microenvironment (TME) and its infiltrating immune cells. Cancer cells are known to modulate the activity of the infiltrating immune cells to bypass immune surveillance. Immune therapy has therefore been designed to stimulate immune cells and potentiate the hosts immune response to specifically targeted tumor cells. Pembrolizumab, a monoclonal antibody normally used in cancer immunotherapy, acts through blockage of the PD-1 receptor on lymphocytes, preventing the binding and activation of programmed death-ligand 1 and 2 (PD-L1 and PD-L2) and causing the activation of T cell-mediated immune response against tumor cells. Patients treated with pembrolizumab in addition to platinum-based chemotherapy, experienced longer overall survival and progression-free survival (Gandhi et al. 2018).

1.3 The Tumor Microenvironment

The TME involves the cellular and non-cellular components of the tumor niche (*Figure 3*). Increasing evidence demonstrates that the TME can dictate aberrant tissue function and play a critical role in the subsequent development of malignancies. The TME consists of the extracellular matrix (ECM), blood and lymphatic vascular networks, and a myriad of cellular components such as myofibroblasts, fibroblasts, neuroendocrine cells, adipose cells, and immune-inflammatory cells (Yuan et al. 2016).

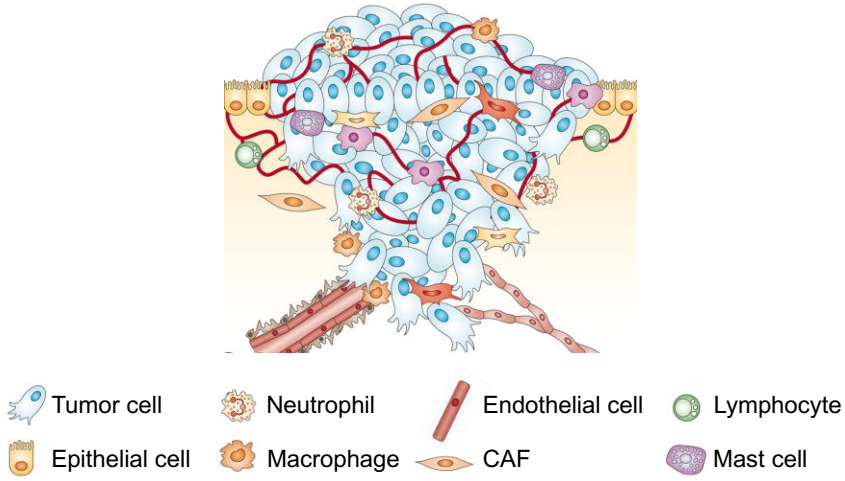

Figure 3. The tumour microenvironment. The tumor stroma is a heterogenic environment where tumor cells are able to recruit CAFs (cancer-associated fibroblasts), epithelial and endothelial cells, fibroblasts, pericytes and immune cells (Taken from Joyce and Pollard 2009).

1.3.1 Cellular components of the tumor microenvironment

The TME consists of cancer cells, immune cells, blood vessels, fibroblasts, lymphocytes, and the ECM, among other components. Specifically, immune cells, such as macrophages, dendritic cells, and lymphocytes have been extensively studied in the context of cancer development and have a key role in either promoting or inhibiting tumor growth. One of the main features driving this process is the complex interaction between cells of the immune system, cancer cells, and the secreted factors that shape their crosstalk (Whiteside 2008).

- Cancer-associated fibroblasts (CAF)

CAFs are a major component of the tumor stroma and can be detected by the expression of markers such as α-smooth muscle actin (α-SMA), fibroblast specific protein-1 (FSP-1), and platelet-derived growth factor receptor (PDGFR). These cells are able to actively remodel and reprogram the ECM and the cellular components of the TME through secretion of a wide range of cytokines (Shiga et al. 2015). CAFs promote tumor cell proliferation and migration by secreting classical growth factors such as epidermal growth factor (EGF), hepatocyte growth factor (HGF), insulin-like growth factors (IGFs), and integrin α11. Additionally, chemokines CXCL12, CXCL14, and CCL5 secreted by CAFs are responsible for the recruitment of bone marrow-derived cells (BMC) and immune cells to tumor sites, which in consequence strengthens the inflammatory profile in the TME (Kalluri 2016).

CAFs can also enhance EMT and angiogenesis by secreting matrix metalloproteinases (MMPs) and are a primary source of VEGF in the tumor stroma (Tao et al. 2017).

- ECM

The ECM is a non-cellular component of the TME composed of a dynamic 3D network of macromolecules, mainly elastin, collagen, and microfibrillar proteins. The primary function of the ECM is to provide homeostasis and maintain the normal architecture of a given tissue (Sainio and Jarvelainen 2014). Increased ECM deposition by CAFs results in tumors that are stiffer than the surrounding tissue as a consequence of collagen crosslinking. This phenomenon modulates tissue fibrosis and facilitates focal adhesions, growth factor signaling, and malignancy (Levental et al. 2009; Balkwill, Capasso, and Hagemann 2012).

- Mast cells

Mouse models of inducible and spontaneous cancer have established that mast cells are among the first immune cells to accumulate and shape the TME. They are key regulators of angiogenesis by secreting heparin, heparanase, histamine, metallo- and serine proteinases, and various growth factors, including basic fibroblast growth factor (bFGF) and VEGF (Dalton and Noelle 2012).

- Macrophages

Macrophages are cells of the innate immune system that originate from monocytes and secrete inflammatory cytokines IL-1, IL-16, and tumor necrosis factor alpha (TNF-α). Their main function is to circulate through tissue and remove pathogens by phagocytosis. After activation, macrophages can also function as antigen presenting cells (APCs), initiating the inflammatory response through stimulation of T cells thus acting as a link between innate resistance and specific immunity (Varol, Mildner, and Jung 2015). Macrophages can become polarized into classically activated M1 macrophages, which produce pro-inflammatory cytokines involved in the Th1 T cell response, such as IL-12 and IL-23, and M2 alternatively activated macrophages triggered by Th2 cytokines, IL-10 and IL-4 (Nahrendorf and Swirski 2016).

Macrophages within the tumor microenvironment are called tumor-associated macrophages (TAMs) and are recruited to the tumor site through secretion of colony stimulating factors (CSFs) and monocyte chemoattractant proteins (MCPs). TAMs can be reprogrammed by cancer cells to produce angiogenic and lymphangiogenic growth factors. Their pro-tumor functions include cancer promotion through production of cytokines such as IL-6 or mitogens that activate the initiation and progression of cancer via the nuclear factor-κB (NF-κB) or signal transducer and activator of transcription 3 (STAT3) signaling pathway in tumor cells. TAMs also secrete IL-10, which results in suppression of T-cell cytotoxicity by T regulatory cells (Tregs). Additionally, CCL18 secreted by TAMs induces tumor metastasis by prompting integrin clustering and enhancing their adherence to the ECM in tumor cells. Finally, secretion of VEGF by TAMs is thought to contribute to angiogenesis in the tumor microenvironment (Yang and Zhang 2017).

- Dendritic cells (DCs)

Dendritic cells are bone marrow-derived leukocytes responsible for the initiation of the adaptive immune response. DCs act as antigen presenting cells and stimulate naïve T cells, resulting in T cell clonal selection and expansion into effector and memory T cells. DCs are a heterogeneous leukocyte population with different phenotypes and localization, forming a cellular system responsible for immune surveillance distributed throughout the body. Their differentiation is driven by key growth factors; Fms-like tyrosine kinase 3 (Flt3), granulocyte macrophage colony-stimulating factor (GM-CSF), and M-CSF. DCs can secrete a variety of cytokines such as, IL-10, IL-13 and TNF-α, among others (Veglia and Gabrilovich 2017). Tumor infiltrating DCs (TIDC) play a major role in cancer immunosurveillance as functional TIDCs migrating to the regional lymph nodes are capable of presenting tumor antigens to naïve

tumor-specific T cells, which subsequently reach the tumor through inflammation-induced ligand/receptor pairs (Ma et al. 2013). Patients with infiltrating DCs in primary tumors display prolonged survival and reduced incidence of metastasis in cases of lung, bladder, and gastric carcinomas. DCs exert their anti-tumor function through type I Interferons (IFN), which promote tumor-specific cytotoxic T-lymphocyte (CTL) priming and also act on innate immune cells to mediate their antitumor effects (Diamond et al. 2011).

- Natural killer (NK) cells

NK cells are large granular bone marrow-derived lymphocytes that share a common progenitor with B and T cells. They are subdivided into “bright” NK cells, which are located in secondary lymphoid organs and influence immune response by the secretion of IFN-γ, and “dim” NK cells, which circulate in peripheral blood and kill transformed or infected cells via perforin/granzyme or death receptor related pathways. Their activity, unlike that of other immune cells, does not require priming and is modulated by an array of inhibitory and activating receptors (Knorr et al. 2014).

In tumors, NK cells are noticeably absent from tumor infiltrates and those present display profound alterations of their phenotype with low cytotoxicity, reduced IFN-γ production, and downregulation of surface markers, suggesting a mechanism by which cancer cells can either hinder their recruitment to tumor sites and/or alter their function (Terry et al. 2017).

- B cells

B cells mediate production of antigen-specific immunoglobulins directed against invasive pathogens and are therefore part of the adaptive humoral immune response. Mature B cells circulate between lymphoid organs until they encounter a cognate antigen. Afterwards, with the help of T cells, a germinal center is established where B cells undergo rounds of proliferation coupled with affinity maturation to produce a B cell pool that can bind antigen with the highest affinity (Nemazee 2017).

Within the TME, B cells are responsible for mediating activation of STAT3 and the inhibitor IKKα through secretion of lymphotoxins, thereby aiding tumor progression. Additionally, B cells can promote tumorigenesis by secreting IL-10 and transforming growth factor beta (TGF-β), hence suppressing CD8 T cell cytotoxicity and recruiting Tregs, which results in a shift in the balance of tumor-specific immune response toward immuno-suppression (Fremd et al. 2013).

1.4 T cells

T cells are white blood cells at the core of adaptive immunity. Their functions are diverse and rely on the different subtypes of mature T cells (Kumar 2018). Tumor Infiltrating lymphocytes (TIL), among which are T cells, play an essential role in mediating response to chemotherapy and can improve clinical outcome in colorectal, ovarian, and lung cancer (Ruffini et al. 2009; Galon et al. 2006; Zhang et al. 2003). However, studies on breast cancer suggest that high density of TILs can have an opposing effect on patient survival. The location and nature of the immune infiltrate is critical for this outcome (Denkert et al. 2018).

1.4.1 T cell development

Development of T cells occurs in primary lymphoid organs, the bone marrow, and thymus, sites of hematopoiesis and clonal expansion of immune cells. In the thymus, progenitor hematopoietic stem cells (HSC) that have migrated from bone marrow give rise to several lineages of blood cells. After maturation, T cells circulate through the blood and the lymphatic system and reside in secondary lymphoid organs, such as organized lymphoid tissues associated with mucosal surfaces like tonsils, bronchial, nasal, and gut-associated lymphoid tissues; the spleen and lymph nodes; where the T-cell mediated immune response takes place (Broere et al. 2011).

T cell progenitors in the thymus, called thymocytes, undergo a series of gene rearrangements that result in the production of a complex T cell receptor (TCR) consisting of the variable α and β polypeptide chains non-covalently associated with non-polymorphic CD3 proteins (*Figure 4*). Previous studies on the stoichiometry of these molecules revealed that CD3 proteins exist as a series of dimers including $\varepsilon\gamma$, $\delta\varepsilon$ and $\zeta\zeta$ associated with a single $\alpha\beta$ heterodimer (Smith-Garvin, Koretzky, and Jordan 2009).

After successful generation of the TCR, progenitor cells lack expression of CD4 and CD8 proteins and are referred to as double negative (DN). CD4 and CD8, are transmembrane proteins found on the surface of T cells and act as co-receptor molecules promoting signaling by the TCR (Broere et al. 2011).

$\alpha\beta$-TCR T cells have a diverse range of antigen recognition receptors and represent mature T cells that circulate through secondary lymphoid organs and modulate adaptive immune responses. A small fraction of T cells expresses $\gamma\delta$-chains in the TCR and are much less heterogenic than $\alpha\beta$-TCR T cells, which reside in skin and certain mucosal surfaces and play a part in the initial response to bacterial invasion. Surface markers CD44 and CD25 have been used to identify distinct intermediate phases that occur between β-chain TCR rearrangements and α-chain TCR development. After successful selection of receptor chains,

T cells begin to express both the TCR and co-receptors CD4 and CD8 and are therefore called double positive (DP) (Broere et al. 2011; Smith-Garvin, Koretzky, and Jordan 2009).

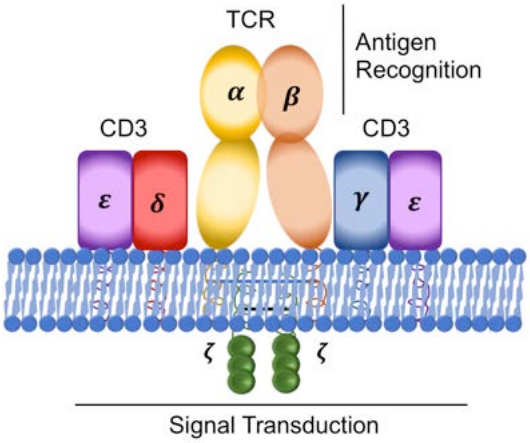

Figure 4. T cell receptor complex. The T cell receptor is composed of heterodimers of two polypeptide chains, α and β, covalently linked by a disulfide linkage. Cells with TCRs containing both chains are referred to as αβ T cells. Other structures associated with the TCR are CD3 and ζ-chain accessory molecules and are non-covalently associated with the αβ chain. CD3 structures are composed of εγ and εδ polypeptide chains that contain specific molecules responsible for the downstream signaling pathway (Adapted from Broere et. al., 2011).

DP cells must undergo a process of selection based on antigen reactivity before they can leave the thymus. Cortical epithelial cells expressing class I and II MHC molecules and self-antigens interact with DP cells. Those with a high enough affinity survive, whereas the rest undergo apoptosis. This process, referred to as positive selection, enriches useful T cells that are potentially reactive to foreign antigens, but not to self-antigens, presented by self-MHC molecules. Subsequently, cells that have survived positive selection migrate to the medulla area of the thymus and bind bone marrow-derived APCs (macrophages and dendritic cells) that highly express self-antigens. Those that interact too strongly with these molecules undergo apoptosis; intending to eliminate self-reactive T cells and avoid auto-immunity. Only 3-5% of developing thymocytes survive the process of maturation (Takaba and Takayanagi 2017). Single positive thymocytes (for co-receptor molecules CD4 or CD8) are exported to supply the peripheral T cell population and their last maturation stage is characterized by the expression profile of markers; CD62L (lymphocyte L-selectin) and CD69 (C-type lectin protein). It is believed that T regulatory cells are produced during this last maturation step in the medulla area of the thymus (Takahama 2006).

1.4.2 T cell activation

Naïve T cells generated in the thymus can be distinguished from other cells of the immune system by the presence of a T cell receptor which provides T cells with the ability to recognize and respond to specific foreign antigen. After maturation, T cells circulate through blood and the lymphatic system until they are exposed to antigen by professional APCs, resulting in activation and differentiation into effector T cells (Smith-Garvin, Koretzky, and Jordan 2009; Masopust and Schenkel 2013).

Antigenic peptides responsible for T cell activation are acquired from pathogens found in vesicular compartments of infected cells or from extracellular proteins internalized by endocytosis. After their processing, peptides are carried to the cell surface as a complex bound to MHC class II molecules, which can only emerge on the surface of professional APCs (macrophages, DCs, and B cells). On the other hand, MHC class I molecules bind to antigenic peptides present in the cytosol of APCs after their processing by proteasomes. Subsequent interaction with a transporter associated with antigen processing proteins (TAP) allows for peptide delivery toward the endoplasmic reticulum, where they translocate to the cell surface. Nearly all cells express MHC class I molecules and are therefore capable of presenting antigen to CD8 CTLs (Broere et al. 2011; Masopust and Schenkel 2013).

Professional APCs can also present T cells with antigen transferred from other cells in a process commonly referred to as “antigen cross-presentation”, which normally involves MHC class I-restricted peptides when antigen cannot be acquired directly. In addition, this process provides an effective way of separating antigen from the inhibitory processes used by viruses and tumor cells to interfere with antigen presentation and subsequent triggering of the immune response (Joffre et al. 2012).

Cross-presentation seems to be vital for an optimal CD8 response and studies have also shown that DCs can initiate a T cell response against MCH class I antigens through the same process (Campana, De Pasquale et al. 2015). It also may serve as a mechanism for T cell tolerance to self-antigen in the periphery (Joffre et al. 2012).

Activation of T cells requires not only antigen presentation but also a complex balance between the interaction of the TCR with co-receptors CD4 and CD8, co-stimulatory and accessory molecules that can further intensify cell-cell interactions (Golubovskaya and Wu 2016). CD4 and CD8 co-receptors assist the TCR signal, whereas costimulatory molecules such as CD28 and CTLA-4 can augment or obstruct it upon their interaction with either CD80 or CD86 membrane proteins on APCs. Accessory molecules LFA-1 or CD2 contribute to signal transduction by providing adhesion at the cell contact site and therefore strengthen the interaction between the T cell and APC (Broere et al. 2011; Malissen and Bongrand 2015). After this initial phase of T cell activation, there is a release of cytokines such as IL-12 and IL-

2 that induce expansion and differentiation into effector T cells (*Figure 5*) (Broere, Apasov et al. 2011).

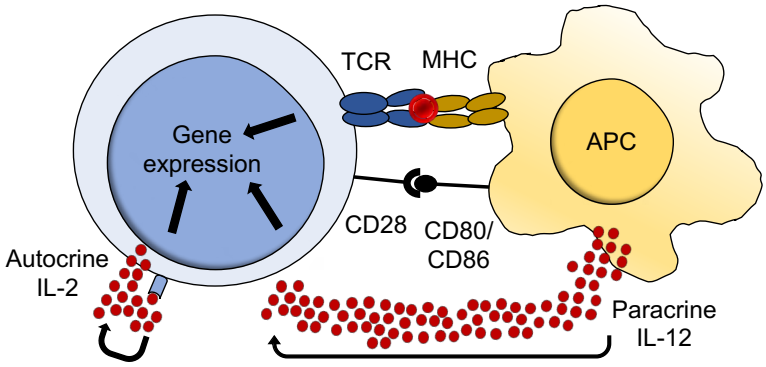

Figure 5. T cell activation. TCR signaling is triggered by presentation of antigen by APCs; next costimulatory interaction can either augment or inhibit TCR signaling, and last cytokine signaling results in the upregulation of genes related to proliferation and differentiation in T cells (Adapted from Broere et. al., 2011).

Activation of the TCR and the subsequent production of IL-2 and binding to its receptor activates intracellular signaling that results in the upregulation of genes responsible for the proliferation and differentiation into effector T cells. This mechanism ensures that T cells differentiate only when a substantial number of lymphocytes simultaneously respond to antigen and levels of IL-2 are effectively high. As mentioned before, the co-receptor associated with the TCR on the surface membrane of T cells will determine which MHC class molecules these cells interact with and their role in the immune response (Golubovskaya and Wu 2016).

1.4.3 CD8 T cells

CD8 T cells are a subpopulation of adaptive lymphocytes that play an important role in the defense against intracellular pathogens and tumor cells. Additionally, some reports have linked these cells to autoimmune and allergic disorders (Huber et al. 2009). Differentiation occurs after naïve CD8 T cells are activated by recognition of specific peptides presented by MHC class I on APCs in peripheral lymphatic organs. CD4 T cells can also influence differentiation of CD8 T cells by supplying co-stimulatory signals and skewing cytokines. After activation, clonal expansion takes place and a large number of cells migrate to the periphery, where they re-encounter antigen and perform their effector functions. After this primary response, a majority of CD8 T cells dies through apoptosis however, a minor fraction persists as memory T cells (Mittrucker, Visekruna, and Huber 2014; Zhang and Bevan 2011).

Cytotoxic T lymphocytes (CTLs) are defined by the production of INF-γ and TNF-α and constitute the best characterized subpopulation of CD8 T cells (Golubovskaya and Wu 2016). They are capable of killing cells carrying a specific antigen through release of cytotoxic

molecules, such as granzymes and perforins. Another subset of CD8 cells are Tc2, which have a very similar cytokine expression profile as the T helper subset; Th2 cells, both develop in the presence of IL-4 and the lineage specific transcription factor GATA3 and produce IL-5 and IL-3 in lesser amounts. Depending on the type of immune response, Tc2 cells can acquire high or low cytotoxicity and their functional properties strongly differ from those of CTLs. Tc2 cells have been associated with contributing to allergic airway inflammation, rheumatoid arthritis and function impairment during influenza infections. Less studied subsets Tc9 and Tc17 have been reported to have similar functions and secrete the same cytokines as their T helper cells counterparts, Th9 and Th17 (Mittrucker, Visekruna, and Huber 2014; Golubovskaya and Wu 2016).

In the context of tumor microenvironment, the presence of CD8 T cells at the tumor site has been associated with increased survival of patients with colorectal cancer and other solid tumors, conferring them with a beneficial role in the context of anti-tumor immunity (Hadrup, Donia, and Thor Straten 2013; Banat et al. 2015).

1.4.4 CD4 T cells

CD4 T cells, also known as T helper cells, modulate adaptive immunity to different pathogens and are involved in autoimmunity, asthma, and allergic responses, as well as tumor immunity (Golubovskaya and Wu 2016). They are able to exert a wide range of functions through differentiation into several subsets: T helper (Th); Th1, Th2, Th9, Th17, Th22, Tregs, and follicular helper T cells (Tfh). Each subset is characterized by different cytokine profiles and requires a specific cytokine and transcription factor combination for its development, as summarized in *Figure 6*. In particular, T helper cells Th1 and Th2 were the first and are now the best-defined Th lineages (Hirahara and Nakayama 2016).

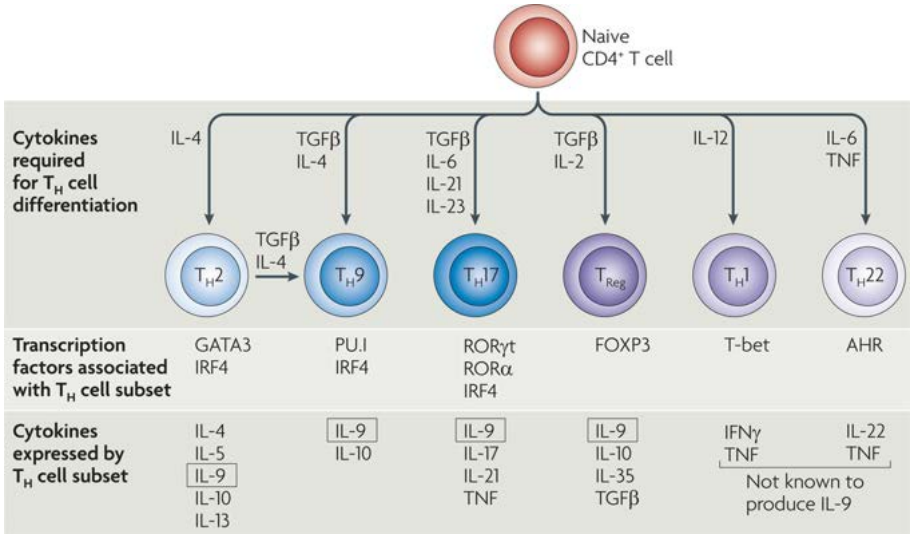

Figure 6. CD4 T helper cell differentiation and lineages. Different cytokines and transcription factors regulate Th cell differentiation into specific subsets. Th1 cells arise after stimulation with IL-12 and upregulation of the transcription factor T-bet. Th2 cell differentiation occurs as a result of IL-2 and IL-4 stimulation and is characterized by expression of the transcription factor GATA3. Differentiation of Th9 and Th17 cells requires the presence of TGF-β in combination with IL-4 and IL-6, respectively. Transcription factor PU.1 and IRF4 are responsible for Th9 differentiation, whereas Stat3 is associated with the Th17 cell lineage (Taken from Noelle and Nowak 2010).

In contrast to data available for CD8 cells, the role of CD4 T cells in the tumor microenvironment is not as straightforward. Evidence can be found for both pro-tumor and anti-tumor effects, which is likely due to the fact that CD4 T cells have more plasticity and carry out dual roles. Thus, depending on the cytokines secreted in the tumor microenvironment, they can differentiate into a specific subtype and convert from pro-tumorigenic to anti-tumorigenic and vice versa (Janssen et al. 2003; Huang et al. 2015; Zheng et al. 2016).

1.4.5 Th1 cells

Th1 cells are characterized by the expression of the transcription factor T-bet and the secretion of INF-γ, IL-2, IL-10, and TNF-α. Their role mainly involves the promotion of cell-mediated immune responses, with its effector cytokines promoting CTL proliferation, production of nitric oxide, and macrophage activation, which in turn leads to phagocytosis helping with the hosts defense against intracellular viral and bacterial pathogens (Zhang et al. 2014; Muraille and Leo 1998). *In vitro* Th1 differentiation occurs through the IFNγ-STAT1-T-bet pathway, which also serves as a powerful amplification mechanism for STAT4 activation by IL-12 and is critical for Th1 responses both *in vitro* and *in vivo*. The differentiation pathways of Th1 and Th2 cells are mutually exclusive, that is, production of INF-γ by Th1 both stimulates further Th1 cell production and inhibits the development of Th2, whereas IL-10, which is produced by Th2 cells, is responsible for the opposite effect (Sekiya and Yoshimura 2016; Hirahara and Nakayama 2016).

In the context of the tumor microenvironment, defined roles for Th1 and Th2 cells have already been established, as mostly anti and pro-tumorigenic, respectively. Th1 cells are believed to hinder tumor growth by the secretion of INF-γ, which induces the infiltration of macrophages and/or CD8 CTLs into the tumor (Pellegrini et al. 1996; Kim and Cantor 2014).

1.4.6 Th2 cells

Th2 cells were one of the first subsets of T helper cells to be described based on the selective production of IL-4 (Swain et al. 1990). These cells mainly modulate the immune response to helminths and other extracellular parasites and are currently defined by the secretion of IL-4, IL-5, IL-6, IL-10, and IL-13. Th2 cells have been shown to be essential in B cell production of IgG, IgA, and IgE (Hirahara and Nakayama 2016). Th2 differentiation occurs under the influence of IL-4 and IL-2 in combination with the transcription factor GATA3, which is able to block expression of IFN-γ, thus inhibiting Th1 differentiation (Zhang et al. 2014). Another key factor modulating Th1/Th2 fate decision is IL-2. In most CD4 T cell subsets, IL-2 is essential for proliferation, but in Th2 cells, IL-2, and the downstream STAT5 signal are crucial in driving naïve T cells toward Th2 differentiation (Cote-Sierra et al. 2004).

Th2 cells and their excessive production of type 2 effector cytokines are known to mediate asthma and chronic allergic inflammation (Leomicronn 2017; Kubo 2017). Although Th2 cells have so far been regarded as tumor promoting due to their role in supporting angiogenesis and tumor growth, they have also been linked to anti-tumor immunity when associated with eosinophils. Hence, their function seems to be related to the cellular and secretory environment (Hung et al. 1998; Nishimura et al. 1999; Ellyard, Simson, and Parish 2007).

1.4.7 T regulatory cells (Tregs)

Tregs are critical mediators of peripheral tolerance and immune suppression. Moreover, previous studies support their involvement in all cell-mediated immune responses directly affecting T and B cell reactions to self and foreign antigen. Other Treg functions include suppression of asthma, allergy, pathogen-induced immunopathology and the protection of commensal bacteria from elimination by the immune system (Broere et al. 2011). T regulatory cells can be subdivided into naturally arising Tregs (nTregs) generated in the thymus and inducible Tregs (iTregs) that are converted to Tregs upon activation in the periphery. nTregs are identified by the expression of both co-receptors CD4 and CD25, a component of the IL-2 receptor, and are therefore positive for CD4 and CD25. nTreg development and function is tightly regulated by the transcription factor Forkhead box P3 (FOXP3), responsible for the upregulation of Treg-related molecules, CD25, CTLA-4 and GITR, that are able to inhibit T cell

activation and downregulate the immune response of neighboring cells. FOXP3 can also inhibit IL-2 transcription, effectively suppressing lymphocyte proliferation and the subsequent differentiation into Th1 and Th2 effector cells (Wolf et al. 2015; Whiteside 2008).

In the context of cancer development, there is increasing evidence that tumor-derived factors promote recruitment of Tregs to tumor sites where their frequency is increased three times from the range in peripheral lymphoid tissues. A high Treg/CD8 ratio is associated with poor prognosis in patients and their role in the tumor microenvironment seems to be the suppression of anti-tumor immunity through inhibition of CTL function (Kim and Cantor 2014).

1.5 Th9 cells

1.5.1 Development and function

Studies on IL-9 expression were done in Th2 cell-mediated immunity with models of *Leishmania*-infected mice and it was formerly considered a Th2 cytokine. Later in 2008, Th9 cells were described as a separate lineage from Th1 and Th2 cells, following studies by two independent research groups (Veldhoen et al. 2008; Dardalhon et al. 2008).

Th9 cell differentiation occurs through a complex network of cytokines and their downstream signaling pathways. TGF-β and IL-4 are central players, although cytokines IL-2, IL-1, IL-33, and IL-25 can also promote IL-9 production in T cells (Kaplan 2015). Th9 development and the signaling pathways triggered by these cytokines are linked with the expression of transcription factors PU.1, IRF4, STAT5, and STAT6 all essential for their differentiation. Th9 cells are now characterized by the production of IL-9, IL-21, and IL-10 and have been associated with contributing to immunopathology in allergy and inflammation, where they have been extensively investigated. Th9 cells are not the only source of IL-9 during an immune response, making it challenging to precisely outline their importance *in vivo* (Chen, Zhang, et al. 2017; Buttrick et al. 2018).

As with other T helper subtypes, Th9 cells have a high level of plasticity, especially in relation to Th2 cells, where it is reported that TGF-β reprograms Th2 cells to lose their expression profile and shift to IL-9 producing cells. Likewise, it has been reported that a minor fraction of Th9 cells *in vivo* can acquire the Th1 cell phenotype, including secretion of their signature cytokine, IFN-γ (Kaplan 2015; Jia and Wu 2014).

1.5.2 Interleukin-9

IL-9, the signature cytokine of Th9 cells, was first referred to as P40, because of its molecular weight of 40 kDa, and described in the late 1980s as a mast and T cell growth factor. Through cloning and the discovery of the complete amino acid sequence, it was revealed that this cytokine is structurally different from other T cell growth factors and was renamed IL-9, based on its biological effects on both myeloid and lymphoid cells (Schmitt and Bopp 2017). This pleotropic cytokine is secreted mostly by long term, antigen-specific and naïve murine T cells. Currently, IL-9 secretion has been reported for Th17, Tregs, and mast cells (Kaplan 2015; Goswami and Kaplan 2011).

As mentioned before, IL-9 has a wide range of effects on both hematopoietic and nonhematopoietic cells. On immune cells, it promotes proliferation of T cells, stimulates IgE production in B cells and enhances Treg function. In addition, previous studies have linked IL-9 to the promotion of Th17-driven inflammation (Koch, Sopel, and Finotto 2017; Nowak et al. 2009). On mast cells, IL-9 is responsible for cell growth, survival and increased expression of IL-6, IL-1β, and IL-5 (Wiener, Falus, and Toth 2004). IL-9 can also enhance chemokine production on epithelial cells, promote maturation of hematopoietic progenitor stem cells and activate production of IL-8, IL-3 and eotaxin by smooth muscle cells (Temann et al. 2007; Kaplan 2015).

IL-9 signal transduction occurs through the IL-9 receptor, a cytokine receptor that consists of a ligand-specific α-subunit and a common γ-chain that is shared with the IL-2, IL-4 and IL-7 receptor complexes. Binding of the cytokine to its receptor increases heterodimerization of the IL-9R α-subunit with the common γ-chain and induces activation of kinases JAK1 and JAK3, which in turn phosphorylate a tyrosine residue on the receptor that serves as a docking site for the STAT3 and STAT5 transcription factors (Goswami and Kaplan 2011).

1.5.3 Th9 cells in tumor biology

Studies on the role of Th9 cells in tumor development have reached a general consensus of potent antitumor activity, particularly in melanoma models (Purwar et al. 2012; Lu et al. 2012; Vegran et al. 2014; Fang et al. 2015). Experiments with RORγt-deficient mice showed a high infiltration of IL-9 producing T cells coupled with reduced tumor growth. Adoptive transfer therapy of antigen specific Th9 cells was also shown to confer anti-tumor properties (Purwar et al. 2012). The underlying mechanisms behind these effects have not been fully elucidated. The reported anti-tumor effects seemingly rely on the ability of Th9 cells to activate and enhance the proliferation of mast cells; another explanation is through the stimulation of epithelial cells to produce CCL20, the ligand of CCR6, which attracts both

dendritic cells and CD8 CTLs into the tumor (Lu et al. 2012; Purwar et al. 2012; Vegran, Apetoh, and Ghiringhelli 2015).

Opposing results have been shown for lymphomas and other non-solid tumor models, where cancer cells are known to overexpress the IL-9 receptor, and IL-9 secretion is responsible for the activations of STAT3 and STAT5 in tumor cells directly promoting survival and proliferation (Lv et al. 2016; Vegran, Apetoh, and Ghiringhelli 2015). In the case of lung cancer, studies point toward an accumulation of Th9 cells due to promotion of cytokine secretion and activation of T regulatory cells (Ye et al. 2012).

1.6 Th17 cells

1.6.1 Development and function

Th17 cells have been defined as a separate CD4 T cell lineage since 2003. Their discovery was prompted by the observation that the newly described IL-23 and not IL-12, responsible for Th1 development, induced a subset of memory CD4 T cells to produce IL-17 (Cua et al. 2003; Aggarwal et al. 2003). Further evidence to support the hypothesis of a new T cell lineage came from studies in rheumatoid arthritis, central nervous system (CNS), and experimental autoimmune encephalomyelitis (EAE) autoimmune models, where researchers identified a role for these novel T cells in granulopoeisis and neutrophil accumulation (Gaffen 2009; Murphy et al. 2003; Gaffen et al. 2014).

Th17 cells were characterized by the production of IL17-A, IL17-F, and IL-6, and their development was shown to be inhibited by IFN-γ and IL-4, bringing about further proof to support their description as a distinct T cell lineage (Langrish et al. 2005; Harrington et al. 2005; Veldhoen et al. 2006). Th17 cells differentiate under the influence of IL-6 and TGF-β, although it has been established that other cytokines such as IL-23 and IL1-β can induce their differentiation independent of TGF-β. Knockout models have elucidated the role of IL-23 in Th17 cell differentiation to be one of maintenance and clonal expansion of these cells (Bedoya et al. 2013; Stritesky, Yeh, and Kaplan 2008). The array of cytokines secreted by Th17 cells has been expanded to include, IL-9, IL-21, IL-22, GM-CSF, IL-10, and IFN-γ, and the transcription factors necessary for their differentiation are RORγT, STAT3, and IRF4 (Bailey et al. 2014).

Th17 cells act as bridge between adaptive and innate immunity, localizing at mucosal surfaces where they trigger inflammatory signals that promote recruitment of neutrophils through granulopoeisis and expression of different factors against bacterial and fungal pathogens. Previous studies have also linked Th17 cells to the promotion of the inflammatory pathology in various autoimmune conditions (Gaffen 2009; Gaffen et al. 2014).

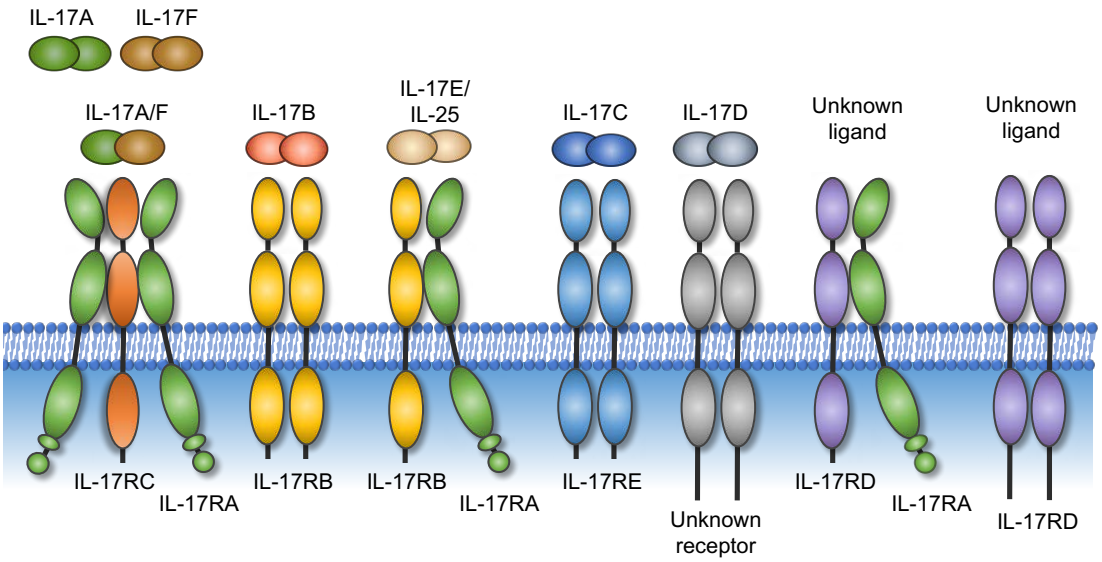

Figure 7. IL-17 cytokine family and their ligand-receptor structural features. The IL-17 cytokine family consists of six homologues: IL-17A, IL-17B, IL-17C, IL-17D, IL-17E, and IL-17F. IL-17A and F were the first to be identified, sharing the highest homology among all family members. These two cytokines are able to form heterodimers and signal through the IL-17RA-RC complex. IL-17B and IL-17C signal through the specific receptors; IL-17RB and IL-17RE, respectively. IL-17E, also known as IL-25, binds with the IL-17RB-RA complex. Some receptor complexes and ligands for other family members have not been identified (Adapted from Gaffen 2009 and Song and Qian 2013).

1.6.2 Interleukin-17 cytokine family

IL-17, formerly referred to as cytotoxic T-lymphocyte-associated antigen 8 (CTLA-8), was discovered in 1993 in a rodent T cell library using subtractive hybridization (Rouvier et al. 1993). Subsequently, through the use of genomic sequencing, several putative IL17-A homologues were identified, and currently constitute the IL-17 family of cytokines, comprising six family members: IL-17A, IL-17B, IL-17C, IL-17D, IL-17E (also known as IL-25) and IL-17F (*Figure 7*) (Gaffen et al. 2014; Amatya, Garg, and Gaffen 2017).

IL-17A and F are highly conserved covalent homodimers that share the strongest homology among all family members, close to 50% and have been extensively investigated (Weaver et al. 2007; Gaffen et al. 2014). These cytokines are able to form A/F heterodimers *in vitro*, where they are produced at much higher levels than IL-17A homodimers. Adding to their similarities, the IL-17 A and F gene loci are located in the same chromosome, whereas all remaining members each map to different chromosomes (Amatya, Garg, and Gaffen 2017).

In particular, IL-17A has been often associated with driving autoimmunity because of its more potent strength of signaling compared to IL-17F, whose responses are 10-30 folds weaker in terms of downstream gene activation, with IL-17 A/F heterodimers acting at an intermediate level. Other than Th17 cells, IL-17 A and F can also be secreted by CD8, γδT, and NK cells (Weaver et al. 2007).

IL-17A is a potent inducer of IL-6 and IL-8 secretion by fibroblasts and both IL-17A and F induce the expression of G-CSF, GM-CSF, CXCL8, CXCL1, and CXCL10. IL-17A and F signal through the ubiquitously expressed IL-17RA-RC complex, which leads to recruitment of the adaptor proteins TRAF6 and Act1 (Amatya, Garg, and Gaffen 2017; Bedoya et al. 2013). NF-κB and mitogen-activated protein kinase (MAPK) activation are mediated by the downstream signaling of IL-17R, which in turn leads to the production of pro-inflammatory cytokines and chemokines and recruitment of neutrophils to the inflamed tissue (Gaffen et al. 2014).

IL-17E is produced by mucosal epithelial cells and other immune cell types and its function is linked to Th2 type response and cytokine production. Other functions include the restriction of Th17 development through inhibition of IL-23 production by macrophages and inducing the expression of CCL5 and CCL11, both important cytokines in the recruitment of eosinophils (Reynolds, Angkasekwinai, and Dong 2010). Less is known about the function and signaling pathways triggered by other family members. Studies suggest that IL-17C is produced by epithelial cells and autocrine signaling in these cells stimulates production of pro-inflammatory cytokines. In a similar fashion, IL-17B might not be a product of lymphocytes and stimulates the transcription of an array of pro-inflammatory genes similar to those induced by IL-17 A and F (Reynolds, Angkasekwinai, and Dong 2010; Jin and Dong 2013).

1.6.3 Th17 cells in tumor biology

Although the contribution of Th17 cells to the promotion of inflammation and autoimmune disorders has been well established, their involvement in tumor immunity has proved contradictory and continues to be highly debated (Bailey et al. 2014; Bedoya et al. 2013; Asadzadeh et al. 2017). Pronounced difference in Th17 form and function appears to be related to several factors, including cancer type, therapeutic approach, and stimuli to which cells are exposed. Evidence can be found of a protective role in leukemia and melanoma, whereas some of its effector cytokines have been associated with impairment of immune surveillance and promotion of tumor growth in mammary tumor models through recruiting of pro-tumorigenic neutrophils (Hus et al. 2013; Bailey et al. 2014; Benevides et al. 2015).

The use of cell surface markers such as CD26 and IL-23R, has helped to distinguish Th17 cells from other T cell subsets; however, findings on T cell plasticity further complicate the detection of these cells in the tumor-bearing host. In particular, previous studies show that Th17 cells can convert into the Th1 lineage in the absence of TGF-β or when exposed to IL-12 and are referred to as non-classical Th1 cells (Basdeo et al. 2017). Studies on tumor infiltrates have only added to the controversy, because although a wide range of tumors have an increased presence of Th17 cells, the role of these cells varies significantly dependending

on tissue type. For example, in colon cancer, pro-inflammatory cytokines secreted by Th17 cells impaired immune surveillance and promoted tumor growth, whereas in melanoma and cervical cancer, Th17 cells directly eradicated tumors in mice to a greater extent than Th1 cells and correlated with increased survival (Muranski et al. 2008; Sharp et al. 2017; Keerthivasan et al. 2014; Yu, Lou, and He 2014). One explanation for this contrasting data is that different types of tumor tissue can foster the generation of different phenotypes of Th17 cells, which is supported by research that has found natural versus induced Th17 cells to be regulated by different signaling pathways (Bailey et al. 2014; Punt et al. 2015).

In the field of lung cancer, previous studies found that patients with NSCLC are characterized by a significantly higher percentage of Th17 and Treg cells when compared to individuals without cancer. However, in NSCLC patients, the levels of the same T cell subsets were inversely correlated in peripheral blood. Higher Treg/Th17 ratios were also observed in patients with stage IV NSCLC compared to stage I-III patients (Duan et al. 2015; Marshall et al. 2016). A better understanding of how Th17 cells affect tumor development and which stimuli or cytokine queues are responsible for the conflicting roles reported in the current literature can only be of use in the development of therapies that can potentiate a hosts immune response to tumor cells.

1.7 Epithelial-Mesenchymal Transition in cancer progression

Organs and adult tissues arise in part through conversion of epithelial cells to mesenchymal cells, a process called epithelial-mesenchymal transition (EMT) (*Figure 8*). These cell types have distinct functions; epithelial cells act as barriers, whereas stromal or mesenchymal cells comprise connective tissue adjacent to epithelia and are loosely organized in a three-dimensional extracellular matrix. EMT involves major phenotypic changes such as loss of cell-cell adhesion, loss of cell polarity, and acquisition of invasive and migratory capacities (Chen, You, et al. 2017).

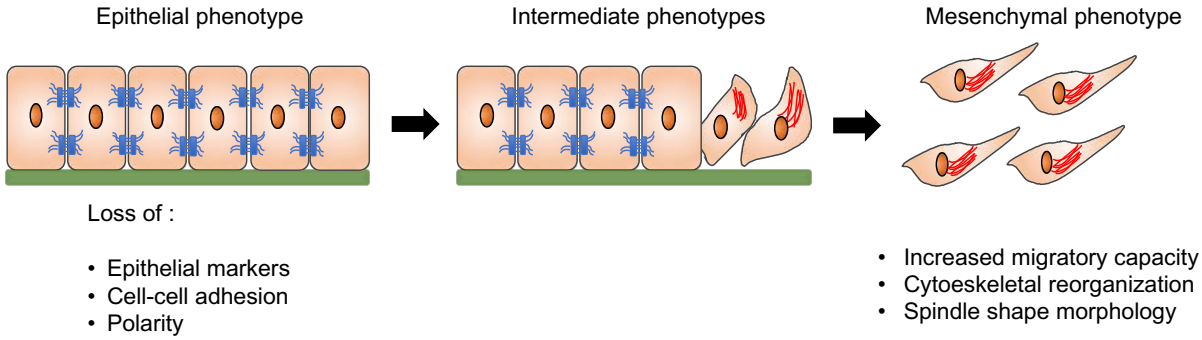

Figure 8. Epithelial-mesenchymal transition. EMT occurs gradually through loss of the epithelial phenotype, characterized by a change in cell polarity and detachment from adjacent cells and the ECM. Cells undergoing EMT exhibit cytoskeletal reorganization with increased migratory capacity and a spindle-shape-like morphology (Adapted from Kalluri and Weinberg 2009).

Histological evidence in the field of embryology in which researchers observed that mesenchymal cells originated from the adjacent epiblast provided the first clues on the existence of EMT. Experimentally, EMT was established by the observation that embryonic and adult epithelial cells embedded in three-dimensional collagen gels transitioned to migratory fibroblast-like cells (Kalluri and Weinberg 2009). In addition to its role in gastrulation of both invertebrates and vertebrates, EMT is critical for the development of the neural crest, organ formation and as a physiological response to injury. Furthermore, EMT has been described in pathologies such as cancer and fibrosis (Terry et al. 2017; Thiery et al. 2009).

Detection of EMT in tumor samples has been challenging and fueled the debate to whether this process happens *in vivo*, although observation of small aggregates of tumor cells extending or detaching from the tumor mass into adjacent stroma has been part of the physiological evidence from the invasive tumor front. It has been proposed that tumors develop an EMT gradient where most of the events occur at the tumor invasive front, which has the hallmark of a mesenchymal phenotype with a poor adhesion system, whereas the main tumor bulk remains epithelial (Thiery et al. 2009; Nieto et al. 2016).

In a particular study from 2014 by Tan and collaborators, a quantitative scoring system based on gene expression profiles was developed and subsequently EMT states from different cancer types were ranked. Interestingly, it was observed that cancers that arise from the mesoderm showed higher EMT scores both *in vivo* and in cell cultured lines. Moreover, EMT ranking consistently predicted overall survival and disease-free survival, leading to the conclusion that although EMT might be a local rather than global event it is still relevant for cancer progression (Tan et al. 2014). The signals that initiate an EMT event in the tumor originate from the interaction between cancer cells and the TME by auto and/or paracrine secretion of mediators such as cytokines, growth factors, and ECM proteins. Experimental data from breast cancer cells stimulated with conditioned media from cancer associated fibroblasts showed induction of EMT and in a similar fashion oral squamous cancer cells via secretion of TGF-β were able to directly induce a myofibroblastic phenotype. EMT not only provides cells with a migratory phenotype but also with stem cells characteristics that can contribute to tumor development and resistance to chemotherapy (Nieto et al. 2016; Iwatsuki et al. 2010).

Irrespective of during metastasis or organ formation EMT occurs in a series of steps; beginning with the disintegration of cell-cell adhesion through loss of the epithelial marker E-cadherin, followed by a loss of baso-apical polarization and gain of front-rear polarization. Subsequently, upregulation of Vimentin supports cytoskeleton remodeling with changes in cortical actin and actin stress fibers and last, adhesion to cell matrix is altered through activation of proteolytic enzymes, such as matrix metalloproteinases (Chen, You, et al. 2017).

Downregulation of E-cadherin is a fundamental event in EMT. This calcium-dependent transmembrane glycoprotein is expressed by most epithelial cells and is responsible for the tight junctions connecting adjacent cells (Nieto et al. 2016). EMT-associated transcription factors (ATF) can repress E-cadherin expression by binding and regulating the activity of its promotor, such is the case for Snail, KLF8 and the ZEB family of transcription factors. Others, such as Twist and FoxC2 can indirectly repress E-cadherin transcription. EMT ATFs not only regulate E-cadherin expression but can also initiate the complete EMT program inhibiting and activating several epithelial and mesenchymal genes. Both ZEB and Snail have been associated with activating invasion and metastasis, resisting cell death and enabling replicative immortality, whereas Twist has been linked with induction of angiogenesis, evasion of growth suppressors, and the sustainment of proliferative signaling. Taking together the role of the EMT ATFs, their function has evolved from simple E-cadherin repressors to inducers of most of the traits necessary for tumor development and metastasis (Sanchez-Tillo et al. 2012).

Additional biomarkers are used to identify EMT, such as cell surface proteins: N-cadherin and Syndecan. Upregulation of N-cadherin has been linked with metastasis and poor prognosis in patients with prostate cancer, while *in vitro* overexpression of N-cadherin increased colony and tumor sphere formation through activation of the ErbB signaling pathway and upregulation of pERK1/2 (Wang et al. 2016; Nakajima et al. 2004).

2. Aim of the Research

Recent evidence highlights the relevance of the immune component within the tumor microenvironment to drive tumor growth and trigger the transformation of epithelial cells to a mesenchymal phenotype, thereby, enabling metastasis. Current studies on T cells in particular, have revealed conflicting data, partly explained due to the heterogeneity of T cell populations in the tumor stroma. The general objective of this dissertation is to investigate the role of Th9 and Th17 T cell subtypes in both human patients and mouse tumor models and determine their contribution to the tumor microenvironment dynamic. Our aim is as follows:

- Determine the effect of the tumor cell-lymphocyte crosstalk on EMT in human and mouse lung tumor cells
- Characterize secreted factors responsible for EMT inducing effects in tumor cells
- Identification of T cell population responsible for the secretion of EMT inducing factors
- Assess the effect of specific T cell subtypes, Th9 and Th17, *in vitro*
- Assess the effect of specific T cell subtypes, Th9 and Th17, in both primary tumor growth and metastasis
- Detection of Th9 and Th17 cell subtypes in patient samples from human lung tumor stroma and determination of the effect of these cells on overall survival
- Characterize gene groups that are upregulated in cancer cells after Co-culture with the specific T cell subtypes Th9 and Th17

Our research highlights the importance of the interaction between cancer cells and T helper cells and, moreover, how cytokines secreted by these cells can affect functional aspects such as migration and proliferation.

3. Materials and Methods

3.1 Experimental Procedures *in vitro*

3.1.1 Human and mouse lung cancer cell lines

Human adenocarcinoma (A549) and mouse Lewis lung carcinoma cells (LLC1) were purchased from American Type Culture Collection (ATCC® CCL-185™ and ATCC® CRL-1642™, USA), maintained in DMEM and RPMI-1640, respectively, and supplemented with 10% fetal calf serum (FCS) and 1% penicillin/streptomycin (100 I.U./mL and 100µg/mL, respectively, by Invitrogen, USA). When cells reached 80-90% confluency, they were sub-cultured and split in a ratio of 1:3 to 1:6 depending on the cell type and density needed. Medium was removed, cells were washed with 1x phosphate buffered saline (1xPBS, Gibco® by Life Technologies) and incubated with 1x trypsin (Thermo Fisher, Germany) for 3-5 minutes at 37°C until cells had detached. Media with FCS or FCS alone was added to the cells to block the trypsin activity, and the cell suspension was collected and centrifuged at 1800 rpm for 5 minutes. The cell pellet was later resuspended in fresh media and cells were plated at the desired ratio.

When cells needed to be frozen, they were trypsinized and the cell pellet was resuspended in freezing medium containing 10% dimethylsulfoxide (DMSO, Sigma Aldrich, USA) and 20% FCS. Cells were frozen in cryovials and stored in liquid nitrogen tank until further use.

3.1.2 Primary human cancer cells

Cancer cells isolated from human tumors were provided by the University of Giessen's Biobank. Cells were grown in DMEM F12 (supplemented with sodium selenite, ethanolamine, phosphorylethanolamine, sodium pyruvate, adenine and HEPES) and kept for a maximum of nine passages. Stimulation and other functional assays were performed as mentioned in Sections 3.1.1 and 3.1.7.

3.1.3 Immunocytochemistry

Cancer cells were seeded in eight-well chamber slides (BD BioSciences, Germany) at a density of $1x10^4$ cells/mL. After stimulation, supernatant was removed, and cells were washed with 1xPBS for 5 minutes. Later, cells were fixed with a cold acetone/methanol mixture (1:1) at -20°C for 30 minutes. After fixation, cells were washed three times with 1x PBS and blocked with 5% BSA/0.1% triton X-100 for 1 hour at room temperature. Primary antibodies E-

cadherin and Vimentin (*Table 2*) were diluted in the blocking solution and added to the cells and incubation took place overnight at 4°C. After incubation, cells were washed four times with 1xPBS and incubated with the fluorescent conjugated secondary antibodies for 1 hour at RT in the dark. Cells were washed four times with 1x PBS and nuclei were counterstained with 4', 6-diamidino-2-phenylindole (DAPI, Life Technologies, USA) diluted 1:100 for 5 minutes. After a final wash with 1xPBS, slides were mounted with Dako fluorescent mounting medium (Dako North America, Inc., USA) and examined under a Leica fluorescent microscope.

Epitope	Species	Catalog No.	Dilution	Manufacturer
α-E-cadherin	Rabbit	3195	1:100	Cell Signaling, USA
α-Vimentin	Rabbit	5741	1:300	Cell Signaling, USA
α-PCNA	Mouse	sc-7907	1:500	Santa cruz, USA
α-vWf	Rabbit	A0082	1:500	DAKO, USA
α-AlexaFluor®488	Goat	A11008	1:1000	Invitrogen, USA
α-AlexaFluor®555	Goat	A27039	1:1000	Invitrogen, USA

Table 2. Antibodies used for Immunofluorescence and Immunocytochemistry

3.1.4 Migration Assays

For the quantification of chemotactic migration, a Boyden chamber transwell assay (8 μm pore size; uncoated filters; BD Biosciences, USA) was used. Either control medium or lymphocyte Co-culture conditioned media (CM) (-/+ PMA; phorbol 12-myristate 13-acetate) or cytokines (IL-9, IL-17 A and F) were provided in the lower chamber and lung tumor cells (A549, LLC1 and primary lung tumor cells) were introduced to the upper chamber at a density of 4×10^4/well in 300 μL serum free medium. Cells were allowed to migrate for 6, 12 and 24 hours depending on cell type. After incubation, filters were washed with 1×PBS and dried from the inner side with a cotton swab to remove dead cells and cells that did not migrate. Filters were submerged in methanol (Roth, Germany) for 3 minutes to fixate, and stained for 10 minutes with a crystal violet solution (Sigma-Aldrich, USA) diluted 1:10 with ddH_2O. After a final wash in ethanol, filters were dried, cut from the inserts, and mounted on slides with Pertex (Medite GmbH, Germany). Slides were scanned with a Nanozoomer 2.0HT digital slide scanner C9600 (Hamamatsu Photonics, Japan) and the migrated cells per membrane were assessed and quantified with the ITCN Runner software plugin to Image J.

3.1.5 Proliferation Assays

Proliferation assays were performed with serum starved cancer cells exposed for 24 or 48 hours to Co-culture CM or cytokines (IL-9, IL-17 A and F). After incubation for 20 hours, bromodeoxyuridine (BrdU) was added and its incorporation was detected using an HRP-coupled antibody by measuring the absorption of the HRP-substrate at 370 nm, according to the manufacturer's instructions (Cell Proliferation ELISA, BrdU colorimetric, Roche, Germany). Detection was performed with the Tecan Infinite M200 Pro and results are reported as an average of six wells.

3.1.6 RNA isolation, cDNA synthesis, real-time PCR

After stimulation of mouse and human cells, RNA was isolated using Trizol® reagent (Invitrogen, USA) according to the manufacturer's instructions. RNA isolation with Trizol® is based on the method developed by Chomczynski and Sacchi for cell lysis and inactivation of RNAses and phenol to dissolve DNA and protein. The addition of chloroform results in phase separation and is followed by centrifugation at 12,000 rpm for 30 minutes at 4ºC. Total RNA was precipitated with isopropanol from the resulting aqueous phase. This mixture was then centrifuged at 12,000 rpm for 10 minutes at 4ºC and the supernatant removed. The pellet was washed twice with 75% ethanol and left to dry. The resulting RNA was resuspended in diethyl pyrocarbonate-treated water. The concentration and purity of the RNA was measured with NanoDrop (Peqlab Biotechnologies GmbH, Germany) and RNA integrity was monitored with 1% agarose gels. Afterwards, RNA was stored at -80ºC until further use.

For cDNA synthesis, only 1000 ng of RNA per sample were used and DNase treatment (Fermentas, Germany) was done to ensure removal of any possible DNA contamination. Using a master mix as described in Table 3, samples were incubated for 30 minutes at 37ºC. Subsequently 1 μL of EDTA was added to each sample to stop the reaction and again incubated for 10 minutes at 65ºC.

	Volume (μL)	Conditions
DNase	1	30 min, 37ºC
DNase buffer	1	
RNAse Inhibitor	0.33	
EDTA	1	10 min, 65ºC

Table 3. DNase treatment summary

RNA was reverse transcribed using the High Capacity cDNA Reverse Transcription kits from Applied Biosystems (Promega, USA) according to the supplier's instructions. First, 10 μL from the master mix (*Table 4*) was pipetted into small tubes to be later completed with 10 μL of sample containing 1 μg of RNA. Subsequently samples were centrifuged and loaded to the thermal cycler. The synthesized cDNA was diluted 1:3 with nuclease-free H_2O before use for qPCR.

Component	Volume(μL)
10x RT buffer	2.0
25x dNTP mix	0.8
10X RT random primers	2.0
MultiScribe™ Reverse Transcriptase	1.0
RNase inhibitor	1.0
Nuclease-free H_2O	3.2
Total reaction volume	10

Table 4. Master mix for cDNA synthesis

All real-time qPCR reactions (*Table 5*) were performed on the Stratagene Mx3005P with the MxPro software and the program "SYBR Green with Dissociation curve" to confirm the specificity of each primer. PCR products were separated on a 3% agarose gel to confirm that every primer yielded one specific product. All primer pairs were blasted with the NCBI primer blast tool (http://www.ncbi.nlm.nih.gov/tools/primer-blast/) and purchased from Metabion (Metabion GmbH, Germany).

Component	Volume(μl)
iQTM SYBR® Green Supermix (2x)	10
Forward primer (10mM)	0.5
Reverse primer (10mM)	0.5
Nuclease-free H_2O	7
cDNA template	2
Total reaction volume	20

Table 5. Reaction mixture for qPCR

Real time PCR was performed with the Platinum® SYBR®Green qPCR SuperMix-UDG (Invitrogen, Life Technologies, USA). Master mixture and cDNA template were pipetted into non-skirted 96-well plates and the reaction was done using the conditions described in Table 6.

Temperature	Time	No. of cycles
95ºC	3 min	1
95ºC	30 sec	40
58 or 60ºC	1 min	
72ºC	30 sec	
95ºC	1 min	1
55ºC	30 sec	1
95ºC	30 sec	1

Table 6. qPCR reaction conditions

PCR data analysis was performed using the MxPro software and GraphPad Prism and mRNA levels are expressed as ΔCt values (Ct value of the housekeeping gene - Ct value of gene of interest). Normalization was done to the expression of HPRT (hypoxanthine phosphoribosyltransferase1) as housekeeping gene. All primers sequences and annealing temperatures are detailed in Table 7.

	Sequence	Annealing temperature (°C)
E-cadherin	FP: 5‘-CCCACCACGTACAAGGGTC-3‘ RP: 5‘-ATGCCATCGTTGTTCACTGGA-3‘	60
Vimentin	FP: 5‘-GGAAATGGCTCGTCACCTTCGT-3‘ RP: 5‘-GCAGAGAAATCCTGCTCTCCTCG-3‘	58
N-cadherin	FP: 5'-TCAGGCGTCTGTAGAGGCTT-3' RP: 5'-ATGCACATCCTTCGATAAGACTG-3'	58
ZO1	FP: 5’-ACGGTCCTCTGAGCCTGTAA-3’ RP: 5’-CTGCTTTCTGTTGAGAGGCTGG-3’	60
ZO2	FP: 5’-GCCCCAGGCATGGAAGAGCTG-3’ RP: 5’- CCCACCCGGGAGCACATCAGA	60
ZEB1	FP: 5’-AGGATGACCTGCCAACAGACCA-3’ RP: 5’-TCCTTTCTGTCATCCTCCCAGCA-3’	60
ZEB2	FP: 5’-AGCCTCTGTAGATGGTCCAGAAGAA-3’ RP: 5’-CACTGTACCATTGTTAATTGCGGTC-3’	60
Smad1	FP: 5’-ACTGCCTCATGTCATTTACTGC-3’ RP:5’-CTATTGGGAGAGTGAGGAAACG-3’	60
Smad3	FP: 5’-CATCGAGCCCCAGAGCAATA-3’ RP: 5’-GTGGTTCATCTGGTGGTCACT-3’	60
Cytokeratin18	FP: 5’-AACAACACCTGCTGTCCGTGT-3’ RP: 5’-TGAAGCTCATGCCCCCAGAAAC-3’	58

Table 7. Primer sequence list

3.1.7 Human and mouse cell stimulations

LLC1 and A549 cells were treated either with cytokines (IL-9, IL-17 A and F) in the following concentrations: 1 and 10 ng/mL (all from R&D Systems, USA diluted as indicated by the manufacturer in PBS with 0.1% bovine serum albumin) or with CM for a period of 24 hours for RNA isolation or 48 hours for protein isolation. After stimulation cells were lysed in RIPA buffer (Thermo Scientific™, Germany) supplemented with protease inhibitor (Santa Cruz, Germany) and phosphatase inhibitors (PMSF at a final concentration of 1mM and sodium orthovanadate at a final concentration of 0.2 mM).

3.1.8 Flow cytometry

Flow cytometry is a laser-based technology widely used to measure the expression of intracellular and surface molecules on cells. It is useful for the definition and characterization of cell types within a heterogeneous cell suspension. This technique allows for the analysis of multiple parameters as well as sorting of cells by separating them in a fluidic system through electronic detection of fluorescent dyes. Flow cytometry allows for the measurement of fluorescence dye-labelled epitopes, granularity, cell size and viability.

All FACS analysis in this study were carried out in *FACSLSRII* and *FACSAriaIII* equipment (BD Biosciences, Germany). First, cells were washed and resuspended in PBS/1%FCS and stained for 15 minutes at 4ºC with the respective antibodies. Labelling of dead cells was performed with LIVE/DEAD Fixable near-IR dead cell stain kit (Thermo Fisher Scientific, USA). After the initial staining, cells were washed again with PBS/1%FCS and treated for either surface or intracellular staining. Surface staining for the co-receptor CD4 was done with a CD4 monoclonal antibody (*Table 8*) and intracellular staining was performed for the detection of cytokines after T cell differentiation.

Intracellular staining requires an additional re-stimulation to prevent cells from releasing cytokines and rather are kept stored in intracellular vesicles. PMA was used to trigger TCR signaling while Brefeldin A was also used to inhibit protein transport from the endoplasmic reticulum to the Golgi apparatus. To access intracellular epitopes, it is necessary to fixate cells with formaldehyde and permeabilize them.

After washing with BSS (balanced salt solution*, See Appendix Table 15*), the cell suspension was incubated with PMA (50 ng/mL), ionomycin (750 ng/mL) and Brefeldin A (10 μg/mL) for 4 hours at 37ºC in RPMI complete media. Afterwards, cells were washed with PBS and fixed with 0.5 mL formaldehyde (2%) for 20 minutes at room temperature. Later, cells were washed in PBS/1%FCS or PBS/1%AB serum and saponin buffer and incubated with the respective antibody dilutions. After a final wash with saponin buffer, cells were resuspended and analyzed.

Epitope	Conjugate	Catalog No.	Dilution	Manufacturer
α-CD4	V450	560470	1:500	BD, USA
α-CD44	PE	12-0441-82	1:500	Affymetrix, USA
α-CD62L	AF700	12-0621-82	1:500	BD, USA
α-IFN-γ	PE	12-7311-41	1:500	Affymetrix, USA
α-IL-9	APC	514105	1:500	BioLegend, USA
α-IL-17	FITC	130-103-007	1:500	Miltenyi Biotec, Germany

Table 8. Antibodies used for FACS sorting and analysis

3.1.9 Cell sorting

Primary murine $CD4^+CD62L^+CD44^-$ T cells were sorted after isolation from spleen to obtain naïve Th cells for differentiation. Murine T cells were stained for 15 minutes at 4ºC with the respective antibodies, washed, and resuspended in PBS/1%FCS. Labelling of dead cells was done (*see Section 3.1.8 Flow cytometry*) with LIVE/DEAD Fixable Near-IR Dead Cell Stain Kit (Thermo Fisher Scientific, USA) for 15 minutes at 4ºC. Sorting was later performed under sterile conditions on a FACSAriaIII (BD Biosciences, Germany) and post sorting analysis confirmed a purity of ≥97%. Sorting also took place after Co-culture of specific Th9 and Th17 subtypes with cancer cells, where cells were detached after 24 hours and stained for the co-receptor CD4 in order to remove all T cells and analyze gene expression of the remaining cancer cells through RNA sequencing.

3.1.10 Leukocyte isolation from PBMCs

Lymphocytes used in Co-culture with cancer cells were isolated from whole blood of healthy donors obtained through Giessen's Blood bank. Density gradient centrifugation using ficoll was applied to obtain an enriched PBMC (peripheral mononuclear cell fraction). Ficoll (Biocoll L6115, Biochrom Germany) is a hydrophilic polysaccharide that has been established by extensive studies from Boyum and collaborators to allow for density-dependent separation of mononuclear and non-nucleated cells. First, anticoagulant-treated blood was diluted with an equal volume of BSS and layered carefully over ficoll followed by centrifugation at 2000 rpm for 35 minutes without brakes. After differential migration of cells during centrifugation, layers containing different cell types are formed: a bottom layer containing erythrocytes, medium layer composed primarily of granulocytes and last an interface between plasma and the ficoll layers made up mainly of mononuclear cells. Plasma was then discarded to obtain the PBMC cell layer and FACS was performed on these cells to isolate naïve human $CD45^+$ cells. For this

purpose, cells were washed twice with PBS/1mM EDTA followed by antibody incubation in 1mL PBS/1%AB serum and sorting for $CD25^{-}CD45RA^{+}CD45RO^{-}$ cells was done.

3.1.11 Murine $CD4^{+}$ T cell preparation

CD57Bl/6 mice were obtained from Charles River Laboratory and all experiments were carried out according to the German animal protection law and the guidelines of local authorities in Giessen. After sacrificing 8-10 weeks old mice, lymph nodes and spleen were surgically removed and stored on ice in BSS medium in order to isolate $CD4^{+}$ T cells. Organs were squashed through 30 μm filters and the resulting cell suspension was washed once with BSS medium followed by treatment with NH_4Cl_2 (6mL per spleen) for 4 minutes to lyse remaining erythrocytes. Cells were later washed with MACS buffer, centrifuged at 1500 rpm for 5 minutes and counted to determine total cell number. Magnetic negative cell separation ($CD4^{+}$ T cell isolation kit, 130-104-454, Miltenyi, Germany) was done to obtain a pure $CD4^{+}$ T cell fraction, and remove labeled unwanted cells such as B cells, macrophages, NK, DC and $CD8^{+}$. Labeling of non-$CD4^{+}$ T cells was achieved through incubation for 15 minutes at 4ºC with the primary FITC-conjugated antibody cocktail detailed in Table 9 at a concentration of 2.5 μL/100x10^6 cells. Afterwards, cells were washed once with MACS buffer (Miltenyi Biotec, Germany) followed by incubation for 20 minutes at 4ºC with biotinylated microbeads (30 μL/100x10^6 cells). Separation of $CD4^{+}$ T cells is completed by placing the microbeads-incubated cell suspension on a magnet at room temperature for 15 minutes and carefully removing the supernatant. Cells were then washed and resuspended in RPMI supplemented with 20% FCS and P/S. Purity was assessed by surface staining with α-CD4 antibody and was usually ≥90%. Purified $CD4^{+}$ T cells were further sorted to obtain naïve T cells ($CD4^{+}CD62L^{+}CD44^{-}$ T cells).

Epitope	Conjugate	Catalog No.	Company
α-msCD8a	FITC	11-0081-82	Affymetrix, USA
α-msCD11b	FITC	11-0112-82	Affymetrix, USA
α-msCD11c	FITC	14-0114-82	Affymetrix, USA
α-msB220	FITC	553929	BD, USA
α-msCD49b	FITC	14-5971-85	Affymetrix, USA
α-msTer119	FITC	13-5921-82	Affymetrix, USA

Table 9. $CD4^{+}$ T cell isolation antibody cocktail

3.1.12 Generation of specific T helper subtypes

For the generation of subtypes Th9 and Th17, negatively purified $CD4^+$ T cells were further sorted on a FACS Arial II (BD Biosciences, Germany) to obtain naive $CD4^+CD62L^+CD44^-$ T cells using α-CD4-V450, α-CD44-PE and α-CD62L-Alexa Fluor 700 monoclonal antibodies (*Table 8*) in a dilution of 1:500. Sorting purity was typically >97% in post-sort analysis. All antibodies were diluted in Saponin Buffer.

TCR activation is necessary for T cell differentiation, additionally, the presence of costimulatory signals and the triggering of cytokine-induced signaling pathways further drive the generation of T cell subtypes. *In vivo*, these signals are provided by APCs and other cells, however *in vitro*, it can be achieved by the use of monoclonal antibodies against the CD3 co-receptor in the TCR, with the addition of the costimulatory molecule CD28 and stimulation with recombinant cytokines (*Table 10*).

For this purpose, murine $CD4^+$ T cells were primed with plate-bound α-CD3 mAb and α-CD28 (both mAbs produced and purified 'in house'). Skewing cytokines were used to achieve Th9 and Th17 cell differentiation and IL-2 was used to promote proliferative survival signals. Cells were stimulated for a period of 3-5 days and were thereafter harvested for intracellular staining, FACS analysis or used in co-culture with cancer cells.

		Th0	Th9	Th17
Coating	α-CD3	10 μg/mL	10 μg/mL	10 μg/mL
	α-CD28	1 μg/mL	1 μg/mL	1 μg/mL
Cytokines	rhIL-2	50 U/mL	50 U/mL	50 U/mL
	α-msIFN-γ	5 μg/mL	5 μg/mL	5 μg/mL
	IL-4	-	20 ng/mL	-
	TGF-β	-	1.5 ng/mL	1 ng/mL
	rIFN-γ	-	± 5 ng/mL	-
	rmIL-6	-	-	20ng/mL

Table 10. T cell differentiation culture conditions

3.1.13 In vitro Co-culture model

Co-culture of cancer cells and immune cells was performed in 10 cm petri dishes (Greiner Bio-one, Germany) where cells were seeded in direct contact in a 1:1 ratio. First, in the case of the human co-cultures, lymphocytes were isolated by ficoll centrifugation gradient from human PBMCs as previously described (*see Section 3.1.9*). After isolation, lymphocytes were activated with PMA (10ng/mL SIGMA, USA) for 24 hours. Subsequently, $2.5x10^6$ A549 cells were seeded with the same amount of PMA activated or non-activated lymphocytes. A549 and lymphocytes (+/- PMA) were seeded separately as controls. DMEM supplemented with 1%FCS and P/S (100U/mL-0.1mg/mL) was used for the Co-culture. After 24 hours, the supernatant (CM) was harvested, centrifuged, filtered and stored at -80°C for further experiments (*Figure 9*).

LLC1 Co-culture with specific T helper subsets was performed once the Th0, Th9 and Th17 cells had been artificially generated (*see Section 3.1.11*). LLC1 cells were seeded in a ratio of 1:1 with the specific Th subtypes in RPMI-1640 supplemented with 2%FCS and P/S (100 U/mL-0.1 mg/mL). LLC1, Th0, Th9, and Th17 cells were also seeded separately at the same confluency as controls. After 24 hours, the CM was harvested, centrifuged, filtered, and stored at -80°C for further experiments. Each Co-culture donor was performed with 3 sets of plates and control supernatant was collected.

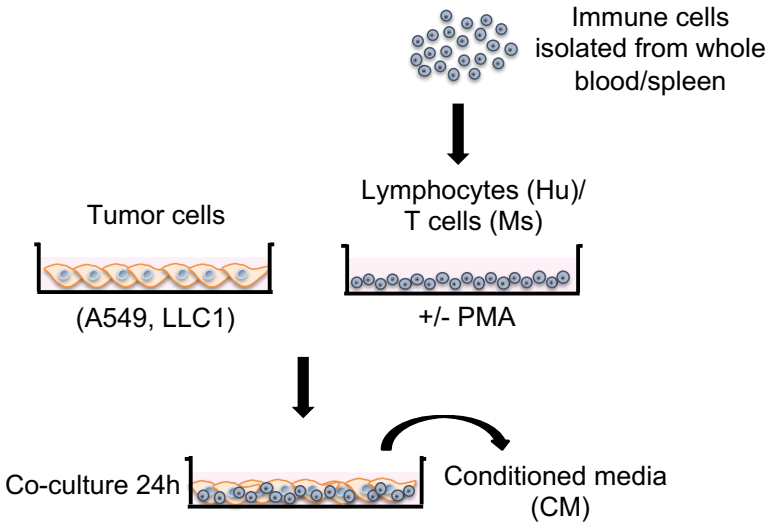

Figure 9. Scheme of cancer-immune cell Co-culture

3.1.14 Enzyme-linked immunosorbent assay

A sandwich ELISA (enzyme-linked immunosorbent assay) was used for the quantification of cytokines in the CM. This technique is based on the specific binding of antibodies to a protein of interest and a color reaction mediated by peroxidase allowing the measurement of protein concentration when compared to a standard curve of known protein values. IL-9, IL17-A and IL17-F levels were quantified in either control, lymphocyte (+/- PMA) or Co-culture-CM (+/- PMA) with the respective human ELISA kit from Biolegend following the supplier's instructions (IL-9, human IL-9 ELISA MAX™ Deluxe CN-434704; IL-17A, LEGEND MAX™ human IL-17A ELISA kit with Pre-coated Plates CN-433917 and IL-17F, LEGEND MAX™ human IL-17F ELISA kit with pre-coated plates CN-435707).

3.1.15 Cytokine array

To obtain an overall picture of the secretome of the CM, a human Cytokine array, Panel A (ARY005 R&D Systems, USA) was performed according to the manufacturer's instructions. First, nitrocellulose membranes spotted with capture antibodies against 36 different cytokines (*Figure 10*) as well as positive and negative controls were blocked. Later, the membranes were incubated with 250 µL of CM of A549, Lymphocyte (-/+ PMA) or Co-culture medium (-/+ PMA) previously mixed with a cocktail of biotinylated detection antibodies. Any cytokine-detection antibody complex present is bound by its cognate immobilized capture antibody and was detected by adding a streptavidin-HRP solution followed by incubation with Chemi Reagent Mix. The reactions were visualized with Amersham Hyperfilm ECL films (GE Healthcare Europe GmbH, Germany). Analysis and quantification were performed with the BioDoc Analyze software from Biometra.

	1	2	3	4	5	6	7	8	9	10	11	12	13	14	15	16	17	18	19	20
A	Ref Spot	Ref Spot	C5/C 5A	C5/C 5A	CD40 ligand	CD40 ligand	G-CSF	G-CSF	GM-CSF	GM-CSF	GR0α	GR0α	I-309	I-309	sICA M-1	sICA M-1	IFN-γ	IFN-γ	Ref Spot	Ref Spot
B			IL-1α	IL-1α	IL-1β	IL-1β	IL-1ra	IL-1ra	IL-2	IL-2	IL-4	IL-4	IL-5	IL-5	IL-6	IL-6	IL-8	IL-8		
C			IL-10	IL-10	IL-12 P70	IL-12 P70	IL-13	IL-13	IL-16	IL-16	IL-17	IL-17	IL-17E	IL-17E	IL-23	IL-23	IL-27	IL-27		
D			IL-32α	IL-32α	IP-10	IP-10	I-TAC	I-TAC	MCP-1	MCP-1	MIF-1	MIF-1	MIP-1α	MIP-1α	MIP-1β	MIP-1β	Serpin E1	Serpin E1		
E	Ref Spot	Ref Spot	Rantes	Rantes	SDF-1	SDF-1	TNF-α	TNF-α	sTREM-1	sTREM-1									Neg Cont	Neg Cont

Figure 10. Cytokine array template coordinates

3.1.16 RNA sequencing

RNA sequencing was performed in collaboration with Dr. Stephan Guenther (MPI, Bad Nauheim). After 24 hours Co-culture of LLC1 cells with Th specific subtypes, cells were detached and stained for the co-receptor CD4. Afterwards, FACS sorting was performed to remove all T cells from the cell suspension, leaving behind live LLC1 cells. Remaining cells were washed with PBS and RNA was isolated using the miRNeasy micro kit (CN-217084 Qiagen, Germany) combined with on-column DNase digestion (DNase-Free DNase set, Qiagen, Germany) to avoid contamination by genomic DNA. RNA and library preparation integrity were verified with a BioAnalyzer 2100 (Agilent, USA) or LabChip Gx Touch 24 (Perkin Elmer, USA). 1 μg of total RNA was used as input for the SMARTer stranded total RNA sample prep kit from HI Mammalian (Clontech USA). Sequencing was performed on the NextSeq500 instrument (Illumina, USA) using v2 chemistry, resulting in an average of 30M reads per library with a 1x75bp single end setup. The resulting raw reads were assessed for quality, adapter content and duplication rates with FastQC (Andrews S. 2010, FastQC: a quality control tool for high throughput sequence data. Available online at: http://www.bioinformatics.babraham.ac.uk/projects/fastqc).

Reaper version 13-100 was employed to trim reads after a quality drop below a mean of Q20 in a window of 10 nucleotides (Davis et al. 2013). Only reads between 30 and 150 nucleotides were cleared for further analyses. Trimmed and filtered reads were aligned versus the Ensembl mouse genome version mm10 (GRCm38) using STAR 2.4.0a with the parameter "--outFilterMismatchNoverLmax 0.1" to increase the maximum ratio of mismatches to mapped length to 10% (Dobin et al. 2013).

The number of reads aligning to genes was counted with featureCounts 1.4.5-p1 tool from the Subread package (Liao, Smyth, and Shi 2014). Only reads mapping at least partially inside exons were admitted and aggregated per gene. Reads overlapping multiple genes or aligning to multiple regions were excluded. Differentially expressed genes were identified using DESeq2 version 1.62 (Love, Huber, and Anders 2014). Only genes with a minimum fold change of +- 1.5 (log2 +-0.59), a maximum Benjamini-Hochberg corrected p-value of 0.05, and a minimum combined mean of 5 reads were deemed to be significantly differentially expressed. The Ensemble annotation was enriched with UniProt data (release 06.06.2014) based on Ensembl gene identifiers (Activities at the Universal Protein Resource (UniProt)).

3.2. Experimental Procedures *in vivo*

3.2.1 Opal staining

Opal Multiplex staining was done on human tissue microarrays (TMA). Samples consisted of resected lung tumors from 66 patients with different stages and types of lung cancer (*Table 11*). TMAs were constructed from paraffin blocks of selected lung specimens. Six 1.0 mm cores from representative areas of the tumor were taken for each patient. All clinical information was obtained from UKM (Universitaetsklinikum Muenchen).

Patient Sample	66
Median age at operation (range), years	65 (38-83)
Median tumor size (range), CM	3 (0.7-13)
Median overall survival (range), months	49 (1-141)
Reached cancer survival end point	57

Gender	
Male	40
Female	26

Subtype	
Adenocarcinoma	32
Squamous cell carcinoma	26
Large cell carcinoma	6
Unidentified	2

Table 11. Patient Information

Opal staining allows for simultaneous detection of multiple biomarkers (maximum eight) on the same tissue. For this purpose, the Opal™ 7-Color Fluorescent IHC Kit (CN-NEL801001KT, Perkin Elmer, USA) was used according to the manufacturer's instructions.

First, TMA blocks were cut to 5 μm sections and later dewaxed with xylene (3 x 10 minutes) and rehydrated through a graded series of ethanol solutions (100% 1 x 10 minutes; 95% 1 x 10 minutes; and rinsed in 70%). After rehydration, slides were washed in distilled water and tissues were fixed in 10% neutral buffered formalin for 20 minutes followed by another wash in distilled water and antigen retrieval in heated AR6 buffer (pH 6.0) for 15 minutes (EZ Retriever microwave, BioGenex, USA). Slides were left to cool and later rinsed in distilled water and TBST and subsequently blocked with 10%FCS in 0.5% Triton/PBS. Each section was put through seven sequential rounds of staining, each including blocking followed by primary antibody incubation (*Table 12*).

Epitope	Concentration	Catalog No.	Company	Opal fluorophore
α-Cytokeratin	1:500	MA1-26237	DAKO, USA	520
α-PU.1	1:200	ab76543	Abcam, USA	540
α-IL-9	1:200	ab181397	Abcam, USA	570
α-STAT3	1:200	12640S	Cell Signaling, USA	690
α-IL-17	1:200	ab79056	Abcam, USA	650
α-CD4	1:100	ab133616	Abcam, USA	620

Table 12. Primary antibodies used for Opal staining

Generation of signal was then performed by adding opal fluorophore working solution and incubating for 10 minutes followed by microwave treatment to remove primary and secondary antibodies. Subsequently, the slides were prepared for the next antibody introduction after rinsing in distilled water and TBST for 2 minutes each (*Figure 11*). The Vectra® 3 automated quantitative pathology imaging system (Perkin-Elmer, USA) was used for image acquisition and inForm® Cell Analysis™ software was used to score the relative abundance of cells expressing a certain marker protein in the epidermis upon tissue segmentation (Carstens et al. 2017; Mezheyeuski et al. 2018).

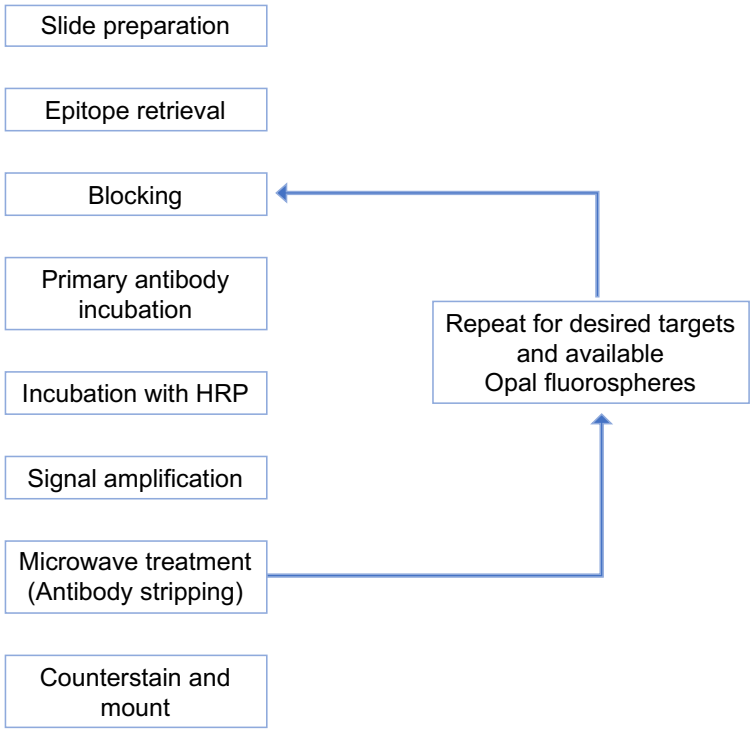

Figure 11. Opal Multiplex staining protocol

3.2.2 Syngeneic subcutaneous model of lung cancer

Primary tumor growth of LLC1 cells was monitored as described (Savai et al. 2007). Local authorities (Regierungspräsidium Darmstadt, Hessen, Germany) approved all animal studies with the application number: V54-19c20/15-B2/1062. All animals used were obtained from The Jackson Laboratory that carries the C57Bl/6 Background and kept under specific-pathogen-free (SPF) conditions and handled in accordance with the European Union Commission on Laboratory animals. First, $1x10^6$ LLC1 cells were subcutaneously co-injected (24 g needle, 0.55x25 mm, Neolus, Terumo Europe, Belgium) with the same amount of either Th0, Th9, or Th17 cells into C57BL/6 WT mice. Tumor growth was measured every 4 days with digital calipers. On day 21, mice were sacrificed, and tumor, lung, liver and spleen were balanced and analyzed for FACS, immunohistochemistry or molecular biology techniques. When necessary RNA was also isolated from tissues by first weighing 50-100 mg that were later homogenized in 1mL Trizol® (Qiagen, Germany) twice at 6500 rpm for 25 seconds using Precellys® Ceramic kit 1.4 (Peqlab Biotechnologies, Germany) and Precellys homogenizer. In the case that protein isolation was needed the same protocol was followed with the exception of RIPA buffer being used instead of Trizol®.

3.2.3 Syngeneic metastatic model of lung cancer

LLC1 cells were co-injected with either Th0, Th9 or Th17 cells at a concentration of $1x10^6$/100 μL in saline solution. C57BL6 control mice were injected with 100 μL saline solution whereas experimental mice with 100 μL of cell suspension into the tail vein of each mouse. The development of tumors was monitored for 21 days post-injection. Lung tissue was harvested from each mouse separately for nodule count and FACS analysis. Tumor volume was calculated as previously described (Salmon et al. 2012). Animals treated with antibodies against IL-9 or IL-17 were injected with LLC1 cells and treatment (IL-9 antibody conc. 30 μg/mice Biolegend, USA and IL-17 antibody conc. 200 μg/mice R&D, USA) was administered 4 days after cancer cell injection and followed by continuous intraperitoneal injections on every fourth day. Lungs were harvested on day 21 post-injection for histological analysis and FACS.

3.2.4 Tumor digestion for FACS analysis

After sacrificing mice on day 21, subcutaneous tumors were prepared for flow cytometry analysis of infiltrating immune cells. Extracted tumors were placed in 35×10 mm petri dishes (Greiner Bio-one, Germany) and cut with a scalpel into small cubes (< 1 mm^3). Later, small pieces were passed through 30 μm filters and 2mL of a digestion solution of 0.2 mg/mL collagenase-D (Roche Diagnostics, Mannheim, Germany), 1 mg/mL Pronase (Roche Diagnostics, Mannheim, Germany), and 2 μL DNAseI (400 U/ml, Promega, Madison, USA) was added to the cell suspension and samples were incubated for 40 minutes at 37°C on a shaker.

The digested tissue was resuspended in 10 mL PBS with 10% FCS to stop the digestion reaction and centrifuged for 5 minutes at 1600 rpm. The pellet was washed with PBS and cells were counted. The cell suspension was then centrifuged, resuspended in 1 mL ice-cold 1% PFA per $1x10^6$ cells, and fixed for 15 minutes on ice. After centrifugation, cells were prepared in Saponin buffer for intracellular staining and flow cytometry (*see Section 3.1.7*).

3.2.5 Histology

After mice were sacrificed, tissues were kept in paraformaldehyde (4%) for 24 hours, afterwards they underwent sequential rounds of dehydrating and finally embedded in paraffin and used for detection of protein markers with the use of immunofluorescence staining or for the calculation of metastatic area and tumor volume which was performed with hematoxylin and eosin stained sections. For the hematoxylin and eosin staining, paraffin-embedded tissues were cut with a microtome into 3 μm sections. Firstly, tissues were rehydrated with a continuous xylol-ethanol (99% ethanol, 90% ethanol, 70% ethanol) row. After washing in distilled water, slides were incubated in fresh hematoxylin (AppliChem, Darmstadt, Germany) for 15 minutes and washed again in distilled water to remove any excess from the tissue. Next, the slides were incubated with freshly prepared eosin (AppliChem, Darmstadt, Germany) for 1 minute. Slides were later washed in distilled water again, dehydrated with ascending ethanol concentrations (70, 90, 99%), and finally mounted with Pertex Mounting Media (Leica Biosystems, Wetzlar, Germany). Pictures of whole H&E stained sections were acquired with Nanozoomer 2.0HT digital slide scanner C9600. Percentage of metastatic area in mice lungs was measured with ImageJ and outlined as the percentage of lung area occupied by metastatic nodules. Tumor volume was also quantitated with the use of ImageJ from H&E stained lung sections and calculations were done as previously described (Salmon et al. 2012)

For the immunofluorescence staining, 3 μm sections were rehydrated, and antigen retrieval was achieved with citrate buffer/heat, trypsin- or proteinase-K treatment. After blocking (5% BSA, 0.2% Triton-X, 0.5 % serum according to secondary AB), sections were incubated with the following primary antibodies: CD31 1:100 from Cell signaling, vonWillebrand factor 1:400 from DAKO and Vimentin 1:200 from Cell Signaling (*see Appendix, Table 13*). Indirect immunofluorescence was conducted by incubation with conjugated secondary antibodies (*Table 2*). Nuclei were counterstained with DAPI, and sections were mounted with fluorescent mounting media (Dako, USA). All fluorescence images were acquired with the same exposure time in 40× and 20× magnification with a Leica DM6000B microscope equipped with the Image Analysis & Processing Software for Quantitative Microscopy Leica QWin (Leica Microsystems GmbH, Wetzlar, Germany).

3.3 Statistical Analysis

Statistical analyses were performed with the GraphPad Prism 7 software following the manufacturer's guidelines. A one-way analysis of variance (ANOVA) followed by Student-Newman-Keuls multiple comparison test was used to compare the means of more than two independent groups. For other analysis, we used two-way ANOVA. Two independent groups were compared with Student's t test. Data are expressed as means ± SD.

4. Results

4.1 Lymphocyte CM induces an EMT Transition in cancer cells

4.1.1 Stimulation with Lymphocyte CM alters protein and mRNA expression levels of epithelial and mesenchymal markers

To dissect the role of lymphocytes and how the crosstalk with cancer cells impacts the tumor microenvironment and cancer development, a direct Co-culture system was used, where resting and PMA-activated lymphocytes isolated from whole blood samples of healthy donors were cultured in direct contact with human lung cancer cells. $CD45^+$ cells (leukocyte common antigen) with a purity of $\geq$97% were obtained through negative selection with magnetic beads.

After incubation of the Co-culture for 24 hours the medium in which both cells were cultured was collected and used as a stimulant on A549 human adenocarcinoma cells (*Figure 12 a*).

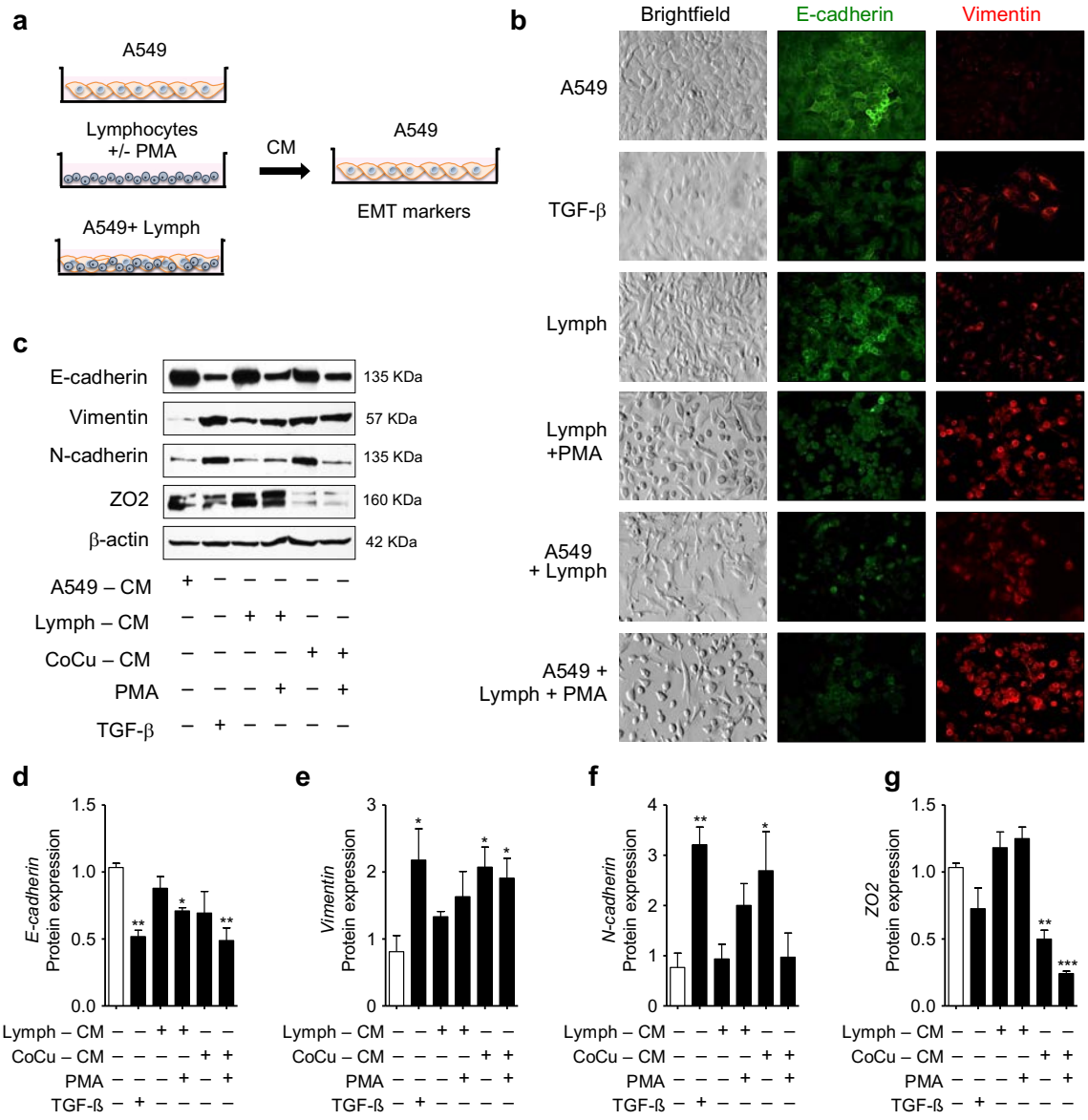

Figure 12. Stimulation of cancer cells with Lymphocyte CM induces loss of epithelial markers and upregulation of mesenchymal markers. a) Scheme of cancer-immune cell co-culture. Lymphocyte CM was used to stimulate A549 cells for 48 hours and changes in EMT markers were evaluated. **b)** Brightfield representative images of cell morphology after CM stimulation and immunocytochemistry of E-cadherin and Vimentin. **c)** Western blot for EMT markers E-cadherin, Vimentin, N-cadherin, and ZO2. β-Actin was used as a loading control. **d-g)** Quantification of western blot analysis of EMT markers. Data are represented as mean ± SEM, n=3 biological replicates, *p≤0.05, **p≤0.01, *** p≤0.001 when compared to A549 control.

A549 cells were stimulated for 48 hours with Lymphocyte CM, and protein expression of known epithelial markers; E-cadherin and ZO2 (Zonula occludens-2) and mesenchymal markers: Vimentin and N-cadherin, was analyzed by ICC and/or Western blot (*Figure 12 b and c*). After stimulation with Lymphocyte CM, human lung tumor cells displayed a spindled-like shape, exhibiting larger gaps between single cells (*Figure 12 b*). The effect of CM on both E-cadherin and Vimentin expression levels in tumor cells was further confirmed by immunostaining. After exposure to PMA activated CM, there was an apparent loss of cell-cell contact and an increase in cytoskeletal filaments in treated A549 cells. Western blot analysis

confirmed that although protein levels of epithelial markers were decreased after stimulation, mesenchymal markers displayed the opposite tendency and were upregulated after stimulation with PMA activated CM (*Figure 12 c*).

Stimulation with Co-culture CM effected the strongest changes in protein expression patterns of all EMT markers when compared with either Lymph-CM or A549 controls (*Figure 12 d, e, f and g*).

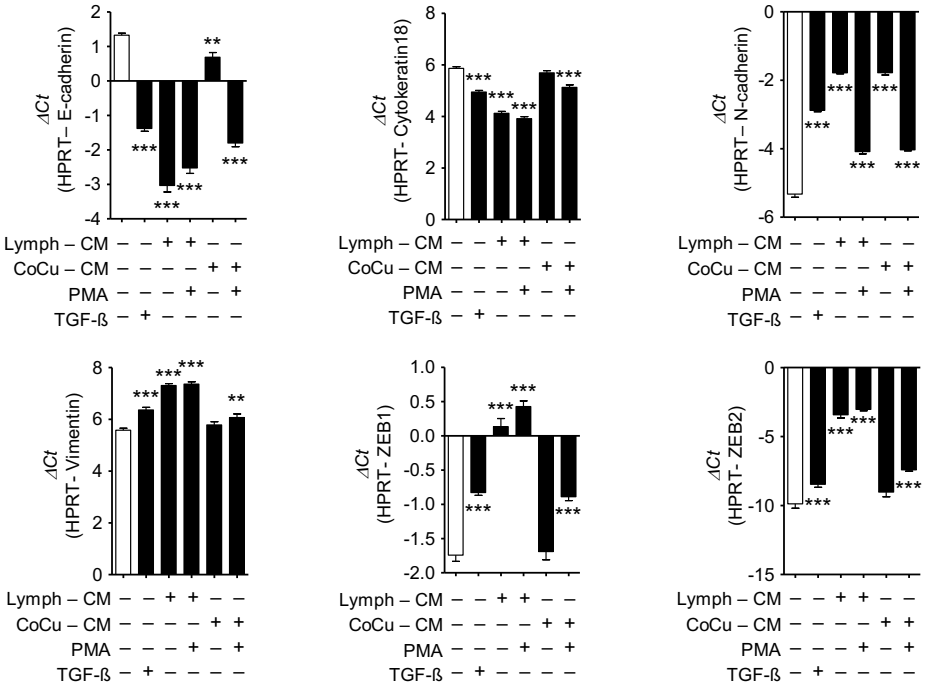

Figure 13. mRNA expression profile of EMT markers after stimulation with CM. A549 cells were stimulated for 24 hours with CM and relative mRNA expression for both EMT associated protein markers and transcription factors was determined. TGF-β was used as a positive control for the transition toward a mesenchymal phenotype. Data represented is the ΔCt of the gene of interest normalized to HPRT as a housekeeping gene. Data are represented as mean ± SEM, n=3 biological replicates, *p≤0.05, **p≤0.01, *** p≤0.001 when compared to A549 control using one-way ANOVA Dunnett's test.

Additionally, mRNA was isolated from A549 cells stimulated for 24 hours with Lymphocyte CM. Real-time PCR analysis showed a noticeable decrease in mRNA expression levels of E-cadherin, Cytokeratin18 and ZO2 in tumor cells. Both the Lymphocyte and Co-culture CM have a strong inhibiting effect on E-cadherin expression, at both protein and mRNA level, although patterns of inhibition were specific to each marker (*Figure 13*).

For mesenchymal markers, Vimentin and N-cadherin, stimulation of A549 cells with CM greatly enhanced their expression. Additionally, EMT-associated transcription factors ZEB1 and ZEB2, were shown to be upregulated in tumor cells after stimulation with Lymph-CM. Taken together, we were able to detect an EMT shift in A549 cells after stimulation with Co-culture CM, confirmed by a deregulation in protein and mRNA expression of known epithelial and mesenchymal markers and EMT- associated transcription factors.

4.1.2 Effect of Lymphocyte CM on migration and proliferation of human lung cancer cells

EMT is also associated with other functional aspects of cell behavior, in particular migration. Cells undergoing EMT become highly migratory and in some cases can shift to a proliferative state. Chemotactic migration and BrdU incorporation were assessed in A549 cells stimulated for 6 to 24 hours with Lymphocyte CM (*Figure 14 a).*

Lymphocyte and Co-culture CM were able to strongly induce proliferation of cancer cells (*Figure 14 b)*. Migration was quantified through use of transwell membrane inserts, with the CM as a chemoattractant stimulus. Although Lymph and Co-culture CM induced migration of A549 cells, the effect was more robust for both the non-activated and activated versions of the Co-culture CM (*Figure 14 c and d)*.

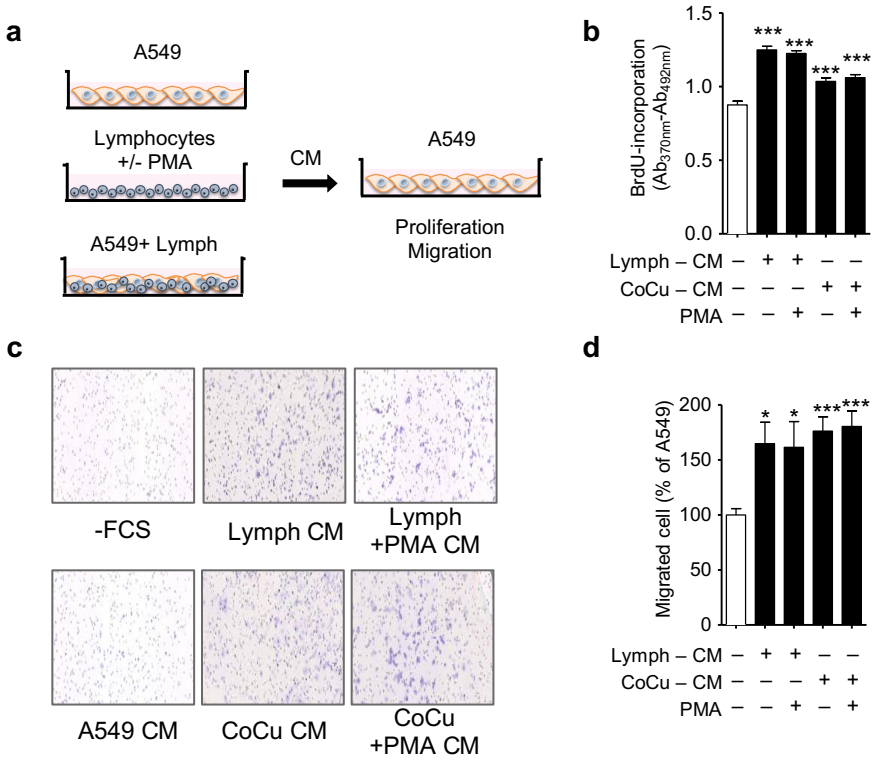

Figure 14. CM enhances the migration of cancer cells. a) Scheme of cancer-immune cell Co-culture. Lymphocyte CM was used to stimulate A549 cells for 6 hours for the quantification of migration or for 24 hours to measure proliferation through BrdU incorporation. **b)** BrdU incorporation by A549 cells after CM stimulation. **c)** Representative migration pictures. **d)** Percentage of migrated cells. Data are represented as mean ± SEM, n=3 biological replicates, *p≤0.05, **p≤0.01, *** p≤0.001 when compared to A549 control using one-way ANOVA Dunnett's test.

Adding to the changes observed in mRNA and protein levels of various EMT markers, the detected increase in proliferation and migration provides further evidence of an EMT transition triggered by secreted factors present in the CM.

4.1.3 Effect of Lymphocyte CM on EMT marker expression, proliferation and migration of primary lung cancer cells

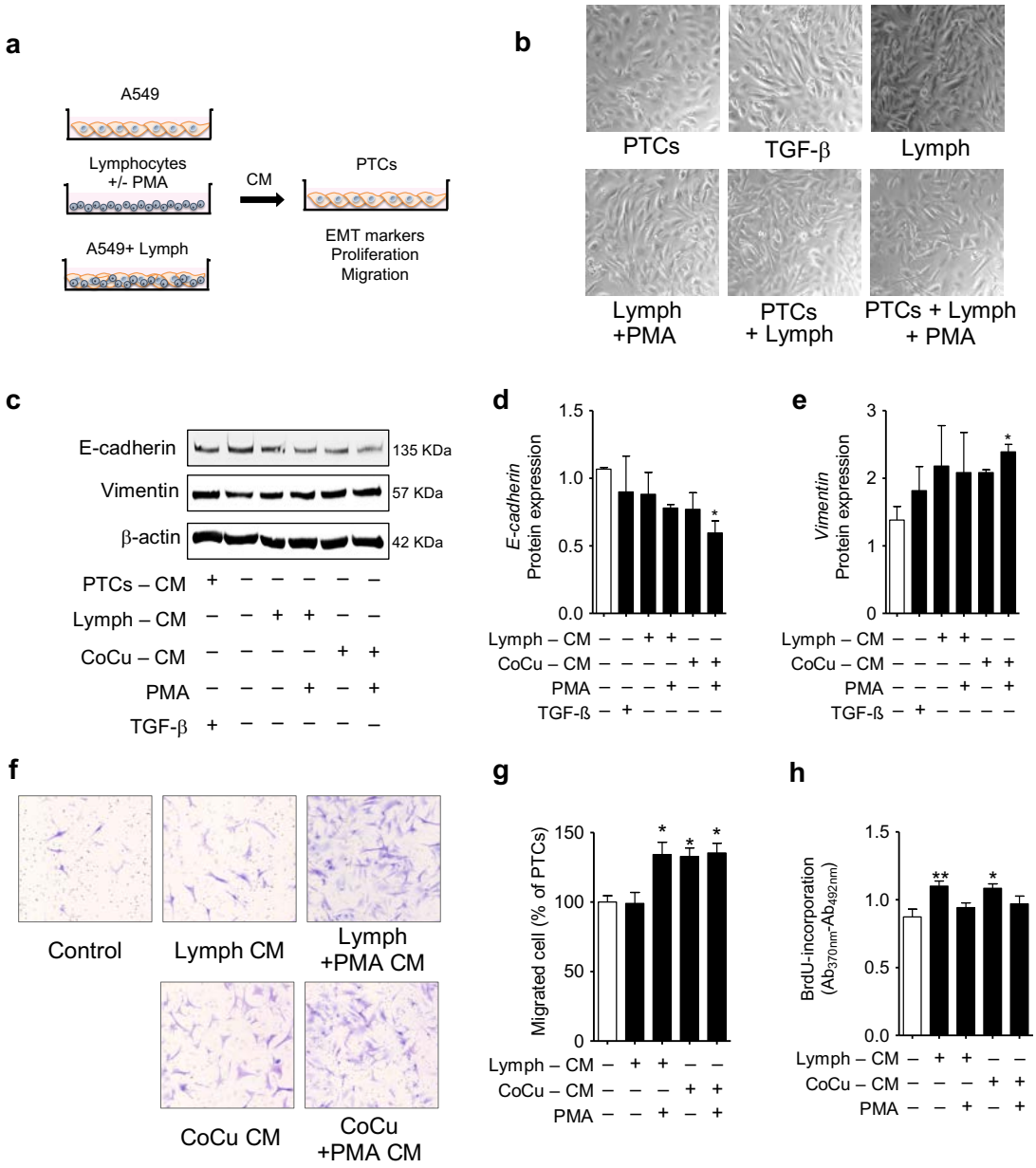

Figure 15. Stimulation of primary cancer cells with Lymphocyte-CM results in increased migration and proliferation. a) Scheme of cancer-immune cell Co-culture. Lymphocyte CM was used to stimulate primary cancer cells and changes in proliferation, chemotactic migration and EMT marker protein expression were quantified. **b)** Brightfield representative images of cell morphology after CM stimulation. **c)** Western blot for EMT markers E-cadherin, Vimentin and N-cadherin. β-Actin was used as a loading control**. d and e)** Quantification of western blot analysis of E-cadherin and Vimentin. **f)** Representative migration pictures. **g)** Percentage of migrated cells. **h)** BrdU incorporation by primary cancer cells. Data are represented as mean ± SEM, n=4 biological replicates, *p≤0.05, **p≤0.01 when compared to non-stimulated cells.

Primary lung cancer cells obtained through Giessen's Biobank were stimulated with Co-Culture CM (*Figure 15 a*). Changes in cell morphology were observed for the PMA activated Co-Culture CM, with cells displaying larger gaps between single cells (*Figure 15 b*). Stimulation with Lymph-CM resulted in similar effects on protein expression of the same EMT markers as in A549 cells (*Figure 15 c*).

For PMA activated Co-Culture CM, expression of epithelial marker E-cadherin was reduced, and mesenchymal marker Vimentin was upregulated (*Figure 15 d and e*). Exposure to CM also affected the migratory profile of primary cancer cells, observing significant changes for both PMA activated Lymph and Co-Culture CM (*Figure 15 f and g*). Proliferation was significantly altered only for the non-activated versions of the CM (*Figure 15 h)*.

Changes observed in EMT markers and functional assays on human lung tumor primary cells provides further evidence of the importance of the crosstalk between cancer cells and immune cells taking place in the tumor microenvironment.

4.1.4 Incubation of cancer cells with PMA-activated lymphocytes prompts secretion of cytokines IL-9 and IL-17

In the interest of gaining an overview of the secreted factors contained in the CM that could be responsible for the functional changes observed in both primary lung cancer cells and A549 cells, a cytokine array was performed (*Figure 16 a*). Each nitrocellulose membrane contains capture antibody spots for 36 different cytokines and was incubated overnight with undiluted CM (*see Section 3.1.15 for complete cytokine array coordinates*).

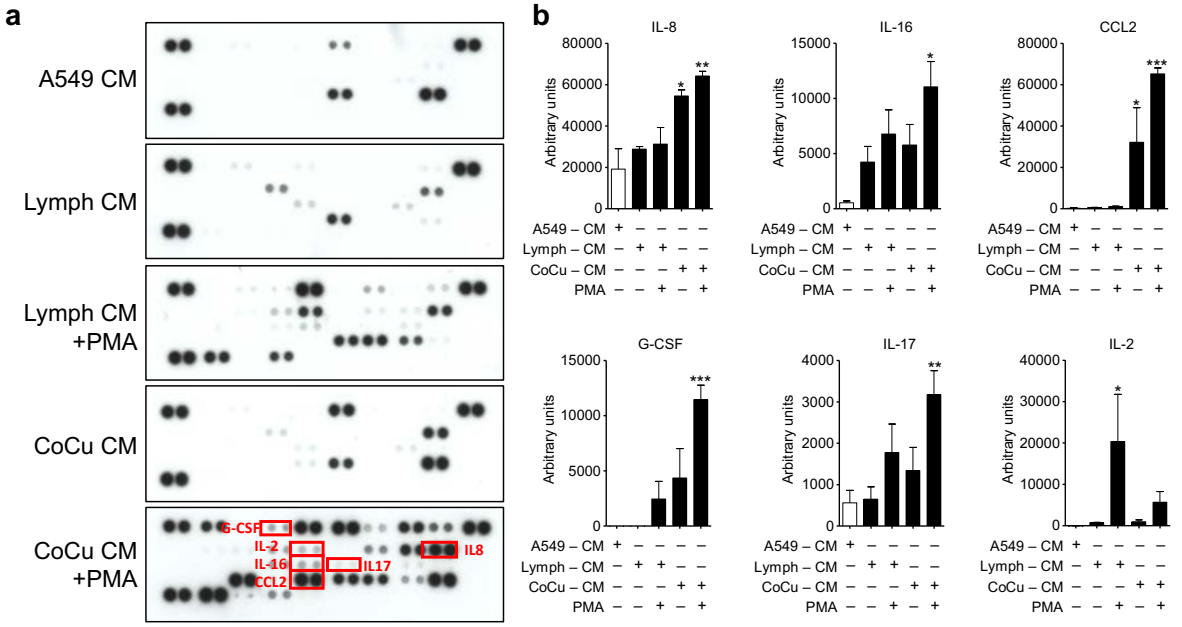

Figure 16. Cytokine profile of CM. a) Representative pictures of antibody spotted membranes after incubation overnight with CM. Upregulated cytokines are highlighted in red. G-CSF, granulocyte-colony stimulating factor; IL-2, Interleukin-2; IL-16, Interleukin-16; IL-17, Interleukin-17; CCL2, C-C motif chemokine ligand 2; IL-8, Interleukin-8. **b)** Quantification of secreted cytokines. Data are represented as a mean ± SEM, n=2 biological replicates, *p≤0.05, **p≤0.01, *** p≤0.001 when compared to Lymphocyte control media.

Within A549 CM, only 3 cytokines were found to be constitutively secreted: CXCL1, a potent chemokine that plays a role in immunity and inflammation; Serpin, a protease inhibitor and lastly MIF, an immune and insulin regulator. As expected, PMA activation of lymphocytes

sharply changed cytokine secretion by immune cells. IL-2, a hallmark cytokine of lymphocyte function was greatly increased in the Lymph+PMA CM, confirming activation of lymphocytes used for Co-Culture. Some of the differentially expressed cytokines in the Co-Culture CM were IL-8, IL-16, CCL2, G-CSF and IL-17 (*Figure 16 b*).

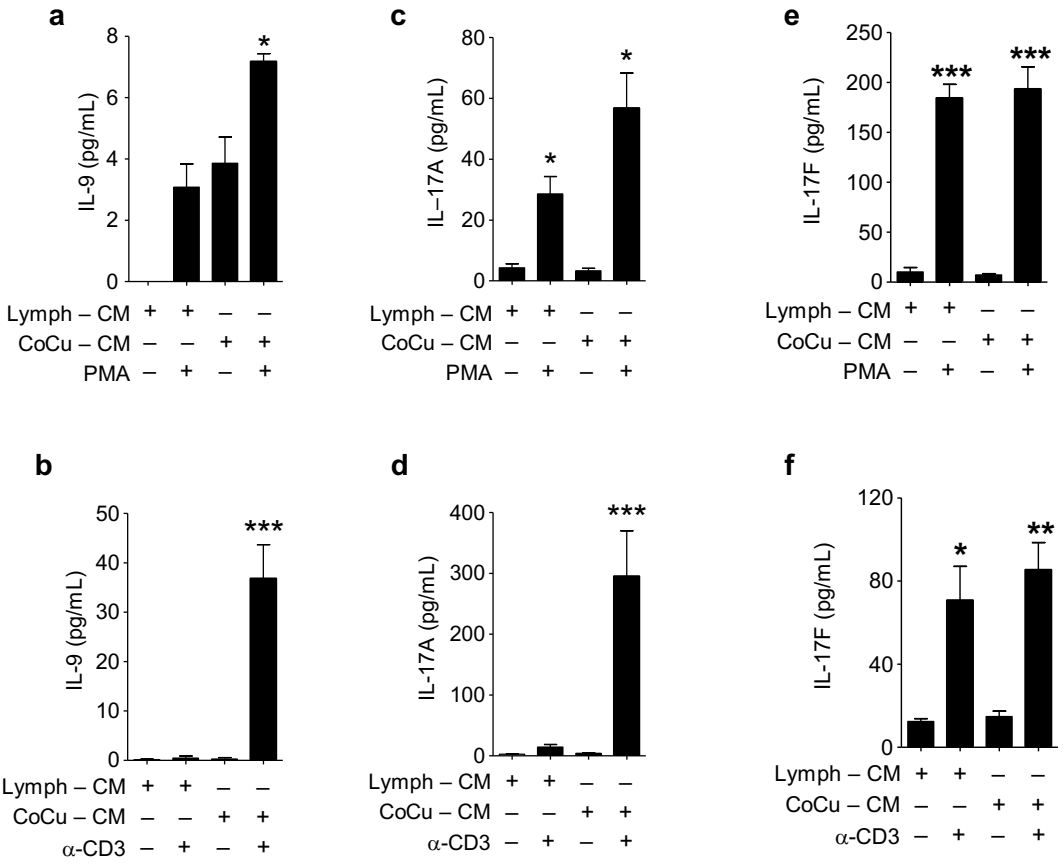

Figure 17. Elevated levels of cytokines IL-9, IL-17A and F were observed in PMA and CD3 activated Co-Culture CM. a and b) IL-9 secretion in PMA and CD3 activated CM. **c and d)** IL-17A secretion in PMA and CD3 activated CM. **e and f)** IL-17F secretion in PMA and CD3 activated CM. Data are represented as a mean ± SEM, n=4 biological replicates, *p≤0.05, **p≤0.01, *** p≤0.001 compared to Lymph-CM.

Additionally, ELISA assays for the detection of IL-9, IL-17A and IL-17F were performed on both CD3-primed and PMA activated Co-Culture CM. Increased levels of IL-9 were found almost exclusively in the Co-Culture CM pointing towards the lymphocyte cancer cell interaction as responsible for the secretion of this cytokine (*Figure 17 a*). Activation of lymphocytes with CD3 proved to be even more potent towards the production of IL-9 (*Figure 17 b)*. IL-17A was also increased in Lymph+PMA CM and the detected amount doubled in the case of the activated Co-Culture CM (*Figure 17 c)*. Activation with CD3 bound antibody did not affect secretion of IL-17A in the Co-culture CM, although similarly as with IL-9, CD3 activation resulted in higher amounts of detected cytokine (*Figure 17 d)*.

Secretion of IL-17F was similar for both the PMA and CD3 activated CM, displaying similarly elevated levels for the Lymph-CM and activated Co-Culture CM (*Figure 17 e and f).*

Elevated levels of these cytokines specifically for Co-Culture CM hints toward their role in directing the pro-proliferative and migratory phenotype observed in tumor cells.

4.1.4 Effect of CM on human lung cancer cells is not TGF-β dependent and involves phosphorylation of ERK1/2

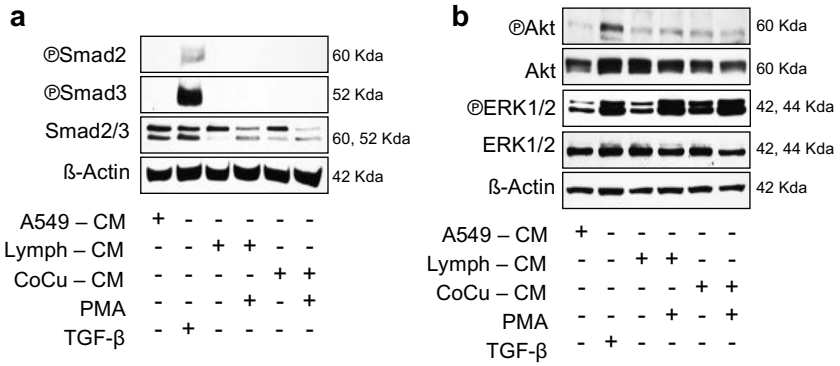

Figure 18. EMT-inducing changes of the CM are not TGF-β dependent and are characterized by ERK1/2 phosphorylation. a) Western blot of phosphorylated Smad2 and 3 and total Smad2/3 after 48 hours of stimulation with CM. **b)** Western blot for EMT-associated downstream signaling proteins: phosphorylated and non-phosphorylated Akt, phosphorylated and non-phosphorylated ERK1/2. β-Actin was used as a loading control.

Switching of the transcription program during EMT is induced by signaling pathways mediated by TGF-β, Wnt and other specific growth factors. To exclude TGF-β as the cytokine responsible for the functional changes observed *in vitro*, A549 cells were stimulated with CM for 48 hours and protein expression of downstream signaling targets of the TGF-β pathway were analyzed. Phosphorylation of Smad2 and 3 was observed only in A549 cells stimulated with TGF-β, supporting the hypothesis that other novel cytokines or growth factors are responsible for the EMT transition observed in cancer cells (*Figure 18 a)*.

Stimulation with CM was characterized by the phosphorylation of ERK1/2 specifically for the activated CM (both the Lymph and Co-Culture CM), which could indicate some involvement of growth factors in the EMT-inducing effects caused by the CM (*Figure 18 b)*.

4.2 Immunostaining of Th9 and Th17 markers allows for simultaneous detection of T cells in human lung cancer samples

4.2.1 Staining of Th9 and Th17 cells in human tumor samples

Opal multiplex immunostaining is a technique that allows for the simultaneous labelling of a maximum of eight markers in a single human tissue section, achieved through covalent binding of detection antibodies to an epitope allowing for subsequent antibody removal or inactivation to clear the tissue for the detection of the next target.

To provide clinical relevance to our *in vitro* findings, we screened T helper cells subpopulations using a multiplex immune-labelling protocol for Opal fluorophores, which allowed for the simultaneous evaluation of characteristic markers for Th9 and Th17 cells.

Staining for the following set of markers was performed: T-cell surface glycoprotein CD4, Cytokeratin, transcription factors Stat3 and PU.1, and cytokines IL-9 and IL-17 with DAPI as a nuclear stain (*Figure 19*). Opal multiplex staining was used on human lung cancer tissue samples or Tissue microarrays (TMA) obtained from 66 patients comprising different types and stages of lung cancer (*see Section 3.2.1 for patient information*) with the purpose of phenotyping and localizing Th9 and Th17 cells in tumor stroma.

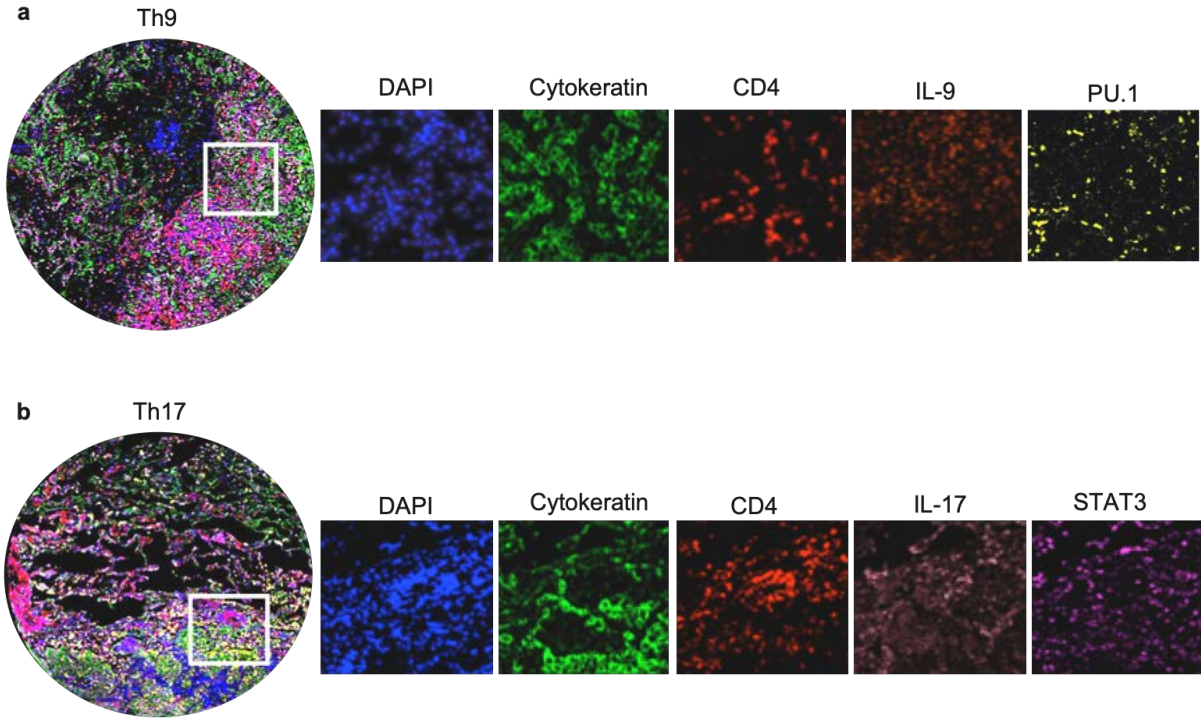

Figure 19. Opal seven-colour multiplex analysis of human lung tumor TMA samples. a) Representative image displaying a TMA core after multispectral imaging for Th9 markers. Enlarged subsection of the core showing each of the individual markers in the composite image after spectral unmixing: DAPI as nuclear marker, Cytokeratin (pseudocolored green, Opal 520), CD4 (pseudocolored red, Opal 620), IL-9 (pseudocolored orange, Opal 570), PU.1 (pseudocolored yellow, Opal 570). **b)** Representative image displaying a TMA core after multispectral imaging for Th17 markers. Enlarged subsection of the core showing each of the individual markers in the composite image after spectral unmixing: DAPI as nuclear marker, Cytokeratin (pseudocolored green, Opal 520), CD4 (pseudocolored red, Opal 620), IL-17 (pseudocolored pink, Opal 650), STAT3 (pseudocolored yellow, Opal 690).

4.2.2 Th9 and Th17 are located in the stromal area of tumors and a low Th/CD4$^+$ ratio correlates with better survival

The spectrally unmixed images were then analyzed to identify different cellular phenotypes, where cells that were positive for CD4, PU.1 and IL-9 were considered as Th9 cells and Th17 cells were defined as positive for CD4, Stat3, and IL-17 with a level of confidence of 50% or higher. Cytokeratin was used to identify epithelial cancer cells in tumor samples and to define tumor and stromal areas. Finally, all other cells not confined within these categories (such as myofibroblasts, macrophages, and so on) were grouped into one category, labelled as “other”. After parameters for the definition of Th9 and Th17 cells were outlined, quantification was done for all patients and results are shown as a percentage in relation to all cells in a given core and as an average per patient.

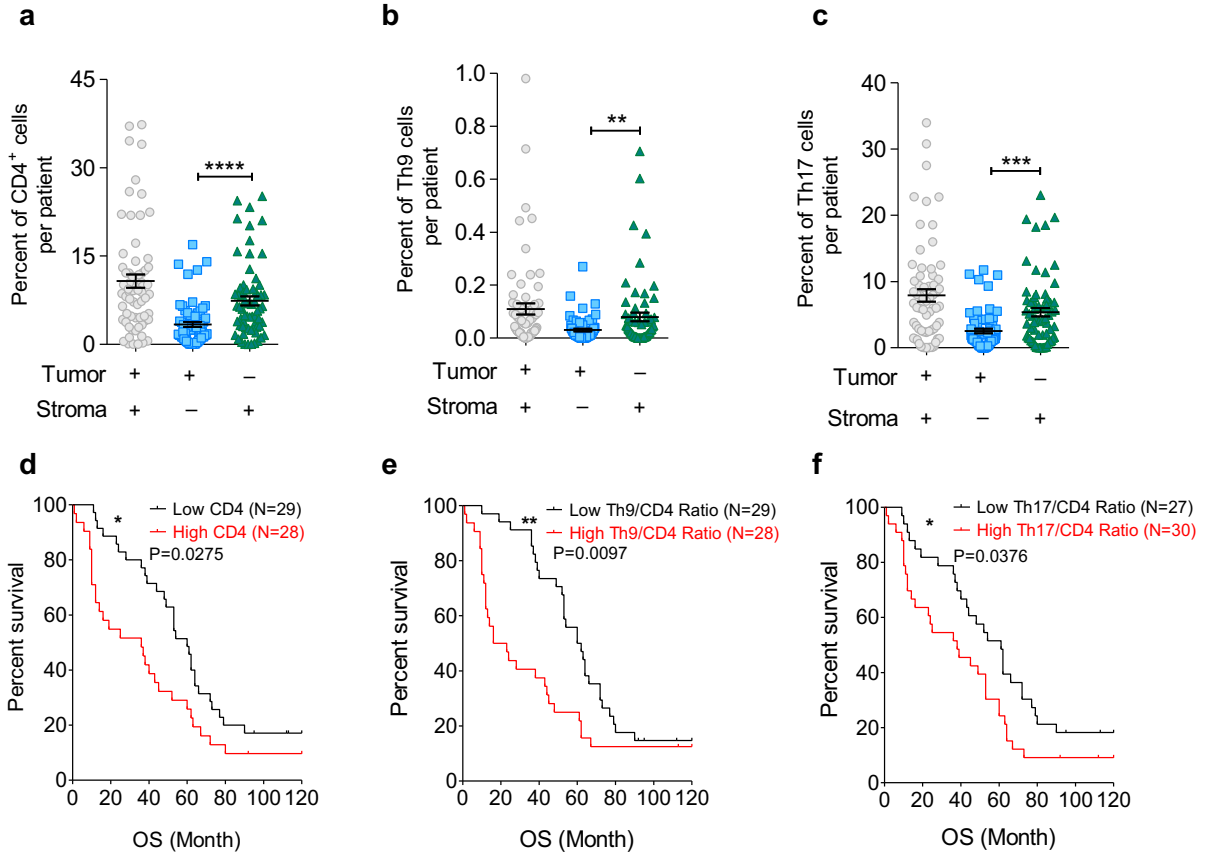

Figure 20. CD4$^+$ T cells are more abundant in the stromal area of tumors and their presence is associated with decreased survival. a, b, c) Percentage of CD4$^+$, Th9, and Th17 cells in tumor and stroma of all patients (n=66). **d, e, f)** Survival analysis of patients based on the Th/CD4$^+$ ratio. High and low infiltration values were divided on the basis of the median percentage of positive cells or ratio.

CD4$^+$ T helper cells in general, including, Th9 and Th17 cells, were located in greater proportion in the stromal area of tumors of lung cancer patients (*Figure 20 a,b,c*). Even though both Th9 and Th17 cells share a tendency to locate in stroma the total amount of Th9 versus Th17 varied significantly. To know what, if any impact, these subpopulations have on overall

patient survival, a Th/CD4$^+$ ratio was calculated and separated into high or low concentration groups, only for CD4$^+$, a total percentage of cells was used to determine survival. Overall, higher amounts of CD4$^+$ cells in tumor samples correlated with a detrimental effect on patient survival (*Figure 20 d*). A low Th9/CD4 ratio in tumor samples significantly correlated with an increase in patient survival, whereas a low Th17/CD4 ratio, though not significant, also exhibited a similar tendency of being favorable to the survival of lung cancer patients (*Figure 20 e and f*).

4.3 Th9 and Th17 CM induces EMT and migration in mouse lung cancer cells

Protocols for the *in vitro* generation of the distinct T helper subtypes have been developed to facilitate the understanding of T cell differentiation and research their pathogenesis in various inflammatory diseases. CD4 naïve lymphocytes can differentiate into specific T helper subtypes in the presence of specific stimulatory cytokines and inhibition of cytokines required for the development of alternative lineages (Huber et al. 2013; Zhao et al. 2016). To understand the role of Th9 and Th17 subsets in tumor development, mouse Th0, Th9 and Th17 cells were artificially generated and seeded in combination with LLC1 cells. Supernatant in which cells were grown was collected and used further as a stimulant to asses changes in EMT protein markers, proliferation, and migration.

4.3.1 Mouse Th9 and Th17 CM decreases expression of the mesenchymal marker ZO2 and increases migration of lung cancer cells

Naive CD44$^-$CD62L$^+$CD4$^+$ T cells were isolated from mice spleen, and later treated under Th0 (without skewing cytokines), Th9 (TGF-β and IL-4) and Th17 (TGF-β and IL-6) conditions for 2 – 5 days (see *Section 3.1.12 Generation of specific T helper subtypes)*. FACS analysis was later performed to assess levels of cytokines IL-9, IL-17, IL-2, and IFN-γ and confirm T cell differentiation profiles (*Figure 21*).

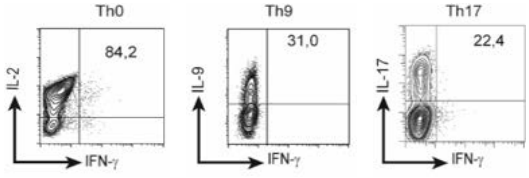

Figure 21. Generation of specific T helper cell subpopulations, Th9 and Th17. Naive CD44$^-$CD62L$^+$CD4$^+$ T cells were isolated from C57BL/6 mice and treated under Th9 (TGF-β and IL-4), Th17 (TGF-β and IL-6), or Th0 (without cytokines) conditions for 2-5 days. Analysis for IL-9, IL-17, IL-2 and IFN-γ production was detected by flow cytometry.

After confirmation by FACS of cytokine production and therefore a phenotype change, supernatant of Th0, Th9 and Th17 cells was used as CM to stimulate mouse lung cancer cells (*Figure 22 a*).

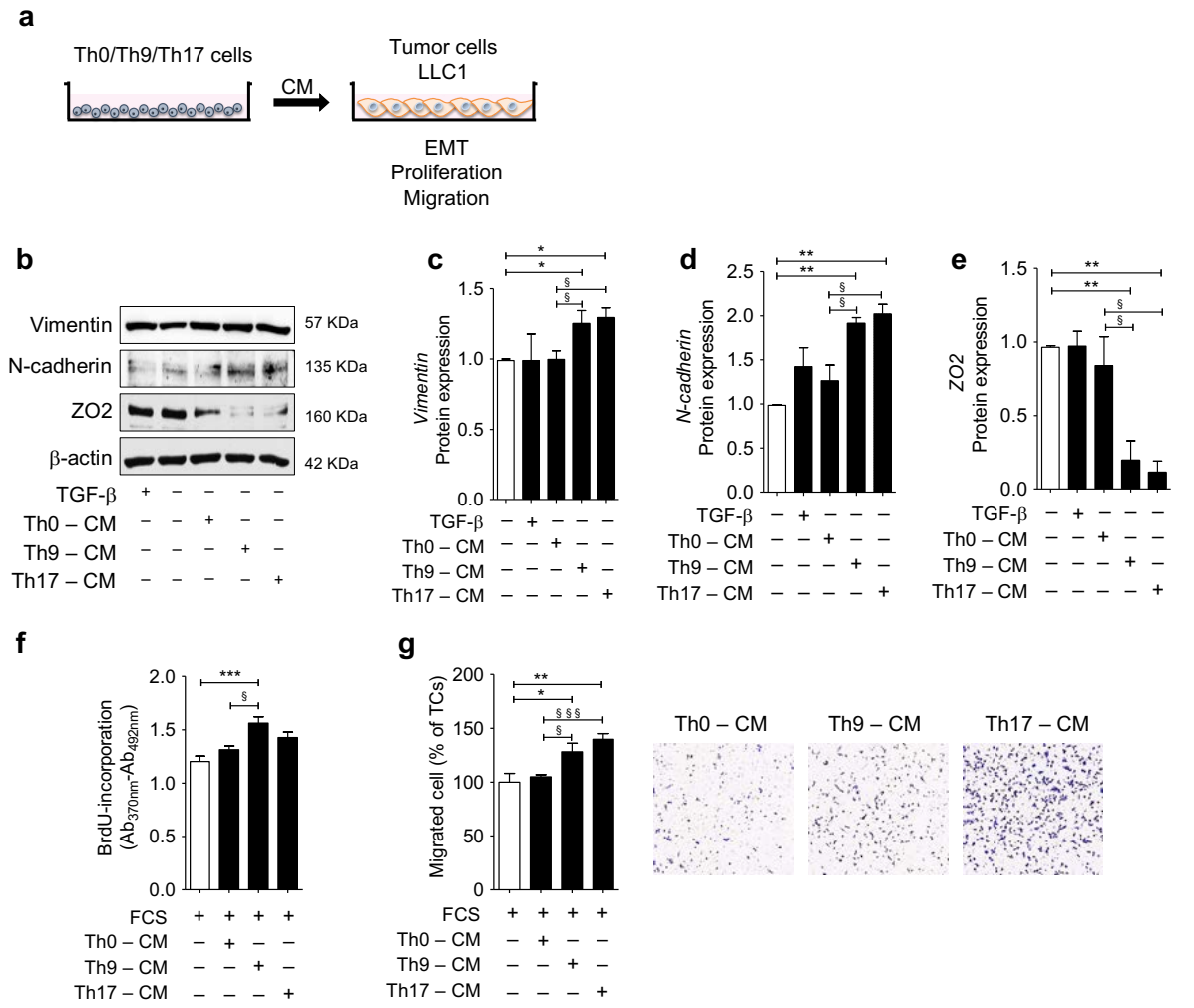

Figure 22. Th9 and Th17 CM induce a decrease in epithelial markers and potentiate migration of mouse cancer cells. a) Schematic of experimental design showing CM from Th0, Th9, or Th17 cells was used to stimulate LLC1 cells. **b)** Western blot analysis of Vimentin, N-cadherin, and ZO2 after 48 hours of stimulation with Th0, Th9 or Th17-CM. β-Actin was used as a loading control. **c, d and e)** Quantification of western blot analysis of EMT markers. **f)** BrdU incorporation by mouse cancer cells after 24 hours stimulation with CM. **g)** Percentage of migrated cells and representative migration pictures after 12 hours stimulation with CM. Data are represented as mean ± SEM, n=3 biological replicates, *p≤0.05, **p≤0.01, when compared to Th0 CM or LLC1 control.

Western blot analysis of LLC1 protein lysates after exposure to Th9 and Th17 CM, displayed significantly decreased ZO2 protein levels when compared to either LLC1 control or Th0 CM (*Figure 22 b and e*). Vimentin and N-cadherin protein levels were increased in LLC1 cells when stimulated with both Th9 and Th17 CM (*Figure 22 b-d*).

Furthermore, migration of tumor cells increased after stimulation with both Th9 and Th17 CM (*Figure 22 g*), whereas only the Th9 CM was able to increase proliferation of tumor cells (*Figure 22 f*).

4.3.2 Th9 and Th17 Co-culture CM strongly induces EMT marker expression and increases migration of mouse lung cancer cells

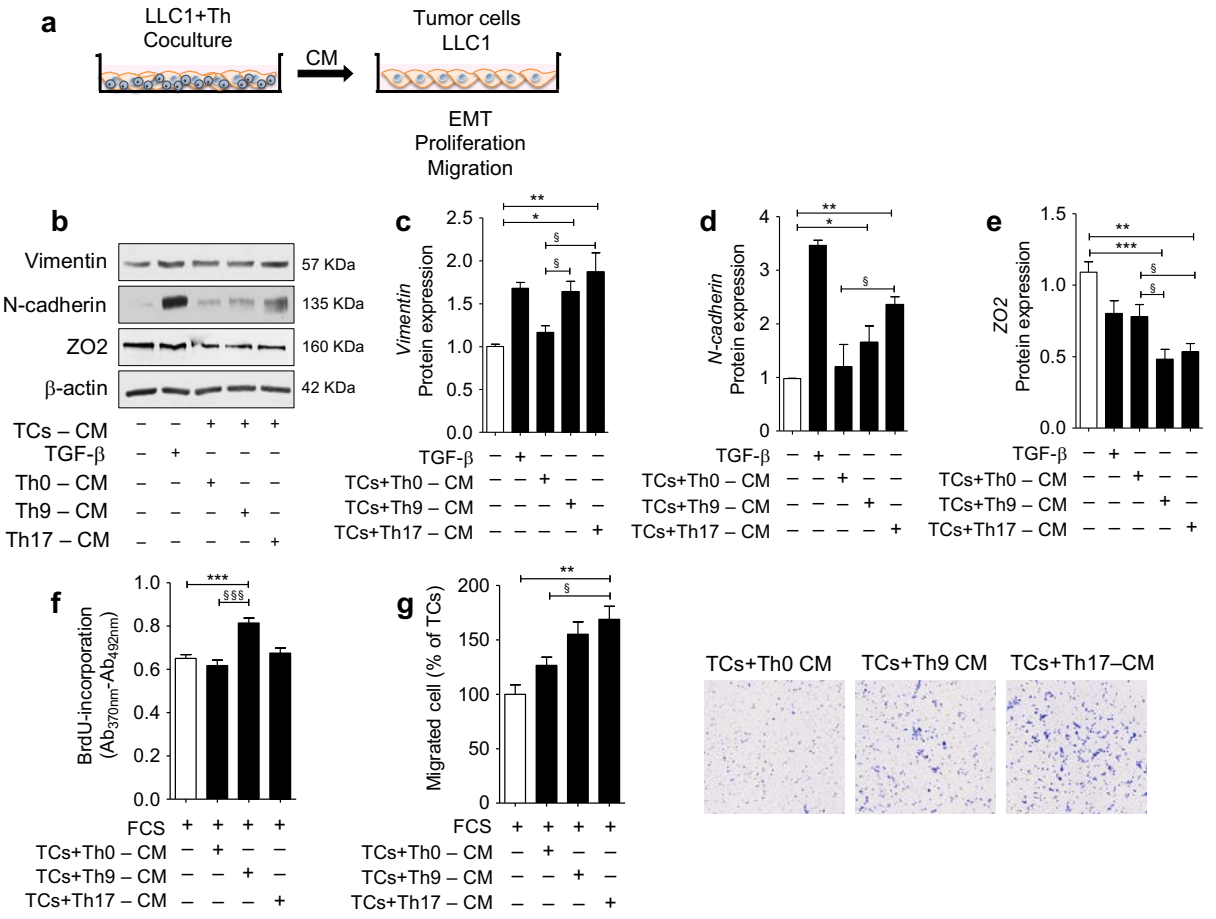

Figure 23. Th9 and Th17 Co-Culture CM induces deregulation of EMT markers and potentiates migration of mouse cancer cells. a) Naive $CD44^{-}CD62L^{+}CD4^{+}$ T cells were isolated from C57BL/6 mice and treated under Th9 (TGF-β and IL-4), Th17 (TGF-β and IL-6) or Th0 (without cytokines) for 2 – 5 days. Analysis for IL-9, IL-17, IL-2 and IFN-γ production was detected by flow cytometry. Differentiated Th subtypes were used in Co-culture with mouse cancer cells for 24 hours and CM was collected and used as a stimulant. **b)** Western blot analysis of Vimentin, N-cadherin and ZO2 after 48 hours stimulation with CM. β-Actin was used as a loading control. **c, d and e)** Quantification of western blot analysis of EMT markers. **f)** BrdU incorporation by mouse cancer cells after 24 hours stimulation with CM. **g)** Percentage of migrated cells and representative migration pictures after 12 hours stimulation with CM**.** Data are represented as a mean ± SEM, n=3 biological replicates, *p≤0.05, **p≤0.01, when compared to Th0 CM or LLC1 control.

Differentiated mouse T helper cells (*Figure 21*) were seeded in a direct Co-culture system with LLC1 cells in a 1:1 ratio and incubated for 24 hours. Afterwards, Co-culture CM was removed and used as stimulant on LLC1 cells to analyze changes in EMT markers, proliferation and migration of cancer cells (*Figure 23 a*). The CM obtained from Co-culture of Th0, Th9 and Th17 with LLC1 cells induced a stronger change of both epithelial (ZO2) and mesenchymal markers (Vimentin and N-cadherin) protein expression in tumor cells when compared to the CM of Th0, Th9 and Th17 cultured alone as observed by WB analysis (*Fig. 23 b-e*). Co-culture CM also induced the migration of mouse cancer cells after stimulation (*Figure 23 g*) whereas effects on the proliferation of tumor cells was observed only for the Th9 Co-culture CM (*Figure 23 f*).

4.4 Co-culturing of LLC1 cells with Th9 or Th17 cells alters their gene expression profile

Following the functional changes observed in cancer cells after stimulation with CM, RNA sequencing was used to examine the effect of Co-culture on the cellular transcriptome of lung tumor cells. Once again, specific T cell subtypes Th9 and Th17, were artificially generated from naïve T cells isolated from mice spleen. Cytokine production was confirmed with flow cytometry (*Figure 24 a*). Th9 and Th17 cells were later used in a direct co-culture with LLC1 cells for 24 hours, afterwards FACS sorting of $CD4^+$ T cells was performed. Sorting of T lymphocytes allowed for the recovery of mouse cancer cells from the Co-culture which were then used for RNA sequencing analysis (*Figure 24 b*). Conservation among biological replicates and reproducibility of the data was evaluated and is represented by Spearman's correlations graphs. Replicates among experimental groups (LLC1+Th0, LLC1+Th9, LLC1+Th17) displayed a high correlation and there was a clear separation between experimental conditions (*Figure 24 c and d*).

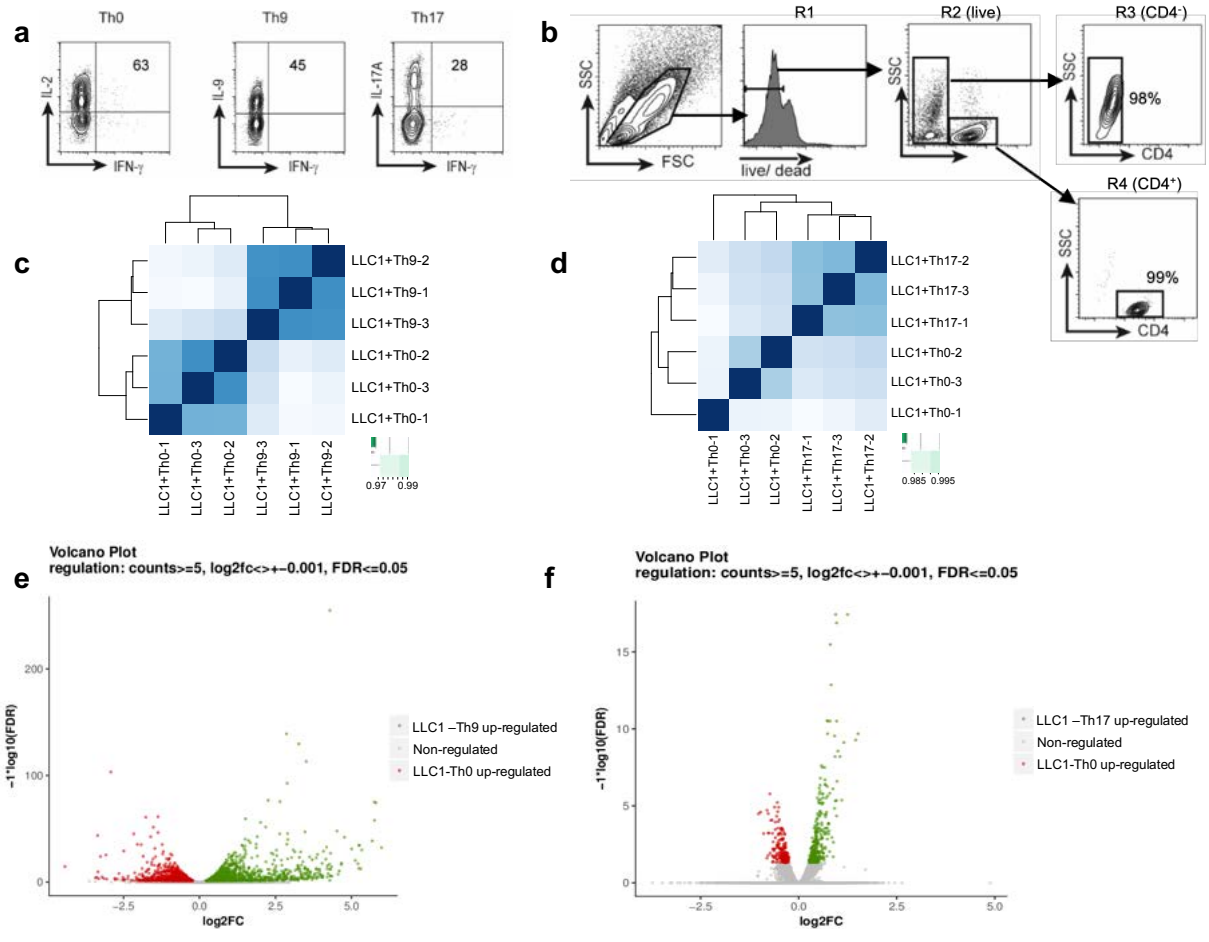

Figure 24. Deregulation of tumor cell gene profile after direct Co-culture with Th9 or Th17 cells. a) Naive $CD44^-CD62L^+CD4^+$ T cells were isolated from C57BL/6 mice and treated under Th9 (TGF-β and IL-4), Th17 (TGF-β and IL-6) or Th0 (without cytokines) conditions for 2 - 5 days. Analysis for IL-9, IL-17, IL-2 and IFN-γ production was detected by flow cytometry. **b)** After 24 hours of Co-culture, cells were sorted to remove all $CD4^+$ T lymphocytes and RNA sequencing was performed on remaining tumor cells. **c and d)** Spearman correlation between samples: LLC1+Th0 vs LLC1+Th9 and LLC1+Th0 vs LLC1+Th17 groups. **e)** Volcano plot representation of differential expression analysis of genes in LLC1+Th0 (red) vs LLC1+Th9 (green) groups. **f)** Volcano plot representation of differential expression analysis of genes in LLC1+Th0 (red) vs LLC1+Th17 (green) groups.

Comparisons between the control group (LLC1+Th0) and cells co-cultured with Th9 lymphocytes indicated a total of 3377 genes that were found to be differentially expressed. Among these genes, 1794 were significantly upregulated after Co-culture (*Figure 24 e*). For the Th17 Co-culture group, close to 500 genes displayed a deregulation, of which 290 were upregulated after Co-culture (*Figure 24 f*).

KOBAS (KEGG orthology-based annotation system) is a web server-based software that allows for the identification of statistically significantly enriched pathways using a hypergeometric test. This computational tool takes an input set of genes or proteins and maps these genes against known pathways in the KEGG pathway database offering information regarding which metabolic and signaling pathways are involved in a given set of samples (Xie et al. 2011).

KOBAS analysis was used to perform further functional classification and pathway assignment of the up-regulated genes in our experimental groups. Both Th9 and Th17 Co-culture groups displayed an upregulation of common pathways such as Integrin signaling pathway, T cell activation and PDGF and EGF receptor signaling (*Figure 25 a and b*).

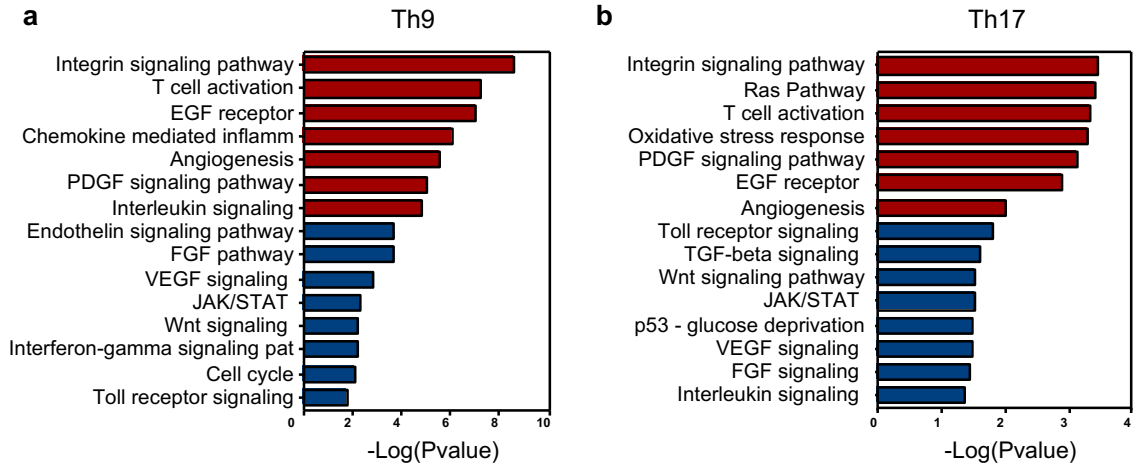

Figure 25. Signaling pathways upregulated after direct Co-culture with Th9 or Th17 cells. The Keggs orthology-based annotation system was used to find frequent and statistically enriched pathways in both experimental groups. **a)** Pathway analysis for differentially regulated genes in tumor cells co-cultured with Th9 cells. **b)** Pathway analysis for differentially regulated genes in tumor cells co-cultured with Th17 cells (n=3 experimental replicates).

Interestingly, both Co-culture conditions showed upregulation of the integrin signaling pathway. Some of the differentially up-regulated pathways for the Th9 Co-culture group were related to chemokine mediated inflammation and angiogenesis-related pathways, whereas the Th17 Co-culture group exhibited an increase in the oxidative stress response and Ras signaling pathways (*Figure 25 a and b*).

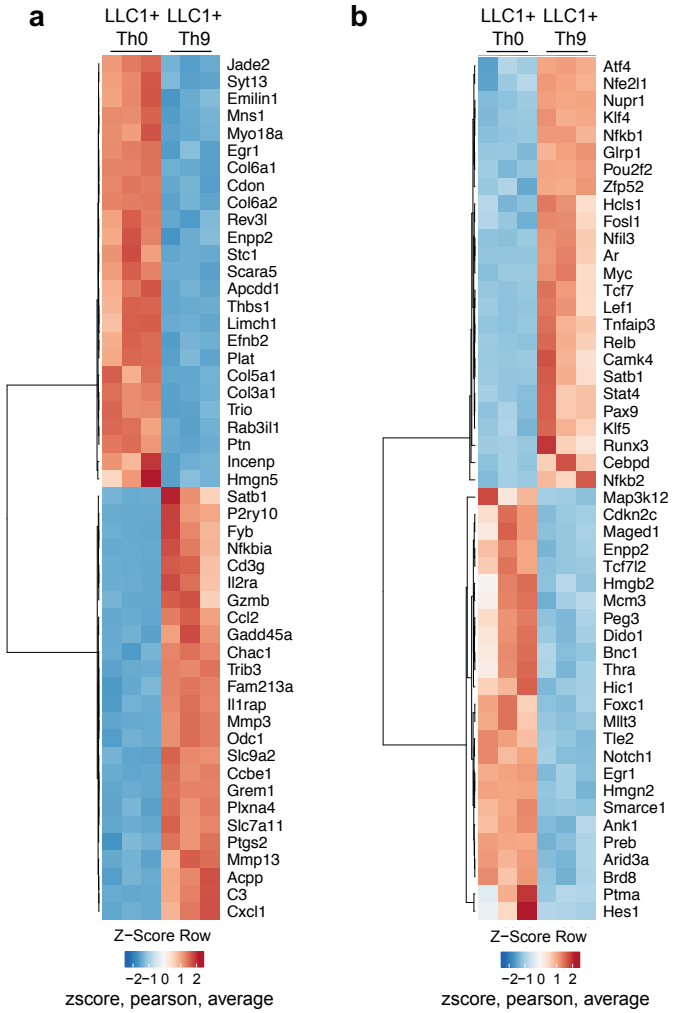

Figure 26. Co-culture of LLC1 cells with Th9 induces the upregulation of genes related to immune cell activation and inflammation. a) Heat map of differentially expressed genes in the LLC1+Th9 group. Genes with higher expression levels are shown in red, whereas genes with lower expression levels are shown in blue. **b)** Heat map of differentially expressed transcription factors in the LLC1+Th9 group. Genes with higher expression levels are shown in red, whereas genes with lower expression levels are shown in blue (n=3 experimental replicates).

Heatmap analysis of RNA-sequencing data allowed us to further consider specific protein coding genes including transcriptions factors that were directly affected by Co-culture with Th9 such as, MMP13, MMP3, PlexinA4, complement component 3 and CxCl1, all of which can be associated with tumor progression and metastasis (*Figure 26 a)*. For the Th9 Co-culture group, well-known tumor suppressor genes Notch1 and Hic1, were found to be downregulated (*Figure 26 b*).

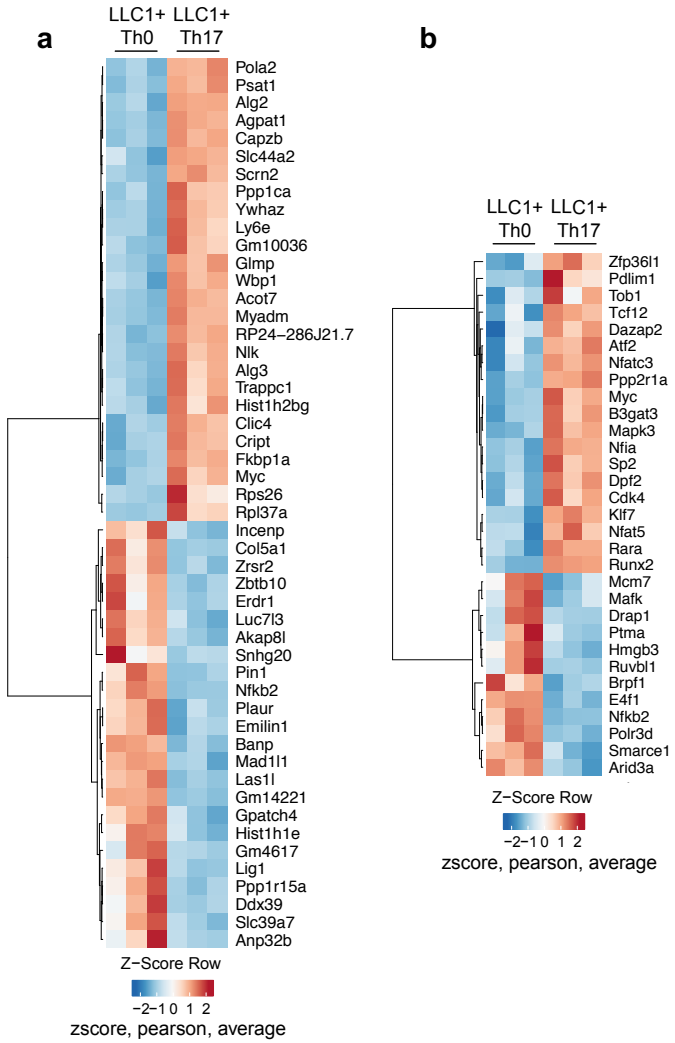

Figure 27. Co-culture of LLC1 cells with Th17 induces the upregulation of genes related to immune cell activation, inflammation and metastatic phenotype. a) Heat map of differentially expressed genes in the LLC1+Th17 group. Genes with higher expression levels are shown in red, whereas genes with lower expression levels are shown in blue. **b)** Heat map of differentially expressed transcription factors in the LLC1+Th17 group. Genes with higher expression levels are shown in red, whereas genes with lower expression levels are shown in blue (n=3 experimental replicates).

For the Th17 Co-culture group, upregulated genes included Ywhaz, Psat1 and Ly6e, which are known to be involved in promotion of epithelial-mesenchymal transition, cell cycle progression, and regulation of tumor blood vessel density, all key aspects of the metastatic phenotype in lung cancer (*Figure 27 a*). A common family of transcription factors upregulated in both the Th9 and Th17 Co-culture groups was Krüppel-like factors (Klf), specifically Klf4 and Klf5 for the Th9 Co-culture group and Klf7 for the Th17 Co-culture group (*Figures 26 b and 27 b*).

4.5 Co-injection of tumor cells and/or Th9/Th17 cells promotes lung cancer growth and metastasis

4.5.1 Co-injection of LLC1 with Th9 cells significantly increases tumor size whereas co-injection with Th17 cells correlated with elevated incidence of metastatic nodules to the lung

A commonly used animal mouse tumor model is the xenograft subcutaneous (s.c.) tumor growth of mouse Lewis lung carcinoma cells, LLC1, in C57BL/6 mice, which have the same genetic background. LLC1 cells ($3x10^6$ cells prepared in 200µL) were injected into the hind flank of WT (Wild type) mice along with artificially generated T cell subtypes, Th9 and Th17. T cell differentiation and cytokine production was confirmed by flow cytometry. After co-injection tumor growth was monitored for 20 days (*Figure 28 a and b*).

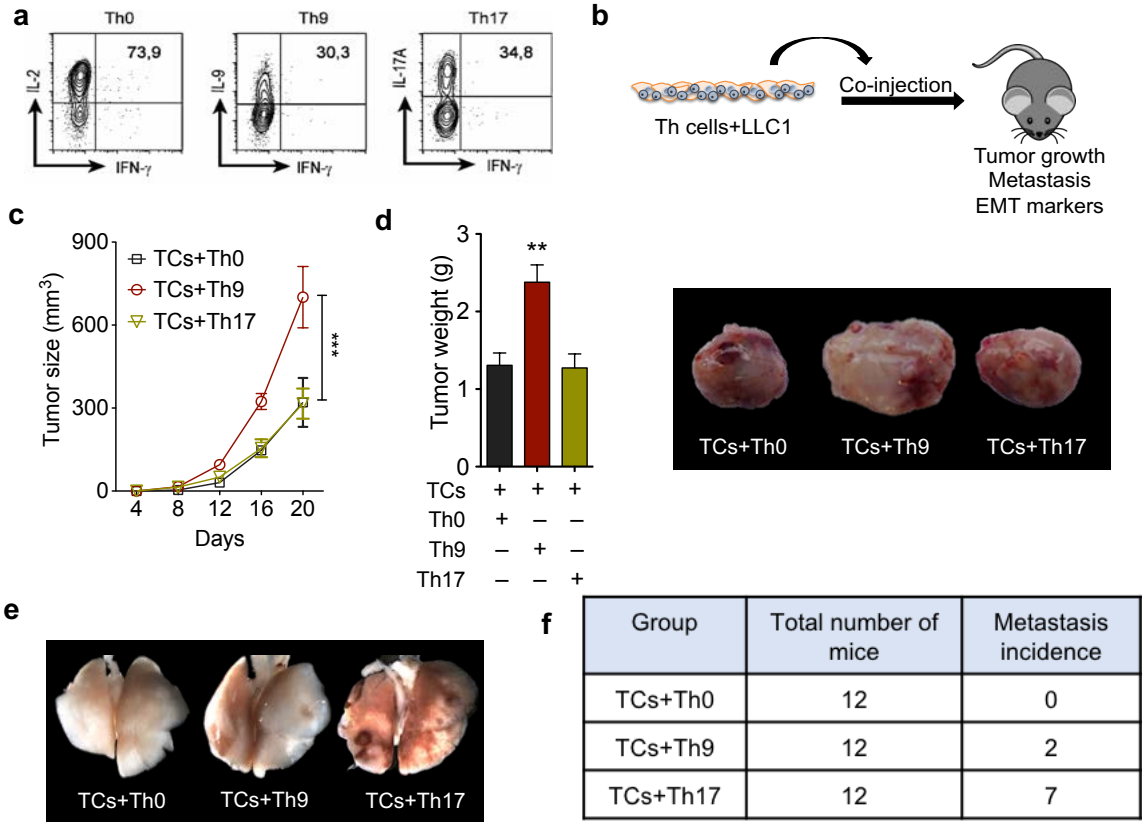

Group	Total number of mice	Metastasis incidence
TCs+Th0	12	0
TCs+Th9	12	2
TCs+Th17	12	7

Figure 28. Co-injection of LLC1 cells with Th9 and Th17 cells leads to increased tumor growth and metastasis *in vivo*. a) Naive $CD44^{-}CD62L^{+}CD4^{+}$ T cells were isolated from C57BL/6 mice and then treated under Th9 (TGF-β and IL-4), Th17 (TGF-β and IL-6) or Th0 (without cytokines) conditions for 2–5 days. Analysis for IL-9, IL-17, IL-2 and IFN-γ production was detected by flow cytometry. **b)** Differentiated Th9 and Th17 cells were s.c. co-injected with LLC1 cells into WT mice and tumor growth was monitored for 20 days. **c and d)** Tumor size, tumor weight and representative pictures of extracted tumors of co-injected groups (n = 6). Data are represented as a mean ± SEM, *p≤0.05, **p≤0.01, *** p≤0.001 when compared to Th0 co-injection group. **e)** Representative pictures of extracted lungs. **f**) Table representing metastasis incidence in mice.

Mice in the Th9 co-injection group (LLC1+Th9) displayed a significant increase in tumor growth and weight when compared to the control group (LLC1+Th0) (*Figure 28 c and d*). Unexpectedly, animals in the Th17 co-injection group exhibited a much greater incidence of metastatic nodules in the lung despite their overall tumor growth remaining unchanged when compared to the control group (*Figure 28 e and f*). Likewise, co-injection of Th9 cells increased the appearance of metastatic nodules in mice indicating that, Th9 and Th17 cells or their signature cytokines might be involved in promoting or facilitating early stages of metastasis.

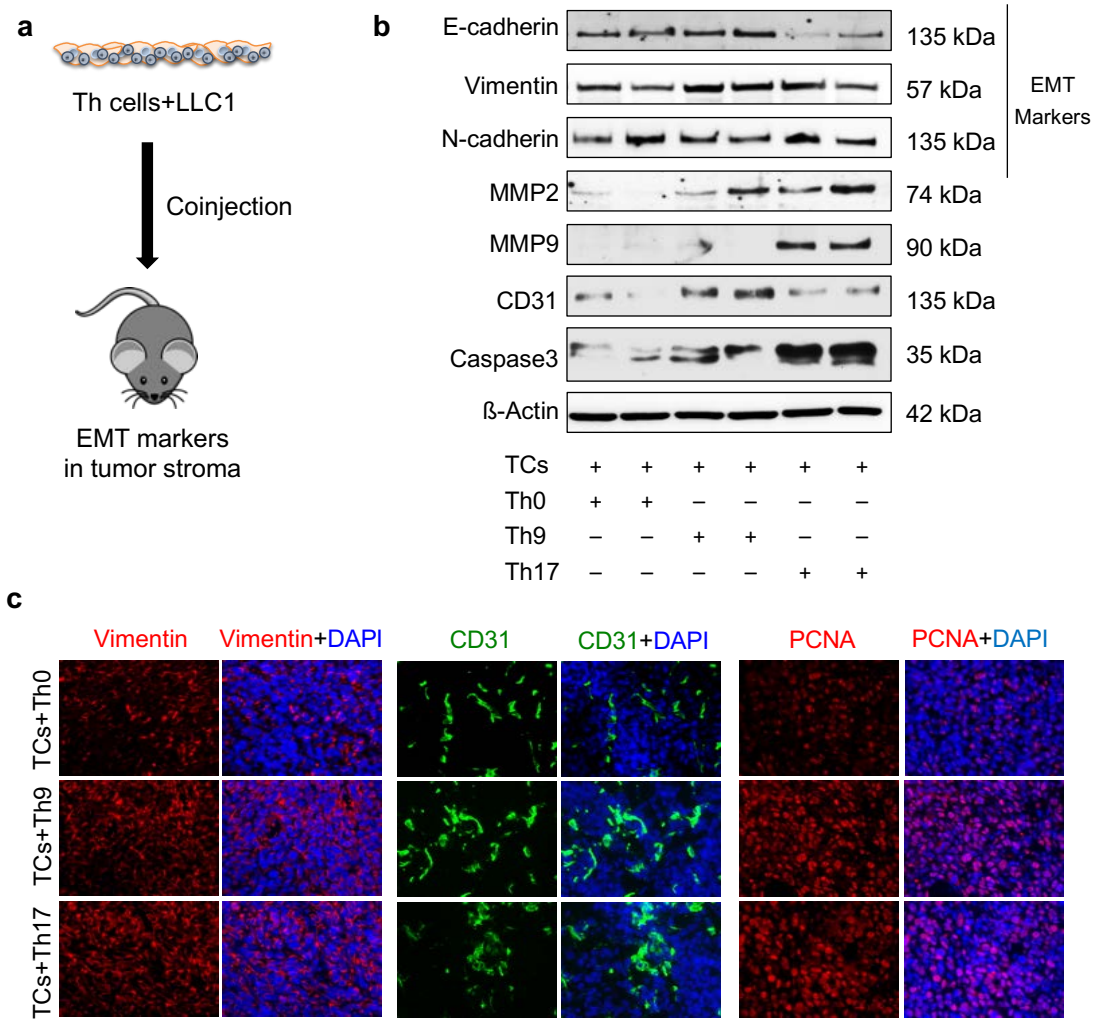

Figure 29. Tumor stroma of mice co-injected with T cells is characterized by an EMT protein profile and upregulation of MMPs. a) T cells were co-injected with LLC1 mouse lung cancer cells and tumor growth was monitored. After day 20 tumors were resected for protein isolation and IHC. **b)** Western blot analysis of E-cadherin, Vimentin, CD31, Caspase 3, MMP2 and MMP9 from tumor homogenates. β-Actin was used as a loading control. **c)** Immunofluorescence for Vimentin (red), CD31 (green), and PCNA (red) in tumor sections.

Analysis of protein lysates from subcutaneous tumors confirmed changes in vascularization by the upregulation of the endothelial marker, CD31 (*Figure 29 b and c*). Moreover, upregulation of EMT markers, such as MMP2 and MMP9 further points toward a migratory phenotype change of LLC1 cells present in tumor stroma. E-cadherin and Vimentin

protein levels in tumors of mice belonging to the Th17 co-injection group were found to be expressed accordingly with an EMT-like transition (*Figure 29 b*). Caspase 3, a mediator of apoptosis, was deregulated in tumor stroma of both experimental groups.

Staining of subcutaneous lung tumor sections also confirmed an increased protein expression of Vimentin for the Th9 and Th17 co-injection groups. Furthermore, angiogenesis (CD31) and proliferation (PCNA) were shown to be enhanced in both co-injection groups (*Figure 29 c*).

Subcutaneous tumors were taken for digestion and subsequent FACS and cytokine secretion analysis to identify a potential shift in the immune and secretory component of the tumor microenvironment after co-injection of cancer cells with either Th9 or Th17 cells (data not shown). A decrease in the percentage of $CD4^+$ T cells was observed in both experimental groups, although it was significantly more pronounced for the Th9 co-injection group. Infiltration of $CD8^+$ T cells was also reduced for both co-injection groups. Likewise, the percentage of macrophages ($CD11b^+$ cells) was reduced, with the Th9 co-injection group displaying significantly less infiltration of macrophages when compared to the control group. Furthermore, Co-injection of Th9 cells altered the secretory profile of the tumor microenvironment, observing increased levels of cytokines IL-9, IL-17A, and IFN-γ. For the Th17 co-injection group, these cytokines remained largely unchanged when compared to the control group (LLC1+Th0).

4.5.2 Intravenous co-injection of LLC1 with both Th9 and Th17 cells significantly increased lung metastasis in mice

Further building upon the observed metastasis in our subcutaneous tumor model and in order to better comprehend the role of both Th9 and Th17 cells in the progression of lung cancer metastasis; co-injections of LLC1 cells with Th9 and Th17 were administered intravenously. On day 20 after co-injection, lungs of experimental mice were harvested in order to analyze metastatic incidence, through tumor nodule count, calculation of percentage of metastatic area and tumor volume. As expected, co-injection of tumor cells with Th9 and Th17 cells increased appearance of lung tumors in mice (*Figure 30 a*). This observation was confirmed by changes in the percentage of metastatic area and tumor volume for both Th9 and Th17 co-injection groups when compared to the control group (*Figure 30 b*). As with subcutaneous tumors, mesenchymal marker Vimentin was increased in the lungs of the Th9 and Th17 co-injection groups. Angiogenesis as detected by the presence of the vonWillebrand marker, was shown to be downregulated in the lungs of mice of the Th17 co-injection group (*Figure 30 c*).

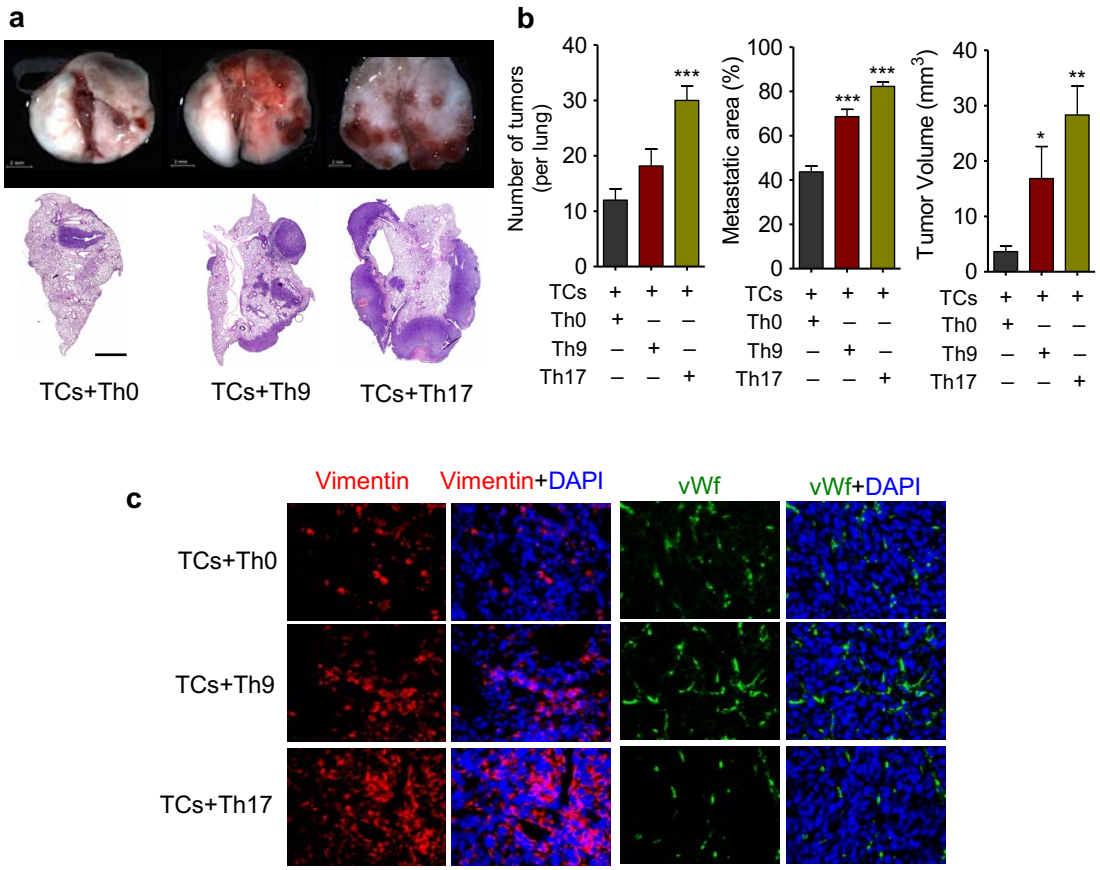

Figure 30. Co-injection of Th9 and Th17 cells leads to increased metastasis *in vivo*. a) Representative pictures of extracted lungs and H&E stained sections on day 20 after i.v injection of LLC1 cells. **b)** Quantification of macroscopic nodules (n = 10), percentage of metastatic area and tumor volume (n = 4). Data are represented as a mean ± SEM, *p≤0.05, **p≤0.01, *** p≤0.001 when compared to Th0 co-injection group. **c)** Immunofluorescence of Vimentin (red) and vonWillebrand factor (green) in sections of lungs with metastatic nodules after co-injections.

Taken collectively, our *in vivo* results strongly support the involvement of Th9 and Th17 cells in the enhancement of tumor growth and metastasis, through deregulation of protein markers associated with an EMT transition and alteration of the cytokine profile within the tumor microenvironment.

Lungs of experimental mice were also used for FACS and cytokine analysis (data not shown), to have an overall assessment of cellular and secretory components in tumor stroma. Unlike results observed in the subcutaneous tumors, total percentage of the immune cells $CD4^+$, $CD8^+$, and $CD11b^+$ were not altered after intravenous co-injection of LLC1 and the Th specific subtypes, Th9 and Th17. Similarly, levels of cytokines IL-17A and IFN-γ showed no changes among experimental groups.

4.6 IL–9 and IL–17 induce EMT in human tumor cells while their neutralization decreases lung cancer metastasis

Thus far our results support the link between $CD4^+$ T cells, Th9 and Th17, and their role in the promotion of EMT. However, to further delineate the effects of these cells versus those of their corresponding cytokines, IL-9 and IL-17, both A549 and tumor primary cells were directly stimulated to asses changes in proliferation, migration, and protein expression of EMT markers *in vitro*.

4.6.1 Stimulation of human lung cancer cells with IL-9 induces an EMT phenotype characterized by increased migration

A549 and tumor primary cells were stimulated with IL-9 (1, 5 and 10 ng/mL) for 48 hours after which, changes in protein expression, BrdU incorporation and chemotactic migration were measured. Stimulation with IL-9, decreased protein levels of E-cadherin in tumor cells, whereas expression of the mesenchymal marker Vimentin was increased, confirmed by western blot analysis and immunostaining. Deregulation of both markers was more efficiently observed at a concentration of 10ng/mL (*Figure 31 a-d*). Alterations of these markers was accompanied by a phenotype change with cells acquiring a fibroblast-like shape as observed by immunostaining (*Figure 31 d*).

Although proliferation remained unaffected for both A549 and primary tumor cells (*Figure 31 e and f*), the observed EMT marker changes corresponded with an elevated percentage of migration for both tumor cell types (*Figure 31 g, h and i*).

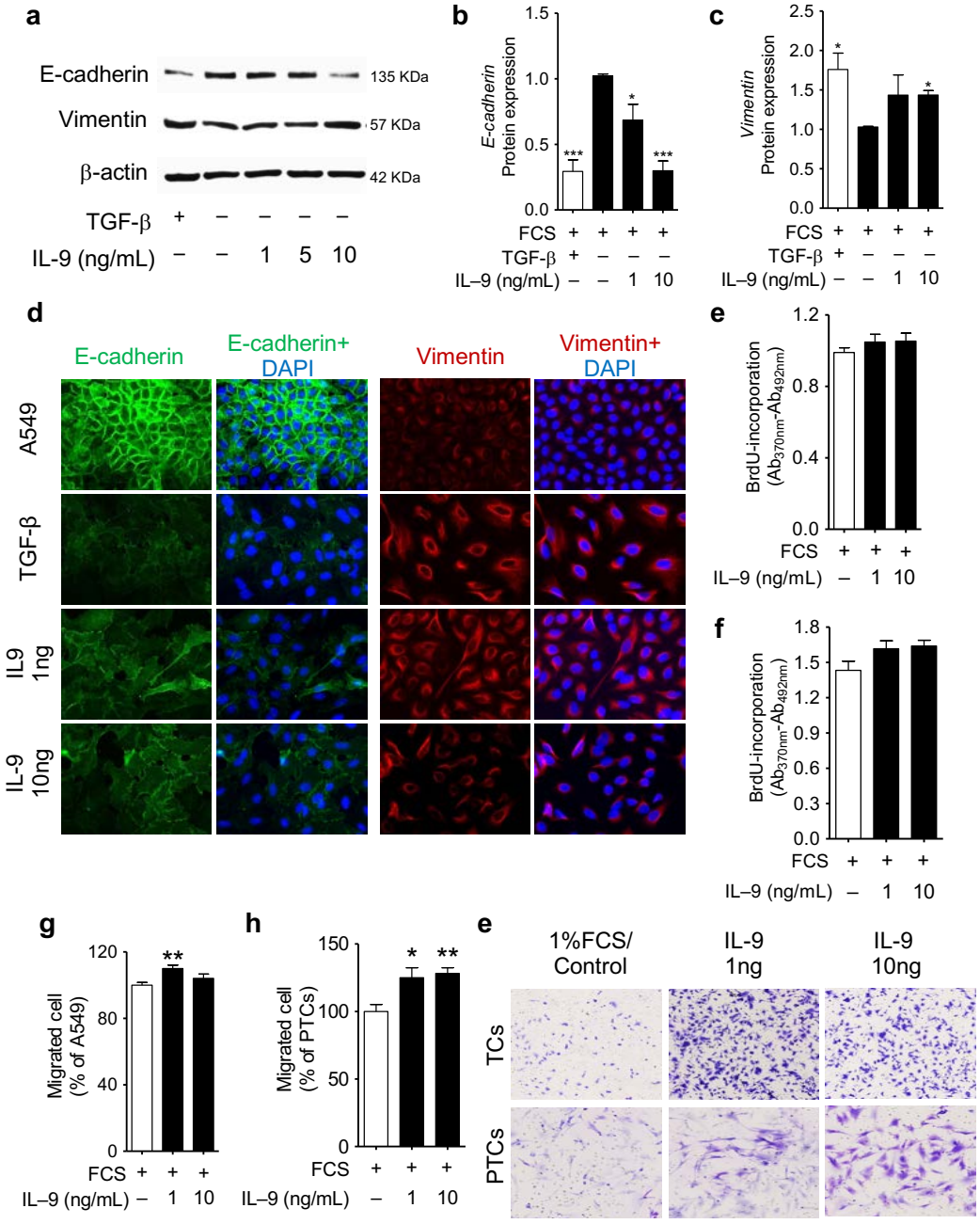

Figure 31. Stimulation with IL-9 results in an EMT-like phenotype in tumor cells. a) Western blot analysis of epithelial (E-cadherin) and mesenchymal (Vimentin) markers from tumor cell lysate after 48 hours stimulation with IL-9. **b and c)** Quantification of western blot analysis of EMT markers. **d)** Immunocytochemistry of E-cadherin (green) and Vimentin (red) after 48 hours of stimulation with IL-9. **e and f)** BrdU incorporation by tumor cells and primary tumor cells, respectively, after 24 hours of stimulation with IL-9. **g)** Percentage of migrated tumor cells after stimulation for 12 hours with IL-9. **h)** Percentage of migrated primary tumor cells after stimulation for 6 hours with IL-9. Data are represented as a mean ± SEM, n=3 experimental replicates, *p≤0.05, **p≤0.01, *** p≤0.001 when compared to non-stimulated cells. **i)** Representative migration pictures.

4.6.2 Stimulation of human lung cancer cells with IL-17 isotypes A and F induces an EMT phenotype

Because Th17 cells secrete IL-17 A, F and the heterodimer A/F, these cytokine subtypes were used to stimulate A549 cells and measure changes in functional aspects of cell behavior. Stimulation with IL17 A/F resulted in unchanged EMT marker protein expression, as well as, no changes in proliferation and migration (data not shown).

IL-17A, the most prominent member of the IL-17 cytokine family, showed similar effects as IL-9, on E-cadherin and Vimentin protein levels in tumor cells at a concentration of 1ng/mL (*Figure 32 a*-d). Immunostaining confirmed changes observed by western blot analysis, additionally depicting changes in cell morphology after 48 hours of cytokine stimulation (*Figure 32 d*). Proliferation was only increased for A549 cells when stimulated with 1 and 10 ng/mL of IL-17A (*Figure 32 e and f*). Increased migration was observed for both A549 and primary tumor cells at a concentration of 1 ng/mL (*Figure 32 g, h and i*).

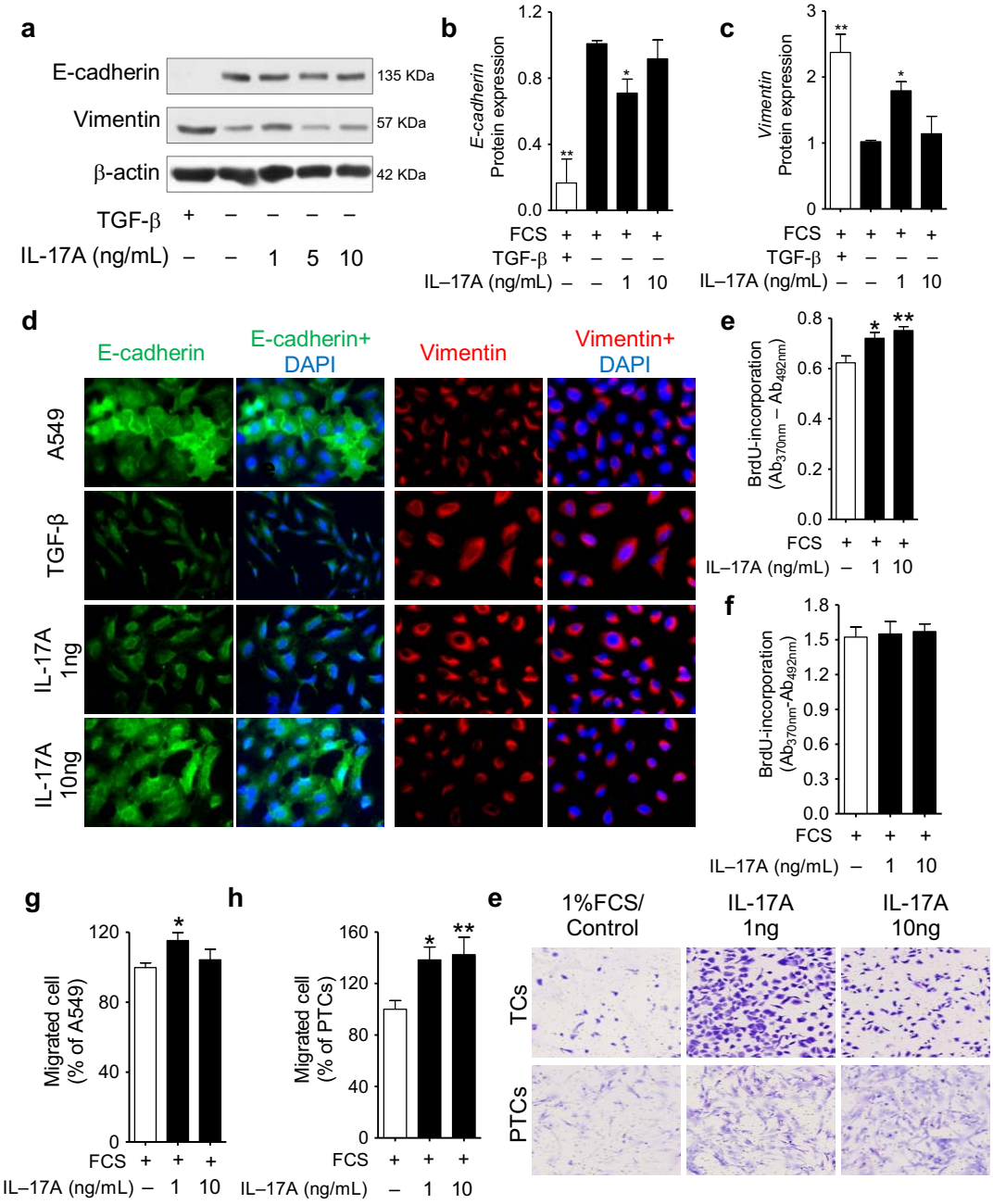

Figure 32. Stimulation with IL-17A results in an EMT-like phenotype in tumor cells. a) Western blot analysis of epithelial (E-cadherin) and mesenchymal (Vimentin) markers from tumor cell lysate after 48 hours stimulation with IL-17A. **b and c)** Quantification of western blot analysis of EMT markers. **d)** Immunocytochemistry of E-cadherin (green) and Vimentin (red) after 48 hours stimulation with IL-17A. **e and f)** BrdU incorporation by tumor cells and primary tumor cells, respectively, after 24 hours stimulation with IL-17A. **g)** Percentage of migrated tumor cells after stimulation for 12 hours with IL-17A. **h)** Percentage of migrated primary tumor cells after stimulation for 6 hours with IL-17A. Data are represented as a mean ± SEM, n=3 experimental replicates, *p≤0.05, **p≤0.01, *** p≤0.001 when compared to non-stimulated cells. **i)** Representative migration pictures.

Exposure to IL-17F, also caused significant changes in protein expression of EMT markers, E-cadherin and Vimentin, in A549 cells at a range of 10ng/mL (*Figure 33 a-c*). Once again, changes in protein levels were confirmed by immunostaining, observing profound cell phenotype alterations (*Figure 33 d*).

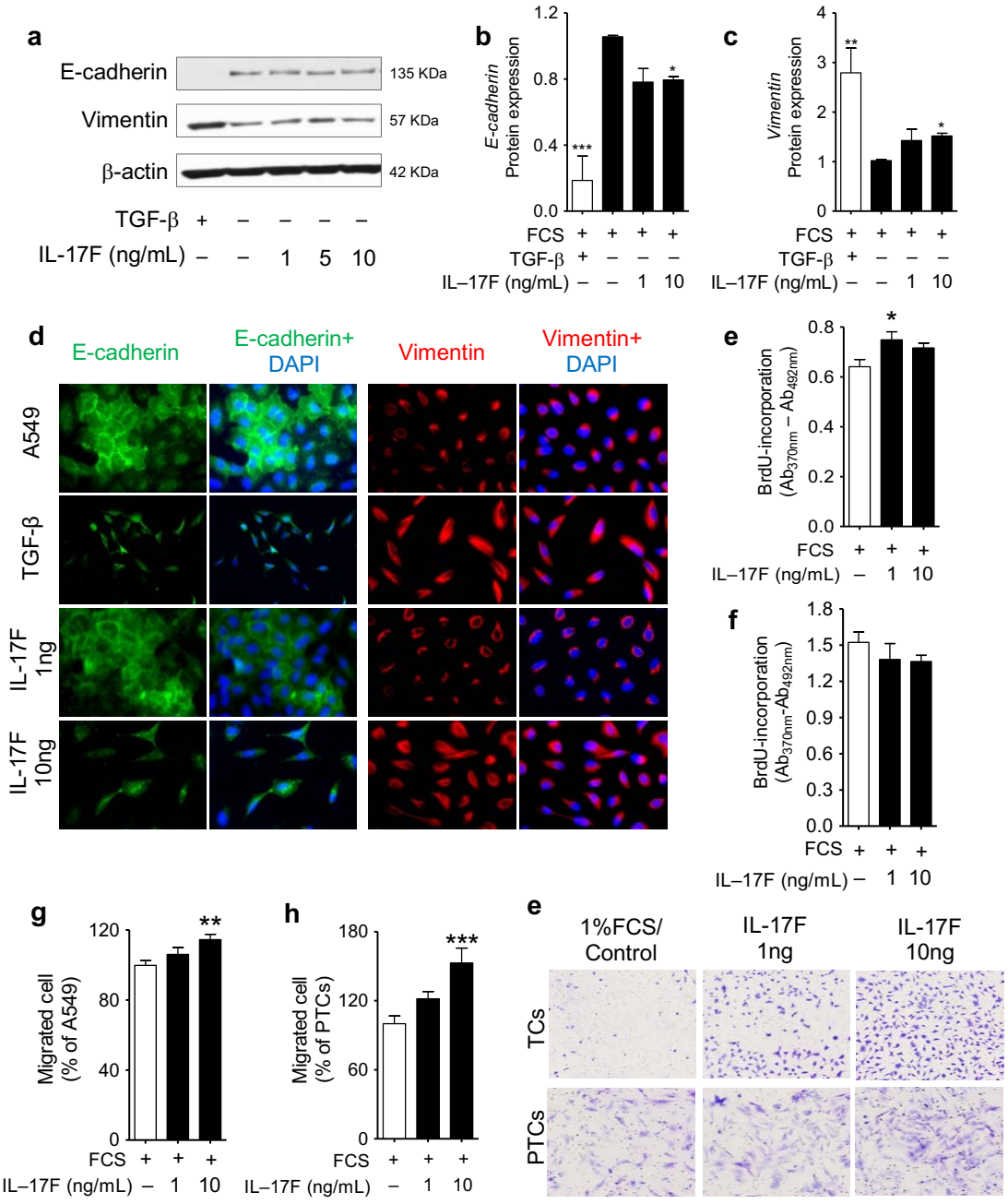

Figure 33. Stimulation with IL-17F results in an EMT- like phenotype in tumor cells. a) Western blot analysis of epithelial (E-cadherin) and mesenchymal (Vimentin) markers from tumor cell lysate after 48 hours stimulation with IL-17F. **b and c)** Quantification of western blot analysis of EMT markers. **d)** Immunocytochemistry of E-cadherin (green) and Vimentin (red) after 48 hours stimulation with IL-17F. **e and f)** BrdU incorporation by tumor cells and primary tumor cells, respectively, after 24 hours stimulation with IL-17F. **g)** Percentage of migrated tumor cells after stimulation for 12 hours with IL-17F. **h)** Percentage of migrated primary tumor cells after stimulation for 6 hours with IL-17F. Data are represented as a mean ± SEM, n=3 experimental replicates, *p≤0.05, **p≤0.01, *** p≤0.001 when compared to non-stimulated cells. **i)** Representative migration pictures.

Proliferation of A549 cells was increased after stimulation with 1ng/mL of IL-17F, whereas for tumor primary cells, no changes were detected (*Figure 33 e and f*). Enhanced migration of both A549 and tumor primary cells was observed after stimulation with 10 ng/mL of IL-17 (*Figure 33 g, h and i*).

4.6.3 Depletion of IL-9 and IL-17 results in decreased lung cancer metastasis in mice

Taken together, our results strongly suggest the involvement of T helper cells, Th9 and Th17 and their signature cytokines in the induction of an EMT phenotype in tumor cells, which results in an increased migratory and pro-proliferative state. Hence, we postulated that by inhibiting the production of these Th9 and Th17 associated cytokines, we could revert the effects observed *in vivo* on tumor growth and metastasis, thereby providing a possible therapeutic aim to our findings.

To test this hypothesis, we employed specific antibodies against IL-9 and IL-17 to inhibit systemic cytokine production in mice. Antibodies were administered 4 days after i.v. injection of LLC1 cells at a concentration of 30 μg/mouse for α-IL-9 and 100 μg/mouse for α-IL-17. Treatment was administered every four days during a total experimental time of 20 days, after which lungs were harvested and metastatic nodules, percentage of metastatic and tumor volume were calculated.

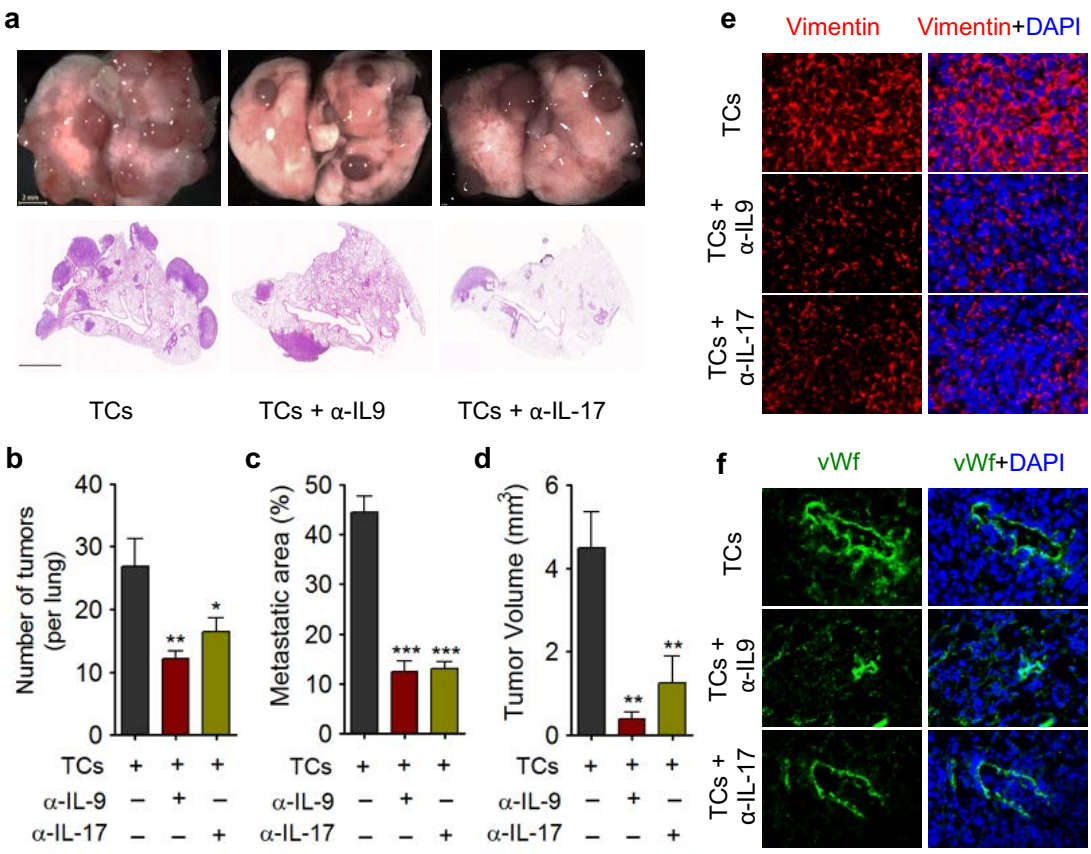

Figure 34. Treatment with neutralizing antibodies against IL-9 and IL-17 reduces lung tumor metastasis *in vivo*. a) Representative pictures of extracted lungs and H&E stained sections on day 20 after i.v. injection of tumor cells. **b, c and d)** Quantification of macroscopic nodules (n = 10), percentage of metastatic area and tumor volume (n = 4). Data are represented as a mean ± SEM, *p≤0.05, **p≤0.01, *** p≤0.001 when compared to control. **e)** Immunofluorescence of Vimentin (red) in sections of lung metastatic nodules after treatment with neutralizing antibodies. **f)** Immunofluorescence of vonWillebrand factor (green) in sections of lung metastatic nodules after treatment with neutralizing antibodies.

Metastatic nodules on the lungs of mice with neutralized IL-9 and IL-17 were significantly reduced after antibody treatment when compared to non-treated mice (*Figure 34 a*). Likewise, tumor volume and percentage of metastatic area in lungs was decreased after treatment with neutralizing antibodies (*Figure 34 b, c and d*). Presence of the mesenchymal marker Vimentin was evaluated in lung tissue sections, where it was noticeably decreased in mice treated with antibodies against IL-9 and in a lesser degree for IL-17 treated mice (*Figure 34 e*). Angiogenesis, as indicated by the presence of vonWillebrand factor, was increased in lung tissue sections of mice treated with neutralizing antibodies against both cytokines (*Figure 34 f*).

5. Discussion

The presence of immune cells at tumor sites was first reported more than a century ago by Virchow who noted a strong leukocyte infiltrate in neoplastic tissues and reasoned that cancer originated at sites of chronic inflammation (Balkwill and Mantovani 2001). Since then, research has linked inflammation as a starting or promoting factor in tumor development. This is supported by evidence of inflammatory cytokines and chemokines, secreted by tumor cells and/or tumor-associated leukocytes that can directly modulate cancer cell proliferation and migration, such as TNF-α, IL-1 or CCL2 among others.

Production of these cytokines during inflammation and the subsequent activation of the NFκB signaling pathway has previously been linked with the direct upregulation of potent EMT inducers including Snail and ZEB factors. Likewise, TNF-α has also been associated with induction of Snail1 promotor activity and stabilization of Snail protein, providing further evidence of a link between inflammation, EMT, and tumor development (Lopez-Novoa and Nieto 2009).

5.1 Lymphocyte CM prompted an Epithelial-Mesenchymal transition in human lung cancer cells

Co-culture models have been used to study the interactions between cell populations and are fundamental in the research of complex multicellular systems such as the tumor microenvironment. These models for cancer cells and lymphocytes are an useful tool allowing researchers to mimic a setting similar to the tumor stroma where lymphocytes would be in close or direct contact with cancer cells and assess how secreted factors affect both tumor cell phenotype and lymphocyte plasticity (Bogdanowicz and Lu 2013).

After exposure of both cancer cells and primary tumor cells to lymphocyte CM we observed some of the hallmarks of an epithelial-mesenchymal transition, a process, that is necessary for tumor cells to invade and metastasize, even though it also takes place during normal development, tissue healing and other non-malignant processes. EMT is characterized by phenotypical alterations, such as, cytoskeletal reorganization, detachment of the ECM, and loss of polarity (Xiao and He 2010). Stimulation of tumor cells with lymphocyte CM caused the expected phenotype change, as well as, deregulation of epithelial and mesenchymal markers, confirmed both at protein and RNA level, and more importantly, enhanced the migratory capacity of lung cancer cells.

Previous studies have revealed a link between lung cancer progression and EMT, for instance, in a large-scale TMA analysis from more than 300 patients, the epithelial-mesenchymal phenotype, characterized through E-cadherin, N-cadherin, Vimentin, MMP9,

and integrin-αvβ6 expression levels was analyzed with IHC staining in both adenocarcinoma and squamous cell tissues and found to be deregulated when compared to normal bronchial epithelium in a manner consistent with an EMT transition. Researchers found the EMT phenotype homogenously present in the lung tumor samples analyzed and therefore reached the conclusion that it must be associated with the development of these specific tumor types (Prudkin et al. 2009). Moreover, studies in patients with surgically resected NSCLC were able to link expression of other EMT markers such as Twist, Slug and periostin with larger tumor size, worse overall survival and shorter recurrence-free survival (Bao et al. 2016; Jiang et al. 2012; Soltermann et al. 2008).

As for the role of immune cells in EMT and tumor progression, research has shown that the supernatant derived from *in vitro* immune reactions was able to induce EMT in lung, breast and liver carcinoma cells. Co-culture of lung tumor cells after induction of EMT with T, B and NK cells resulted in the promotion of a number of immune-modulatory mechanisms. A549 cells specifically, seemed to strongly modulate immune cell behavior by, reducing NK cell viability and proliferation and hampering T and B cell proliferation without significant induction of regulatory B and T cells, all of which contributed to the escape of tumor cells from immune checkpoints (Ricciardi et al. 2015).

In similar fashion, our findings demonstrate that the *in vitro* interaction between tumor cells and lymphocytes triggers the secretion of factors capable of inducing an EMT transition in cancer cells characterized by the modification of cell phenotype towards a more migratory and highly proliferative state.

5.2 Co-culture of lymphocytes and cancer cells triggers secretion of a wide array of pro-inflammatory cytokines

After the characterization of an EMT phenotype caused by stimulation with lymphocyte CM we hypothesize that factors secreted during the crosstalk of cancer cells and immune cells were able to induce the transition of tumor cells into a more mesenchymal phenotype. Indeed, with the use of a broad-spectrum cytokine array we were able to confirm that the Co-culture CM has a distinct and more heterogeneous profile of secreted cytokines in comparison to the supernatant of either cell (lymphocyte or A549 control), corroborating that the interaction between activated lymphocytes and cancer cells is vital for cytokine production.

Among some of the upregulated cytokines in the Co-culture CM are IL-8, IL-6, CCL2 and IL-17, in spite of being a wide-ranging group of cytokines, the majority function as chemoattractant stimuli for other immune cells such as neutrophils or macrophages. Additionally, these cytokines can be secreted by a large number of both immune and non-immune cells. Excluded from this group is IL-17, which can only be secreted by cells of the

adaptive immune system, with its major source being Th17 cells. Considering that Th17 cells also contribute to the secretion of IL-9 the levels of both these cytokines were then analyzed with an ELISA assay.

Whether lymphocyte activation was done artificially (by use of PMA) or by the use of antibodies against the T-cell receptor (α-CD3 activation) higher amounts of cytokines IL-9 and IL-17 (Isotypes A and F) were consistently detected in all Co-culture CM. Similarly, studies in inflammatory breast cancer have linked cytokine production with an EMT transition in cancer cells. Specifically, TNF-α secreted by activated T cells, was able to induce the EMT phenotype and enhance metastasis of breast cancer cells, whereas when CM was supplemented with neutralizing antibodies against TNF-α, IL-6, and TGF-β, cancer cells exhibited a less pronounced EMT effect (Cohen et al. 2015).

5.3 Th9 cells and IL-9 in tumor progression and metastasis

Th9 cells are characterized by the production of IL-9, IL-21, and IL-10, and their differentiation occurs in the presence of TGF-β and IL-4, which then induce the expression of transcription factors PU.1 and IRF4. They have been extensively researched in cases of chronic allergic inflammation and autoimmune disease. Additionally, they are critical for host defense against helminth infections (Chen, Zhang, et al. 2017; Buttrick et al. 2018).

In the field of tumor immunology, Th9 cells have been strongly connected with anti-tumor responses *in vivo,* specifically in melanoma models where adoptive transfer therapy of tumor specific Th9 cells was able to mediate tumor regression resulting in long-term survival in mice. In another melanoma model using ROR-γ knockout mice, which are deficient in Th17 cells, IL-9 levels were found to be upregulated and linked to a significant inhibition of primary tumor growth (Lu et al. 2018; Purwar et al. 2012).

Conversely, in models of HCC and pancreatic cancer, IL-9 significantly promoted proliferation, migration, and invasion of cancer cells *in vitro*, in the case of hepatocellular carcinoma (HCC) through phosphorylation of STAT3 and JAK2, whereas in pancreatic cancer cells, the effect of this cytokine was linked to the regulation of the miR200a/β-catenin axis (Lei et al. 2017; Hu et al. 2017). Specifically, for lung cancer, researchers found that A549 cells had high levels of expression of the IL-9 receptor and through phosphorylation of STAT3, IL-9 significantly promoted proliferation and migration of this cell line. Additionally, both IL-9 and IL-17 were able to inhibit apoptosis induced by IFN-γ and facilitate intercellular adhesion of lung cancer cells to pleural mesothelial cell monolayers (Ye et al. 2012).

Evidently, the role of Th9 and its effector cytokine IL-9, in tumor development and progression seems to be distinctive to the tissue type and could therefore be modulated by different molecules.

Despite *in vitro* and *in vivo* evidence for the role of Th9 cells in tumor development, to the best of our knowledge, only studies in HCC have been done to assess the impact of these cells in overall patient survival. In this particular study, researchers found that patients had elevated serum levels of IL-9 and a higher frequency of circulating Th9 cells in PBMCs, peritumor, and tumor tissues. Th9 cells upregulated in HCC appear to exert their effects through CCL20 and STAT3 and patients in the high Th9 frequency group had significantly shorter disease-free survival periods after resection (Tan, Wang, and Zhao 2017).

Through Opal Multiplex staining, we were able to confirm the presence of IL-9 producing $CD4^+$ T cells in human lung tumors and correlate the presence of these cells (both Th9 and Th17) with a reduction in patient survival, adding to existing data in other tumor models of the beneficial effects of Th9 cells in cancer development.

Both the specific Th9 CM and IL-9 strongly induced migration and proliferation and caused the expected deregulation of EMT markers in tumor cells, which would lead to the conclusion of some consistent activation in signaling pathways associated with these cellular processes. Indeed, results from RNA sequencing indicate that Co-culture is followed by a deregulation in the gene expression pattern of cancer cells. Co-culture of tumor cells with Th9 resulted in the upregulation of known EMT markers, MMPs. These enzymes facilitate detachment of epithelial cells from the surrounding tissue and degrade cell-cell junctions. MMP3 and MMP13 specifically, are both upregulated after Co-culture with Th9 cells and have been linked with EMT and metastasis in models of breast cancer and melanoma (Sternlicht et al. 1999; Radisky et al. 2005; Zigrino et al. 2009).

Our results raised the issue of neutralizing antibodies as a way to counteract the effects of IL-9 in the tumor microenvironment. Accordingly, the use of neutralizing antibodies as treatment after injection of cancer cells confirmed a decrease in metastasis, as observed in both the amount of overall lung tumor nodules, as well as the area and volume occupied by these nodules. As expected, Vimentin and vonWillebrand factor, markers previously used to assess the tumor microenvironment, were shown to be reduced as a result of the antibody therapy. Similarly, neutralization of IL-9 coupled with anti-4-1BB treatment (or CDw137, a transmembrane protein expressed by activated T cells) in subcutaneous models of breast cancers resulted in rejection of the primary tumor and the generation of a protective memory response in mice, seemingly through modulation of Treg function (Smith et al. 2011). However, in models of melanoma, it was reported that treatment with antibodies against IL-9 increased the number of tumor nodules to the lung and substantially decreased leukocyte subsets in lung tissues, providing more evidence to a tissue specific behavior of Th9 cells in tumor development (Lu et al. 2012).

Our study provides novel evidence regarding the role of Th9 and IL-9 in lung tumor development and metastatic progression.

5.4 Th17 cells and Il-17 in tumor progression and metastasis

Th17 cells, another specific subset of $CD4^+$ T cells, with the ability to secrete IL-17, IL-9, IL-21, and IL-22 among others, are crucial in the host defense against extracellular pathogens by mediating the recruitment of neutrophils and macrophages. The master regulator of Th17 cell differentiation is ROR-γ whose expression is induced when T cells are in the presence of TGF-β and IL-6. Research on the role of Th17 cells in the tumor stroma has so far been controversial, with contradictory evidence for both a promoting and suppressing role in tumor growth depending on the cancer model and therapeutic intervention (Bailey et al. 2014).

With the use of Opal Multiplex staining, we were able to detect IL-17 producing $CD4^+$ T cells in TMAs of human lung tumors and correlate presence of these cells (for both Th9 and Th17) with a reduction in overall patient survival. Opposite results have been reported in leukemia and thyroid cancer, where studies have observed an improved prognosis in patients with higher infiltration of Th17 cells in tumors (Punt et al. 2015; Cunha et al. 2012). Increased frequency of Th17 cells among PBMCs also appears to improve patient survival, though conflicting evidence has been reported for gastric cancer and HCC, where the balance between Th17 cells and other T helper cells (Th1/Th22) was considered a prognostic factor for the severity of the disease (Abousamra, Salah El-Din, and Helal 2013; Liao et al. 2013; Sarnaik et al. 2011; Yan et al. 2014; Liu et al. 2012).

In particular, for lung cancer, research in NSCLC confirms our results of a correlation between IL-17-producing cells and decreased patient survival. Researchers were able to link intratumoral IL-17 positive cell frequency with lymphatic vessel density (LVD) and therefore explain how Th17 cells could be promoting tumor development by enhancing lymphangiogenesis (Chen et al. 2010).

Stimulation with both IL-17 A and F and the supernatant of Th17 cells consistently resulted in decreased levels of the epithelial markers E-cadherin and ZO-2 in both mouse and human cancer cell lines and human tumor primary cells. Repeatedly, we were able to detect an increase in the migratory capacity of tumor cells after stimulation with either Th17 cells or their effector cytokine, IL-17. Protein expression patterns from subcutaneous tumors obtained from *in vivo* co-injection models of cancer cells with Th17, displayed epithelial and mesenchymal markers regulated accordingly with an EMT transition, linking the increase in migration observed in cancer cells to the hypothesis that Th17 cells could be modulating cancer cell motility and consequently be involved in the promotion of metastasis.

Interestingly, MMP9 was upregulated in the tumor stroma of mice co-injected with Th17 cells, further pointing to MMPs as essential factors mediating the effects seen in our studies. Extensive evidence in breast cancer, NSCLC, and gastric cancer has identified a critical role

for MMP9 in metastasis. MMP9 knockdown in human breast cancer cells significantly reduced migration and mice injected with stably transfected MMP9-targeted lentiviral shRNA cells showed a complete reduction of metastasis to the lung when compared to controls (Mehner et al. 2014). In NSCLC, higher levels of MMP9 were reported for resected tumors compared to adjacent normal tissue and phosphorylation of EGFR was shown to activate MMP9 and promote cancer invasiveness (Li et al. 2015). Likewise, expression of MMP9 in gastric tumors was positively correlated with tumor size and lymph node metastasis (Zheng et al. 2006).

The link between Th17 cells and an increase in metastasis was further confirmed by tail vein injections of mouse tumor cells, where mice co-injected with Th17 cells and tumor cells, displayed a significant increase in lung tumor nodules. Fitting to this observation, deregulation of Vimentin and vonWillebrand factor, signals an EMT transition resulting in an increased metastatic potential of cancer cells present in the tumor stroma. Similar observations on the potential link of Th17 cells in the development of metastasis, have been recently reported in patients and *in vitro* models. In resected tissue from patients with gastric cancer, IL-17 and the Th17 associated transcription factor RORγt, were up to 30-fold upregulated in metastasis patients. Similarly, in patients with lung adenocarcinoma frequency of Th17 cells was higher than in healthy controls and was associated with tumor invasion and metastasis. Although most studies point to Th17 cells as the major source of IL-17 production, others report that γδT cells (another subset of T cells with a gamma-delta (γδ) heterodimer TCR) also have a role in cytokine production (Bao et al. 2016; Kulig et al. 2016; Su et al. 2014).

Neutralization of IL-17 in our metastasis model leads to a strong decrease in lung tumor nodules, with other studies also reporting decreased tumor growth and metastasis in models of mammary carcinoma and lymphoma. These reports suggest that IL-17 has an effect on the tumor microenvironment by modulating other immune cells, on the one hand by preventing the migration of pro-tumorigenic neutrophils and on the other by inhibiting $CD8^+$ T cell infiltration and increasing the amount of myeloid-derived suppressor cells (MDSC), which are known to have a major role in immunosuppression at tumor sites (Benevides et al. 2015; He et al. 2010).

Additionally, Vimentin and vonWillebrand factor, were shown to reduce as a result of the neutralizing antibody therapy providing a complete picture of cancer cells with a distinct mesenchymal phenotype present in the stroma and a tumor microenvironment supporting angiogenesis.

5.5 Effect on LLC1 cells from Co-culture with Th9 and Th17 cells is characterized by the upregulation of common transcription factors associated with EMT and tumor progression

To gain insight into the pathways that are activated during Co-culture of cancer cells and the specific Th9 and Th17 subsets, RNA of previously sorted co-cultured cancer cells was sequenced. One of the upregulated genes in cancer cells after Co-culture with Th9 was Plxna4, which codes for the PlexinA-4 protein, necessary for signaling by class 3 semaphorins and therefore modulates cytoskeletal reorganization. Reports for melanoma have associated this protein with tumor progression and angiogenesis because of its ability to form a complex with the VEGFR-2 receptor and modulate VEGF signaling (Kigel et al. 2011). Adding to these results, upregulation in tumor homogenate of the angiogenesis marker, CD31, for the Th9 co-injection group further supports a role for Th9 cells as promotors of angiogenesis in tumor development.

Similarly, complement component 3 (C3), a protein with a central role in innate immunity, was upregulated after Co-culture. Although predominantly synthetized by hepatocytes, it has been reported to be secreted by malignant cells, where it was able to inhibit E-cadherin expression and was regulated by the transcription factor Twist, a known EMT promotor (Cho et al. 2016).

Sequencing data obtained from LLC1 in co-culture with Th17 cells exhibited expression changes in the Ywhaz gene, encoding 14-3-3 protein zeta/delta, a highly conserved protein that regulates signal transduction pathways through binding of phosphoserine proteins. Proteins in the 14-3-3 family are involved in a variety of cellular processes raging from cell cycle control and protein trafficking to cell adhesion and motility. Overexpression of Ywhaz has been correlated with increased tumor size and high rate of lymph node metastasis in gastric carcinoma, adenocarcinoma of the esophago-gastric junction, and breast cancer (Watanabe et al. 2016; Lu et al. 2009; Nishimura et al. 2013). Upregulation of the Ywhaz protein product has already been reported in lung cancer, where its overexpression correlated with stage and grading of NSCLC and inversely related to patient survival (Fan et al. 2007). *In vitro* studies revealed that cells transfected with a YWHAZ construct displayed increased cell invasiveness and migration and mice injected with YWHAZ transfected cells developed more pulmonary metastasis nodules. Levels of N-cadherin, Vimentin, and Slug were increased in YWHAZ transfected cells compared with the control. The same study found that the metastatic activity of YWHAZ was mediated through prevention of β-catenin ubiquitination and subsequent nuclear accumulation leading to the deregulation of EMT markers (Chen et al. 2012).

Both the Co-culture with Th9 and Th17 cells lead to the upregulation of Krüppel-like factors (Klfs) in tumor cells; Klfs comprise a family of 17 zinc finger DNA-binding proteins that regulate gene expression. Some Klfs upregulated during Co-culture such as Klf7, have been found to be significantly upregulated in oral squamous cell carcinoma and are associated with lymph node metastasis in patients. Knockdown of Klf7 in cells leads to decreased migration and an increase in E-cadherin whereas mesenchymal markers N-cadherin and Vimentin were downregulated (Ding et al. 2017). Klf5 has also been associated with more aggressive and metastatic tumors, with reports confirming that Klf5 can bind to GC-boxes of the VEGFA promoter and regulate its transcription in tumor cells (Gao et al. 2015).

The results reported in this study reveal novel evidence on the specific role of Th17 and IL-17 in lung tumor development and metastatic progression.

5.6 Conclusion

The crosstalk between immune and cancer cells in the tumor microenvironment plays an important role in tumor progression and metastasis. In this work, we studied how the interaction between immune cells, specifically Th9 and Th17 cells, and cancer cells affects their phenotype and function. Indeed, both Th9 and Th17 cells and their effector cytokines IL-9 and IL-17 were able to induce epithelial-mesenchymal transition in lung cancer cells, characterized by loss of epithelial markers, gain of mesenchymal markers and a heightened migratory profile.

Co-injection of Th9 cells resulted in larger primary tumor size, whereas Th17 cells specifically impacted metastasis for both subcutaneous and intravenous cancer cell injection. RNA sequencing data of mouse cancer cells after co-culture with differentiated Th9 and Th17 points toward possible target genes that could account for the observed effects in this study, such as Plexin A4, Ywhaz, and commonly regulated Krüppel-like factors. However, further research must be done to elucidate their involvement in the observed EMT-inducing effects of Th9 and Th17 cells in the tumor microenvironment.

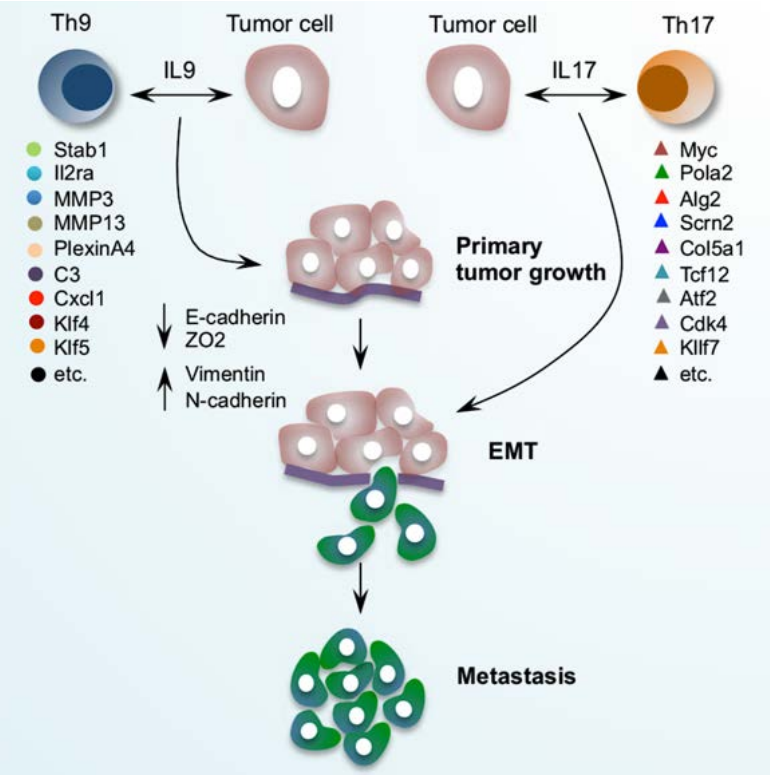

Figure 35. Summary figure with proposed players in the pro-metastatic and EMT-inducing effect of Th9 and Th17 cells in lung cancer. The specific subsets through secretion of their signature cytokines; IL-9 and IL-17, induce the transition of tumor cells to a highly migratory mesenchymal phenotype characterized by loss of epithelial markers (E-cadherin, ZO2) and gain of mesenchymal markers (Vimentin, N-cadherin). This effect is associated with corresponding EMT- and migration- related protein and transcription factor gene regulation in tumor cells that are in direct crosstalk with a specific Th subtype.

5.7 Outlook

With the use of Co-culture systems, *in vitro* research, and primary tumor and metastasis models, we have provided evidence that Th9 and Th17 cells contribute to the progression of lung cancer and metastasis. However, many aspects of this effect remain unclear and require further research to fully elucidate the signaling pathways at play.

In particular, experiments with immunocompetent mice depleted for Th9 and Th17 cells should be done to reveal whether the observed effects on metastasis are reversed. Furthermore, it would be important to carry out intravenous cancer cell injection experiments in IL-17RA, IL-17-RC and IL-9 knockout mice to distinguish between the effects of the immune cells and their effector cytokines.

Additional work must to be done to research the targets obtained by RNA-sequencing, especially on those that were upregulated by both cell types, which could hint at an activation of a shared signaling pathway, such was the case for Krüppel-like transcription factors (Klfs). Another important player seems to be MMPs, which were found to be upregulated both in protein in primary tumor stroma and RNA after Co-culture with both Th9 and Th17 cells and

have been extensively linked with EMT transition and metastasis progression. In both cases, *in vitro* migration and protein expression experiments with inhibitors for these targets could provide more information toward their involvement in the effects observed in cancer cells.

Further efforts aimed at identifying a specific signaling pathway that is regulated during this process could later provide the means to precisely inhibit or block the effects observed *in vivo* and hence serve as a therapeutic approach to counteract the detrimental effects of Th9 and Th17 cells on cancer cell behavior.

6. Summary

Immune cells in the tumor microenvironment have a critical role in lung cancer control versus progression and metastasis. In this study, we explored the role of tumor-infiltrating-lymphocyte subpopulations in lung cancer progression by performing in vitro co-culturing, in vivo mouse tumor models and human lung cancer tissue staining. CM from the Co-culture of activated lymphocytes and lung cancer cells was able to induce an EMT transition in both human and mouse tumor cells, characterized by deregulation of epithelial and mesenchymal markers and increased migration. Co-Culture CM displayed a distinct secretome profile when compared to the supernatant of either lymphocytes or cancer cells alone. Specifically, cytokines IL-9, IL-17 A and F were increased in Co-Culture CM.

Detection of Th9 and Th17 cells in tissue microarrays from human lung cancer tissue correlated with a decrease in patient survival and these cells were frequently identified in the stromal area of tumors. Co-Culture of lung cancer cells with the specific Th9 and Th17 subtypes replicated the deregulation of EMT markers and migration induction observed with Lymphocyte CM, thereby pointing toward these cells as responsible for the observed effects on cancer cell behavior. Additionally, Co-culturing of lung cancer cells with Th9 or Th17 cells modulated the expression profile of genes implicated in EMT, metastasis, and angiogenesis, such as MMPs and the Klf family of transcription factors. Stimulation with the individual effector cytokines, IL-9 and IL-17, reproduced the results observed by exposure to CM, further supporting the involvement of Th9 and Th17 cells, and their effector cytokines, in tumor development and progression.

Co-injection of Th9 and/or Th17 cells with tumor cells in mouse lung cancer models promoted primary tumor growth and metastasis. Th9 specially affected tumor size and weight after subcutaneous injection, whereas Th17 cells had a specific effect on metastasis in models of primary tumor and metastasis. Consequently, inhibition of IL-9 or IL-17 cytokines by neutralizing antibodies decreased protein expression of EMT markers and slowed lung cancer progression and metastasis.

In conclusion, our results assign Th9 and Th17 lymphocytes a prominent role in the induction of lung cancer cell EMT, thereby promoting migration and metastatic spreading, and could provide novel therapeutic strategies targeting some of the targets described in our work.

7. Zussamenfassung

Immunzellen im Tumormikromilieu von Lungenkrebs spielen eine wichtige Rolle bei Kontrolle gegenüber dem Fortschreiten des Erkrankungsverlaufs und der Metastasierung. Ziel dieser Studie ist es, die Bedeutung tumorinfiltrierender Subpopulationen von Lymphozyten in der Progression von Lungenkrebs mittels *in vitro* Kokulturen, *in vivo* Maus-Tumormodellen und humanem Lungenkrebsgewebe zu untersuchen.

Es konnte gezeigt werden, dass konditionelles Medium (CM) von aktivierten Lymphozyten ko-kultiviert mit Lungenkrebszellen epithelial-mesenchymale Transition (EMT), die durch Deregulierung von Epithel- und Mesenchym-Markern sowie erhöhter Migration charakterisiert ist, in humanen und murinen Tumorzellen auslöst. Im Vergleich zu überständen von Lymphozyten oder Krebszellen allein, zeigte das Ko-Kultur-CM ein eindeutig verändertes Sekretom, wobei besonders stark erhöhte Mengen der Zytokine IL-9, IL-17A und F detektiert werden konnten.

Detektion von Th9- und Th17-Zellen durch Microarrays von humanem Lungenkrebsgewebe korrelierte mit erniedrigter Überlebenszeit der Patienten. Zudem konnten diese Zellen häufig im Tumorstroma identifiziert werden. Die durch Lymphozyten-CM ausgelöste Deregulierung der EMT Marker und der Zellmigration konnte durch Ko-Kultur von Lungenkrebszellen mit den Th9- und Th17-Subtypen nachgeahmt werden. Dies deutet darauf hin, dass sie für die Änderung im Verhalten der Tumorzellen verantwortlich sind. Zusätzlich konnte ein verändertes Expressionsprofil von Genen wie MMPs und der Klf-Transkriptionsfaktorfamilie, die mit EMT, Metastasierung und Angiogenese assoziiert sind, in den mit Th9- und Th17-Zellen ko-kultivierten Lungenkrebszellen gezeigt werden. Stimulation mit den Effektorzytokinen IL-9 und IL-17 reproduzierten die durch CM-Behandlung beobachteten Ergebnisse, wodurch weiter unterstützt wird, dass Th9- und Th17-Zellen sowie ihre Effektorzytokine, in der Tumorentwicklung und im Tumorwachstum involviert sind.

Ko-injektion von Th9- und/oder Th17-Zellen mit Tumorzellen im Maus-Lungenkrebsmodell verstärkte primäres Tumorwachstum und Metastasierung. Besonders Th9-Zellen zeigten einen Effekt auf Tumorgröße und -gewicht nach subkutaner Injektion, wobei Th17-Zellen spezifisch auf Metastasierung im Primärtumor- und Metastase-Mausmodell wirkten. Inhibition von IL-9 oder IL-17 durch neutralisierende Antikörper verringerten Proteinexpression von EMT Markern und verlangsamten Lungenkrebswachstum und Metastasierung.

Abschließend kann aus unseren Ergebnissen geschlussfolgert werden, dass Th9- und Th17-Lymphozyten in der Einleitung von EMT bei Lungenkrebs eine bedeutende Rolle spielen, wodurch Zellmigration und Metastasierung erhöht wird. Die in dieser Arbeit beschriebenen Zielmoleküle können daher als Grundlage zur Entwicklung neuartiger Therapien dienen.

8. References

Abousamra, N. K., M. Salah El-Din, and R. Helal. 2013. 'Prognostic value of Th17 cells in acute leukemia', *Med Oncol*, 30: 732.

Aggarwal, S., N. Ghilardi, M. H. Xie, F. J. de Sauvage, and A. L. Gurney. 2003. 'Interleukin-23 promotes a distinct CD4 T cell activation state characterized by the production of interleukin-17', *J Biol Chem*, 278: 1910-4.

Al-Zoughool, M., J. Pintos, L. Richardson, M. E. Parent, P. Ghadirian, D. Krewski, and J. Siemiatycki. 2013. 'Exposure to environmental tobacco smoke (ETS) and risk of lung cancer in Montreal: a case-control study', *Environ Health*, 12: 112.

Amatya, N., A. V. Garg, and S. L. Gaffen. 2017. 'IL-17 Signaling: The Yin and the Yang', *Trends Immunol*, 38: 310-22.

Asadzadeh, Z., H. Mohammadi, E. Safarzadeh, M. Hemmatzadeh, A. Mahdian-Shakib, F. Jadidi-Niaragh, G. Azizi, and B. Baradaran. 2017. 'The paradox of Th17 cell functions in tumor immunity', *Cell Immunol*, 322: 15-25.

Bailey, S. R., M. H. Nelson, R. A. Himes, Z. Li, S. Mehrotra, and C. M. Paulos. 2014. 'Th17 cells in cancer: the ultimate identity crisis', *Front Immunol*, 5: 276.

Balkwill, F., and A. Mantovani. 2001. 'Inflammation and cancer: back to Virchow?', *Lancet*, 357: 539-45.

Balkwill, F. R., M. Capasso, and T. Hagemann. 2012. 'The tumor microenvironment at a glance', *J Cell Sci*, 125: 5591-6.

Banat, G. A., A. Tretyn, S. S. Pullamsetti, J. Wilhelm, A. Weigert, C. Olesch, K. Ebel, T. Stiewe, F. Grimminger, W. Seeger, L. Fink, and R. Savai. 2015. 'Immune and Inflammatory Cell Composition of Human Lung Cancer Stroma', *PLoS One*, 10: e0139073.

Bandera, E. V., J. L. Freudenheim, and J. E. Vena. 2001. 'Alcohol consumption and lung cancer: a review of the epidemiologic evidence', *Cancer Epidemiol Biomarkers Prev*, 10: 813-21.

Bao, Z., G. Lu, D. Cui, Y. Yao, G. Yang, and J. Zhou. 2016. 'IL-17A-producing T cells are associated with the progression of lung adenocarcinoma', *Oncol Rep*, 36: 641-50.

Basdeo, S. A., D. Cluxton, J. Sulaimani, B. Moran, M. Canavan, C. Orr, D. J. Veale, U. Fearon, and J. M. Fletcher. 2017. 'Ex-Th17 (Nonclassical Th1) Cells Are Functionally Distinct from Classical Th1 and Th17 Cells and Are Not Constrained by Regulatory T Cells', *J Immunol*, 198: 2249-59.

Baskar, R., K. A. Lee, R. Yeo, and K. W. Yeoh. 2012. 'Cancer and radiation therapy: current advances and future directions', *Int J Med Sci*, 9: 193-9.

Bedoya, S. K., B. Lam, K. Lau, and J. Larkin, 3rd. 2013. 'Th17 cells in immunity and autoimmunity', *Clin Dev Immunol*, 2013: 986789.

Benevides, L., D. M. da Fonseca, P. B. Donate, D. G. Tiezzi, D. D. De Carvalho, J. M. de Andrade, G. A. Martins, and J. S. Silva. 2015. 'IL17 Promotes Mammary Tumor Progression by Changing the Behavior of Tumor Cells and Eliciting Tumorigenic Neutrophils Recruitment', *Cancer Res*, 75: 3788-99.

Bogdanowicz, D. R., and H. H. Lu. 2013. 'Studying cell-cell communication in co-culture', *Biotechnol J*, 8: 395-6.

Breathnach, O. S., B. Freidlin, B. Conley, M. R. Green, D. H. Johnson, D. R. Gandara, M. O'Connell, F. A. Shepherd, and B. E. Johnson. 2001. 'Twenty-two years of phase III trials for patients with advanced non-small-cell lung cancer: sobering results', *J Clin Oncol*, 19: 1734-42.

Broere, Femke, Sergei G. Apasov, Michail V. Sitkovsky, and Willem van Eden. 2011. 'A2 T cell subsets and T cell-mediated immunity.' in F. P. Nijkamp and Michael J. Parnham (eds.), *Principles of Immunopharmacology: 3rd revised and extended edition* (Birkhäuser Basel: Basel).

Buttrick, T. S., W. Wang, C. Yung, K. G. Trieu, K. Patel, S. J. Khoury, X. Ai, and W. Elyaman. 2018. 'Foxo1 Promotes Th9 Cell Differentiation and Airway Allergy', *Sci Rep*, 8: 818.

Carstens, J. L., P. Correa de Sampaio, D. Yang, S. Barua, H. Wang, A. Rao, J. P. Allison, V. S. LeBleu, and R. Kalluri. 2017. 'Spatial computation of intratumoral T cells correlates with survival of patients with pancreatic cancer', *Nat Commun*, 8: 15095.

Chen, C. H., S. M. Chuang, M. F. Yang, J. W. Liao, S. L. Yu, and J. J. Chen. 2012. 'A novel function of YWHAZ/beta-catenin axis in promoting epithelial-mesenchymal transition and lung cancer metastasis', *Mol Cancer Res*, 10: 1319-31.

Chen, H., L. Zhang, P. Wang, H. Su, W. Wang, Z. Chu, L. Zhang, X. Zhang, and Y. Zhao. 2017. 'mTORC2 controls Th9 polarization and allergic airway inflammation', *Allergy*, 72: 1510-20.

Chen, T., Y. You, H. Jiang, and Z. Z. Wang. 2017. 'Epithelial-mesenchymal transition (EMT): A biological process in the development, stem cell differentiation, and tumorigenesis', *J Cell Physiol*, 232: 3261-72.

Chen, X., J. Wan, J. Liu, W. Xie, X. Diao, J. Xu, B. Zhu, and Z. Chen. 2010. 'Increased IL-17-producing cells correlate with poor survival and lymphangiogenesis in NSCLC patients', *Lung Cancer*, 69: 348-54.

Cho, M. S., R. Rupaimoole, H. J. Choi, K. Noh, J. Chen, Q. Hu, A. K. Sood, and V. Afshar-Kharghan. 2016. 'Complement Component 3 Is Regulated by TWIST1 and Mediates Epithelial-Mesenchymal Transition', *J Immunol*, 196: 1412-8.

Cohen, E. N., H. Gao, S. Anfossi, M. Mego, N. G. Reddy, B. Debeb, A. Giordano, S. Tin, Q. Wu, R. J. Garza, M. Cristofanilli, S. A. Mani, D. A. Croix, N. T. Ueno, W. A. Woodward, R. Luthra, S. Krishnamurthy, and J. M. Reuben. 2015. 'Inflammation Mediated Metastasis: Immune Induced Epithelial-To-Mesenchymal Transition in Inflammatory Breast Cancer Cells', *PLoS One*, 10: e0132710.

Cote, M. L., M. Liu, S. Bonassi, M. Neri, A. G. Schwartz, D. C. Christiani, M. R. Spitz, J. E. Muscat, G. Rennert, K. K. Aben, A. S. Andrew, V. Bencko, H. Bickeboller, P. Boffetta, P. Brennan, H. Brenner, E. J. Duell, E. Fabianova, J. K. Field, L. Foretova, S. Friis, C. C. Harris, I. Holcatova, Y. C. Hong, D. Isla, V. Janout, L. A. Kiemeney, C. Kiyohara, Q. Lan, P. Lazarus, J. Lissowska, L. Le Marchand, D. Mates, K. Matsuo, J. I. Mayordomo, J. R. McLaughlin, H. Morgenstern, H. Mueller, I. Orlow, B. J. Park, M. Pinchev, O. Y. Raji, H. S. Rennert, P. Rudnai, A. Seow, I. Stucker, N. Szeszenia-Dabrowska, M. Dawn Teare, A. Tjonnelan, D. Ugolini, H. F. van der Heijden, E. Wichmann, J. K. Wiencke, P. J. Woll, P. Yang, D. Zaridze, Z. F. Zhang, C. J. Etzel, and R. J. Hung. 2012. 'Increased risk of lung cancer in individuals with a family history of the disease: a pooled analysis from the International Lung Cancer Consortium', *Eur J Cancer*, 48: 1957-68.

Cote-Sierra, J., G. Foucras, L. Guo, L. Chiodetti, H. A. Young, J. Hu-Li, J. Zhu, and W. E. Paul. 2004. 'Interleukin 2 plays a central role in Th2 differentiation', *Proc Natl Acad Sci U S A*, 101: 3880-5.

Cua, D. J., J. Sherlock, Y. Chen, C. A. Murphy, B. Joyce, B. Seymour, L. Lucian, W. To, S. Kwan, T. Churakova, S. Zurawski, M. Wiekowski, S. A. Lira, D. Gorman, R. A. Kastelein, and J. D. Sedgwick. 2003. 'Interleukin-23 rather than interleukin-12 is the critical cytokine for autoimmune inflammation of the brain', *Nature*, 421: 744-8.

Cukic, V. 2017. 'The Association Between Lung Carcinoma and Tuberculosis', *Med Arch*, 71: 212-14.

Cunha, L. L., E. C. Morari, A. C. Guihen, D. Razolli, R. Gerhard, S. Nonogaki, F. A. Soares, J. Vassallo, and L. S. Ward. 2012. 'Infiltration of a mixture of immune cells may be related to good prognosis in patients with differentiated thyroid carcinoma', *Clin Endocrinol (Oxf)*, 77: 918-25.

Dalton, D. K., and R. J. Noelle. 2012. 'The roles of mast cells in anticancer immunity', *Cancer Immunol Immunother*, 61: 1511-20.

Dardalhon, V., A. Awasthi, H. Kwon, G. Galileos, W. Gao, R. A. Sobel, M. Mitsdoerffer, T. B. Strom, W. Elyaman, I. C. Ho, S. Khoury, M. Oukka, and V. K. Kuchroo. 2008. 'IL-4 inhibits TGF-beta-induced Foxp3+ T cells and, together with TGF-beta, generates IL-9+ IL-10+ Foxp3(-) effector T cells', *Nat Immunol*, 9: 1347-55.

Davis, M. P., S. van Dongen, C. Abreu-Goodger, N. Bartonicek, and A. J. Enright. 2013. 'Kraken: a set of tools for quality control and analysis of high-throughput sequence data', *Methods*, 63: 41-9.

Denkert, C., G. von Minckwitz, S. Darb-Esfahani, B. Lederer, B. I. Heppner, K. E. Weber, J. Budczies, J. Huober, F. Klauschen, J. Furlanetto, W. D. Schmitt, J. U. Blohmer, T. Karn, B. M. Pfitzner, S. Kummel, K. Engels, A. Schneeweiss, A. Hartmann, A. Noske, P. A. Fasching, C. Jackisch, M. van Mackelenbergh, P. Sinn, C. Schem, C. Hanusch, M. Untch, and S. Loibl. 2018. 'Tumour-infiltrating lymphocytes and prognosis in different subtypes of breast cancer: a pooled analysis of 3771 patients treated with neoadjuvant therapy', *Lancet Oncol*, 19: 40-50.

Diamond, M. S., M. Kinder, H. Matsushita, M. Mashayekhi, G. P. Dunn, J. M. Archambault, H. Lee, C. D. Arthur, J. M. White, U. Kalinke, K. M. Murphy, and R. D. Schreiber. 2011. 'Type I interferon is selectively required by dendritic cells for immune rejection of tumors', *J Exp Med*, 208: 1989-2003.

Ding, X., X. Wang, Y. Gong, H. Ruan, Y. Sun, and Y. Yu. 2017. 'KLF7 overexpression in human oral squamous cell carcinoma promotes migration and epithelial-mesenchymal transition', *Oncol Lett*, 13: 2281-89.

Dobin, A., C. A. Davis, F. Schlesinger, J. Drenkow, C. Zaleski, S. Jha, P. Batut, M. Chaisson, and T. R. Gingeras. 2013. 'STAR: ultrafast universal RNA-seq aligner', *Bioinformatics*, 29: 15-21.

Duan, M. C., W. Han, P. W. Jin, Y. P. Wei, Q. Wei, L. M. Zhang, and J. C. Li. 2015. 'Disturbed Th17/Treg Balance in Patients with Non-small Cell Lung Cancer', *Inflammation*, 38: 2156-65.

Durham, A. L., and I. M. Adcock. 2015. 'The relationship between COPD and lung cancer', *Lung Cancer*, 90: 121-7.

Ellyard, J. I., L. Simson, and C. R. Parish. 2007. 'Th2-mediated anti-tumour immunity: friend or foe?', *Tissue Antigens*, 70: 1-11.

Fan, T., R. Li, N. W. Todd, Q. Qiu, H. B. Fang, H. Wang, J. Shen, R. Y. Zhao, N. P. Caraway, R. L. Katz, S. A. Stass, and F. Jiang. 2007. 'Up-regulation of 14-3-3zeta in lung cancer and its implication as prognostic and therapeutic target', *Cancer Res*, 67: 7901-6.

Fang, Y., X. Chen, Q. Bai, C. Qin, A. O. Mohamud, Z. Zhu, T. W. Ball, C. M. Ruth, D. R. Newcomer, E. J. Herrick, and M. B. Nicholl. 2015. 'IL-9 inhibits HTB-72 melanoma cell growth through upregulation of p21 and TRAIL', *J Surg Oncol*, 111: 969-74.

Ferlay, J., M. Colombet, I. Soerjomataram, T. Dyba, G. Randi, M. Bettio, A. Gavin, O. Visser, and F. Bray. 2018. 'Cancer incidence and mortality patterns in Europe: Estimates for 40 countries and 25 major cancers in 2018', *Eur J Cancer*, 103: 356-87.

Forde, P. M., and D. S. Ettinger. 2013. 'Targeted therapy for non-small-cell lung cancer: past, present and future', *Expert Rev Anticancer Ther*, 13: 745-58.

Fremd, C., F. Schuetz, C. Sohn, P. Beckhove, and C. Domschke. 2013. 'B cell-regulated immune responses in tumor models and cancer patients', *Oncoimmunology*, 2: e25443.

Gaffen, S. L. 2009. 'Structure and signalling in the IL-17 receptor family', *Nat Rev Immunol*, 9: 556-67.

Gaffen, S. L., R. Jain, A. V. Garg, and D. J. Cua. 2014. 'The IL-23-IL-17 immune axis: from mechanisms to therapeutic testing', *Nat Rev Immunol*, 14: 585-600.

Galon, J., A. Costes, F. Sanchez-Cabo, A. Kirilovsky, B. Mlecnik, C. Lagorce-Pages, M. Tosolini, M. Camus, A. Berger, P. Wind, F. Zinzindohoue, P. Bruneval, P. H. Cugnenc, Z. Trajanoski, W. H. Fridman, and F. Pages. 2006. 'Type, density, and location of immune cells within human colorectal tumors predict clinical outcome', *Science*, 313: 1960-4.

Gandhi, L., D. Rodriguez-Abreu, S. Gadgeel, E. Esteban, E. Felip, F. De Angelis, M. Domine, P. Clingan, M. J. Hochmair, S. F. Powell, S. Y. Cheng, H. G. Bischoff, N. Peled, F. Grossi, R. R. Jennens, M. Reck, R. Hui, E. B. Garon, M. Boyer, B. Rubio-Viqueira, S. Novello, T. Kurata, J. E. Gray, J. Vida, Z. Wei, J. Yang, H. Raftopoulos, M. C. Pietanza, M. C. Garassino, and Keynote- Investigators. 2018. 'Pembrolizumab plus Chemotherapy in Metastatic Non-Small-Cell Lung Cancer', *N Engl J Med*.

Gao, Y., K. Wu, Y. Chen, J. Zhou, C. Du, Q. Shi, S. Xu, J. Jia, X. Tang, F. Li, K. Hui, D. He, and P. Guo. 2015. 'Beyond proliferation: KLF5 promotes angiogenesis of bladder cancer through directly regulating VEGFA transcription', *Oncotarget*, 6: 43791-805.

Garcia Lavandeira, J. A., A. Ruano-Ravina, K. T. Kelsey, M. Torres-Duran, I. Parente-Lamelas, V. Leiro-Fernandez, M. Zapata, J. Abal-Arca, I. Vidal-Garcia, C. Montero-Martinez, M. Amenedo, O. Castro-Anon, A. Golpe-Gomez, R. Guzman-Taveras, C. Martinez, M. Provencio, M. J. Mejuto-Marti, S. Garcia-Garcia, A. Fernandez-Villar, M. Pineiro, and J. M. Barros-Dios. 2018. 'Alcohol consumption and lung cancer risk in never smokers: a pooled analysis of case-control studies', *Eur J Public Health*, 28: 521-27.

Golubovskaya, V., and L. Wu. 2016. 'Different Subsets of T Cells, Memory, Effector Functions, and CAR-T Immunotherapy', *Cancers (Basel)*, 8.

Goswami, R., and M. H. Kaplan. 2011. 'A brief history of IL-9', *J Immunol*, 186: 3283-8.

Hadrup, S., M. Donia, and P. Thor Straten. 2013. 'Effector CD4 and CD8 T cells and their role in the tumor microenvironment', *Cancer Microenviron*, 6: 123-33.

Hamilton, W., and D. Sharp. 2004. 'Diagnosis of lung cancer in primary care: a structured review', *Fam Pract*, 21: 605-11.

Harrington, L. E., R. D. Hatton, P. R. Mangan, H. Turner, T. L. Murphy, K. M. Murphy, and C. T. Weaver. 2005. 'Interleukin 17-producing CD4+ effector T cells develop via a lineage distinct from the T helper type 1 and 2 lineages', *Nat Immunol*, 6: 1123-32.

He, D., H. Li, N. Yusuf, C. A. Elmets, J. Li, J. D. Mountz, and H. Xu. 2010. 'IL-17 promotes tumor development through the induction of tumor promoting microenvironments at tumor sites and myeloid-derived suppressor cells', *J Immunol*, 184: 2281-8.

Hensing, T., A. Chawla, R. Batra, and R. Salgia. 2014. 'A personalized treatment for lung cancer: molecular pathways, targeted therapies, and genomic characterization', *Adv Exp Med Biol*, 799: 85-117.

Hirahara, K., and T. Nakayama. 2016. 'CD4+ T-cell subsets in inflammatory diseases: beyond the Th1/Th2 paradigm', *Int Immunol*, 28: 163-71.

Hirsch, F. R., G. V. Scagliotti, J. L. Mulshine, R. Kwon, W. J. Curran, Jr., Y. L. Wu, and L. Paz-Ares. 2017. 'Lung cancer: current therapies and new targeted treatments', *Lancet*, 389: 299-311.

Hu, B., H. Qiu-Lan, R. E. Lei, C. Shi, H. X. Jiang, and S. Y. Qin. 2017. 'Interleukin-9 Promotes Pancreatic Cancer Cells Proliferation and Migration via the miR-200a/Beta-Catenin Axis', *Biomed Res Int*, 2017: 2831056.

Huang, Y., C. Ma, Q. Zhang, J. Ye, F. Wang, Y. Zhang, P. Hunborg, M. A. Varvares, D. F. Hoft, E. C. Hsueh, and G. Peng. 2015. 'CD4+ and CD8+ T cells have opposing roles in breast cancer progression and outcome', *Oncotarget*, 6: 17462-78.

Huber, M., S. Heink, H. Grothe, A. Guralnik, K. Reinhard, K. Elflein, T. Hunig, H. W. Mittrucker, A. Brustle, T. Kamradt, and M. Lohoff. 2009. 'A Th17-like developmental process leads to CD8(+) Tc17 cells with reduced cytotoxic activity', *Eur J Immunol*, 39: 1716-25.

Huber, M., S. Heink, A. Pagenstecher, K. Reinhard, J. Ritter, A. Visekruna, A. Guralnik, N. Bollig, K. Jeltsch, C. Heinemann, E. Wittmann, T. Buch, O. Prazeres da Costa, A. Brustle, D. Brenner, T. W. Mak, H. W. Mittrucker, B. Tackenberg, T. Kamradt, and M. Lohoff. 2013. 'IL-17A secretion by CD8+ T cells supports Th17-mediated autoimmune encephalomyelitis', *J Clin Invest*, 123: 247-60.

Hung, K., R. Hayashi, A. Lafond-Walker, C. Lowenstein, D. Pardoll, and H. Levitsky. 1998. 'The central role of CD4(+) T cells in the antitumor immune response', *J Exp Med*, 188: 2357-68.

Hus, I., A. Bojarska-Junak, S. Chocholska, W. Tomczak, J. Wos, A. Dmoszynska, and J. Rolinski. 2013. 'Th17/IL-17A might play a protective role in chronic lymphocytic leukemia immunity', *PLoS One*, 8: e78091.

Imielinski, M., A. H. Berger, P. S. Hammerman, B. Hernandez, T. J. Pugh, E. Hodis, J. Cho, J. Suh, M. Capelletti, A. Sivachenko, C. Sougnez, D. Auclair, M. S. Lawrence, P.

Stojanov, K. Cibulskis, K. Choi, L. de Waal, T. Sharifnia, A. Brooks, H. Greulich, S. Banerji, T. Zander, D. Seidel, F. Leenders, S. Ansen, C. Ludwig, W. Engel-Riedel, E. Stoelben, J. Wolf, C. Goparju, K. Thompson, W. Winckler, D. Kwiatkowski, B. E. Johnson, P. A. Janne, V. A. Miller, W. Pao, W. D. Travis, H. I. Pass, S. B. Gabriel, E. S. Lander, R. K. Thomas, L. A. Garraway, G. Getz, and M. Meyerson. 2012. 'Mapping the hallmarks of lung adenocarcinoma with massively parallel sequencing', *Cell*, 150: 1107-20.

Iwatsuki, M., K. Mimori, T. Yokobori, H. Ishi, T. Beppu, S. Nakamori, H. Baba, and M. Mori. 2010. 'Epithelial-mesenchymal transition in cancer development and its clinical significance', *Cancer Sci*, 101: 293-9.

Janssen, E. M., E. E. Lemmens, T. Wolfe, U. Christen, M. G. von Herrath, and S. P. Schoenberger. 2003. 'CD4+ T cells are required for secondary expansion and memory in CD8+ T lymphocytes', *Nature*, 421: 852-6.

Jia, L., and C. Wu. 2014. 'Differentiation, regulation and function of Th9 cells', *Adv Exp Med Biol*, 841: 181-207.

Jiang, W., X. G. Pang, Q. Wang, Y. X. Shen, X. K. Chen, and J. J. Xi. 2012. 'Prognostic role of Twist, Slug, and Foxc2 expression in stage I non-small-cell lung cancer after curative resection', *Clin Lung Cancer*, 13: 280-7.

Jin, W., and C. Dong. 2013. 'IL-17 cytokines in immunity and inflammation', *Emerg Microbes Infect*, 2: e60.

Joffre, O. P., E. Segura, A. Savina, and S. Amigorena. 2012. 'Cross-presentation by dendritic cells', *Nat Rev Immunol*, 12: 557-69.

Joyce, J. A., and J. W. Pollard. 2009. 'Microenvironmental regulation of metastasis', *Nat Rev Cancer*, 9: 239-52.

Kaatsch, Peter, Claudia Spix, Alexander Katalinic, Stefan Hentschel, Sabine Luttmann, and Christa Stegmaier. Robert Koch-Institut.

Kadara, H., P. Scheet, Wistuba, II, and A. E. Spira. 2016. 'Early Events in the Molecular Pathogenesis of Lung Cancer', *Cancer Prev Res (Phila)*, 9: 518-27.

Kalluri, R. 2016. 'The biology and function of fibroblasts in cancer', *Nat Rev Cancer*, 16: 582-98.

Kalluri, R., and R. A. Weinberg. 2009. 'The basics of epithelial-mesenchymal transition', *J Clin Invest*, 119: 1420-8.

Kaplan, M. H. 2015. 'The Development and in vivo function of TH9 cells', *Nat Rev Immunol*, 15: 295-307.

Keerthivasan, S., K. Aghajani, M. Dose, L. Molinero, M. W. Khan, V. Venkateswaran, C. Weber, A. O. Emmanuel, T. Sun, D. J. Bentrem, M. Mulcahy, A. Keshavarzian, E. M. Ramos, N. Blatner, K. Khazaie, and F. Gounari. 2014. 'beta-Catenin promotes colitis

and colon cancer through imprinting of proinflammatory properties in T cells', *Sci Transl Med*, 6: 225ra28.

Kigel, B., N. Rabinowicz, A. Varshavsky, O. Kessler, and G. Neufeld. 2011. 'Plexin-A4 promotes tumor progression and tumor angiogenesis by enhancement of VEGF and bFGF signaling', *Blood*, 118: 4285-96.

Kim, H. J., and H. Cantor. 2014. 'CD4 T-cell subsets and tumor immunity: the helpful and the not-so-helpful', *Cancer Immunol Res*, 2: 91-8.

Knorr, D. A., V. Bachanova, M. R. Verneris, and J. S. Miller. 2014. 'Clinical utility of natural killer cells in cancer therapy and transplantation', *Semin Immunol*, 26: 161-72.

Koch, S., N. Sopel, and S. Finotto. 2017. 'Th9 and other IL-9-producing cells in allergic asthma', *Semin Immunopathol*, 39: 55-68.

Kubo, M. 2017. 'Innate and adaptive type 2 immunity in lung allergic inflammation', *Immunol Rev*, 278: 162-72.

Kulig, P., S. Burkhard, J. Mikita-Geoffroy, A. L. Croxford, N. Hovelmeyer, G. Gyulveszi, C. Gorzelanny, A. Waisman, L. Borsig, and B. Becher. 2016. 'IL17A-Mediated Endothelial Breach Promotes Metastasis Formation', *Cancer Immunol Res*, 4: 26-32.

Kumar, V. 2018. 'T cells and their immunometabolism: A novel way to understanding sepsis immunopathogenesis and future therapeutics', *Eur J Cell Biol*, 97: 379-92.

Langrish, C. L., Y. Chen, W. M. Blumenschein, J. Mattson, B. Basham, J. D. Sedgwick, T. McClanahan, R. A. Kastelein, and D. J. Cua. 2005. 'IL-23 drives a pathogenic T cell population that induces autoimmune inflammation', *J Exp Med*, 201: 233-40.

Lei, R. E., C. Shi, P. L. Zhang, B. L. Hu, H. X. Jiang, and S. Y. Qin. 2017. *IL-9 promotes proliferation and metastasis of hepatocellular cancer cells by activating JAK2/STAT3 pathway*.

Leomicronn, B. 2017. 'T Cells in Allergic Asthma: Key Players Beyond the Th2 Pathway', *Curr Allergy Asthma Rep*, 17: 43.

Levental, K. R., H. Yu, L. Kass, J. N. Lakins, M. Egeblad, J. T. Erler, S. F. Fong, K. Csiszar, A. Giaccia, W. Weninger, M. Yamauchi, D. L. Gasser, and V. M. Weaver. 2009. 'Matrix crosslinking forces tumor progression by enhancing integrin signaling', *Cell*, 139: 891-906.

Li, J., H. Wang, H. Ke, and S. Ni. 2015. 'MiR-129 regulates MMP9 to control metastasis of non-small cell lung cancer', *Tumour Biol*, 36: 5785-90.

Liao, Y., G. K. Smyth, and W. Shi. 2014. 'featureCounts: an efficient general purpose program for assigning sequence reads to genomic features', *Bioinformatics*, 30: 923-30.

Liao, Y., B. Wang, Z. L. Huang, M. Shi, X. J. Yu, L. Zheng, S. Li, and L. Li. 2013. 'Increased circulating Th17 cells after transarterial chemoembolization correlate with improved

survival in stage III hepatocellular carcinoma: a prospective study', *PLoS One*, 8: e60444.

Lissowska, J., L. Foretova, J. Dabek, D. Zaridze, N. Szeszenia-Dabrowska, P. Rudnai, E. Fabianova, A. Cassidy, D. Mates, V. Bencko, V. Janout, R. J. Hung, P. Brennan, and P. Boffetta. 2010. 'Family history and lung cancer risk: international multicentre case-control study in Eastern and Central Europe and meta-analyses', *Cancer Causes Control*, 21: 1091-104.

Liu, T., L. Peng, P. Yu, Y. Zhao, Y. Shi, X. Mao, W. Chen, P. Cheng, T. Wang, N. Chen, J. Zhang, X. Liu, N. Li, G. Guo, W. Tong, Y. Zhuang, and Q. Zou. 2012. 'Increased circulating Th22 and Th17 cells are associated with tumor progression and patient survival in human gastric cancer', *J Clin Immunol*, 32: 1332-9.

Lopez-Novoa, J. M., and M. A. Nieto. 2009. 'Inflammation and EMT: an alliance towards organ fibrosis and cancer progression', *EMBO Mol Med*, 1: 303-14.

Love, M. I., W. Huber, and S. Anders. 2014. 'Moderated estimation of fold change and dispersion for RNA-seq data with DESeq2', *Genome Biol*, 15: 550.

Lu, J., H. Guo, W. Treekitkarnmongkol, P. Li, J. Zhang, B. Shi, C. Ling, X. Zhou, T. Chen, P. J. Chiao, X. Feng, V. L. Seewaldt, W. J. Muller, A. Sahin, M. C. Hung, and D. Yu. 2009. '14-3-3zeta Cooperates with ErbB2 to promote ductal carcinoma in situ progression to invasive breast cancer by inducing epithelial-mesenchymal transition', *Cancer Cell*, 16: 195-207.

Lu, Y., S. Hong, H. Li, J. Park, B. Hong, L. Wang, Y. Zheng, Z. Liu, J. Xu, J. He, J. Yang, J. Qian, and Q. Yi. 2012. 'Th9 cells promote antitumor immune responses in vivo', *J Clin Invest*, 122: 4160-71.

Lu, Y., Q. Wang, G. Xue, E. Bi, X. Ma, A. Wang, J. Qian, C. Dong, and Q. Yi. 2018. 'Th9 Cells Represent a Unique Subset of CD4(+) T Cells Endowed with the Ability to Eradicate Advanced Tumors', *Cancer Cell*, 33: 1048-60 e7.

Lv, X., L. Feng, X. Ge, K. Lu, and X. Wang. 2016. 'Interleukin-9 promotes cell survival and drug resistance in diffuse large B-cell lymphoma', *J Exp Clin Cancer Res*, 35: 106.

Ma, Y., G. V. Shurin, Z. Peiyuan, and M. R. Shurin. 2013. 'Dendritic cells in the cancer microenvironment', *J Cancer*, 4: 36-44.

Malissen, B., and P. Bongrand. 2015. 'Early T cell activation: integrating biochemical, structural, and biophysical cues', *Annu Rev Immunol*, 33: 539-61.

Marshall, E. A., K. W. Ng, S. H. Kung, E. M. Conway, V. D. Martinez, E. C. Halvorsen, D. A. Rowbotham, E. A. Vucic, A. W. Plumb, D. D. Becker-Santos, K. S. Enfield, J. Y. Kennett, K. L. Bennewith, W. W. Lockwood, S. Lam, J. C. English, N. Abraham, and W. L. Lam. 2016. 'Emerging roles of T helper 17 and regulatory T cells in lung cancer progression and metastasis', *Mol Cancer*, 15: 67.

Masopust, D., and J. M. Schenkel. 2013. 'The integration of T cell migration, differentiation and function', *Nat Rev Immunol*, 13: 309-20.

Mehner, C., A. Hockla, E. Miller, S. Ran, D. C. Radisky, and E. S. Radisky. 2014. 'Tumor cell-produced matrix metalloproteinase 9 (MMP-9) drives malignant progression and metastasis of basal-like triple negative breast cancer', *Oncotarget*, 5: 2736-49.

Mezheyeuski, A., C. H. Bergsland, M. Backman, D. Djureinovic, T. Sjoblom, J. Bruun, and P. Micke. 2018. 'Multispectral imaging for quantitative and compartment-specific immune infiltrates reveals distinct immune profiles that classify lung cancer patients', *J Pathol*, 244: 421-31.

Mittrucker, H. W., A. Visekruna, and M. Huber. 2014. 'Heterogeneity in the differentiation and function of CD8(+) T cells', *Arch Immunol Ther Exp (Warsz)*, 62: 449-58.

Mounawar, M., A. Mukeria, F. Le Calvez, R. J. Hung, H. Renard, A. Cortot, C. Bollart, D. Zaridze, P. Brennan, P. Boffetta, E. Brambilla, and P. Hainaut. 2007. 'Patterns of EGFR, HER2, TP53, and KRAS mutations of p14arf expression in non-small cell lung cancers in relation to smoking history', *Cancer Res*, 67: 5667-72.

Muraille, E., and O. Leo. 1998. 'Revisiting the Th1/Th2 paradigm', *Scand J Immunol*, 47: 1-9.

Muranski, P., A. Boni, P. A. Antony, L. Cassard, K. R. Irvine, A. Kaiser, C. M. Paulos, D. C. Palmer, C. E. Touloukian, K. Ptak, L. Gattinoni, C. Wrzesinski, C. S. Hinrichs, K. W. Kerstann, L. Feigenbaum, C. C. Chan, and N. P. Restifo. 2008. 'Tumor-specific Th17-polarized cells eradicate large established melanoma', *Blood*, 112: 362-73.

Murphy, C. A., C. L. Langrish, Y. Chen, W. Blumenschein, T. McClanahan, R. A. Kastelein, J. D. Sedgwick, and D. J. Cua. 2003. 'Divergent pro- and antiinflammatory roles for IL-23 and IL-12 in joint autoimmune inflammation', *J Exp Med*, 198: 1951-7.

Nahrendorf, M., and F. K. Swirski. 2016. 'Abandoning M1/M2 for a Network Model of Macrophage Function', *Circ Res*, 119: 414-7.

Nakajima, S., R. Doi, E. Toyoda, S. Tsuji, M. Wada, M. Koizumi, S. S. Tulachan, D. Ito, K. Kami, T. Mori, Y. Kawaguchi, K. Fujimoto, R. Hosotani, and M. Imamura. 2004. 'N-cadherin expression and epithelial-mesenchymal transition in pancreatic carcinoma', *Clin Cancer Res*, 10: 4125-33.

Nemazee, D. 2017. 'Mechanisms of central tolerance for B cells', *Nat Rev Immunol*, 17: 281-94.

Nieto, M. A., R. Y. Huang, R. A. Jackson, and J. P. Thiery. 2016. 'Emt: 2016', *Cell*, 166: 21-45.

Nishimura, T., K. Iwakabe, M. Sekimoto, Y. Ohmi, T. Yahata, M. Nakui, T. Sato, S. Habu, H. Tashiro, M. Sato, and A. Ohta. 1999. 'Distinct role of antigen-specific T helper type 1 (Th1) and Th2 cells in tumor eradication in vivo', *J Exp Med*, 190: 617-27.

Nishimura, Y., S. Komatsu, D. Ichikawa, H. Nagata, S. Hirajima, H. Takeshita, T. Kawaguchi, T. Arita, H. Konishi, K. Kashimoto, A. Shiozaki, H. Fujiwara, K. Okamoto, H. Tsuda, and E. Otsuji. 2013. 'Overexpression of YWHAZ relates to tumor cell proliferation and malignant outcome of gastric carcinoma', *Br J Cancer*, 108: 1324-31.

Noelle, R. J., and E. C. Nowak. 2010. 'Cellular sources and immune functions of interleukin-9', *Nat Rev Immunol*, 10: 683-7.

Nowak, E. C., C. T. Weaver, H. Turner, S. Begum-Haque, B. Becher, B. Schreiner, A. J. Coyle, L. H. Kasper, and R. J. Noelle. 2009. 'IL-9 as a mediator of Th17-driven inflammatory disease', *J Exp Med*, 206: 1653-60.

Okazaki, I., S. Ishikawa, and Y. Sohara. 2014. 'Genes associated with succeptibility to lung adenocarcinoma among never smokers suggest the mechanism of disease', *Anticancer Res*, 34: 5229-40.

Park, Y. R., S. H. Bae, W. Ji, E. J. Seo, J. C. Lee, H. R. Kim, S. J. Jang, and C. M. Choi. 2017. 'GAB2 Amplification in Squamous Cell Lung Cancer of Non-Smokers', *J Korean Med Sci*, 32: 1784-91.

Pellegrini, P., A. M. Berghella, T. Del Beato, S. Cicia, D. Adorno, and C. U. Casciani. 1996. 'Disregulation in TH1 and TH2 subsets of CD4+ T cells in peripheral blood of colorectal cancer patients and involvement in cancer establishment and progression', *Cancer Immunol Immunother*, 42: 1-8.

Prudkin, L., D. D. Liu, N. C. Ozburn, M. Sun, C. Behrens, X. Tang, K. C. Brown, B. N. Bekele, C. Moran, and Wistuba, II. 2009. 'Epithelial-to-mesenchymal transition in the development and progression of adenocarcinoma and squamous cell carcinoma of the lung', *Mod Pathol*, 22: 668-78.

Punt, S., G. J. Fleuren, E. Kritikou, E. Lubberts, J. B. Trimbos, E. S. Jordanova, and A. Gorter. 2015. 'Angels and demons: Th17 cells represent a beneficial response, while neutrophil IL-17 is associated with poor prognosis in squamous cervical cancer', *Oncoimmunology*, 4: e984539.

Purwar, R., C. Schlapbach, S. Xiao, H. S. Kang, W. Elyaman, X. Jiang, A. M. Jetten, S. J. Khoury, R. C. Fuhlbrigge, V. K. Kuchroo, R. A. Clark, and T. S. Kupper. 2012. 'Robust tumor immunity to melanoma mediated by interleukin-9-producing T cells', *Nat Med*, 18: 1248-53.

Radisky, D. C., D. D. Levy, L. E. Littlepage, H. Liu, C. M. Nelson, J. E. Fata, D. Leake, E. L. Godden, D. G. Albertson, M. A. Nieto, Z. Werb, and M. J. Bissell. 2005. 'Rac1b and reactive oxygen species mediate MMP-3-induced EMT and genomic instability', *Nature*, 436: 123-7.

Reveliotis, K., G. Kalavrouziotis, K. Skevis, A. Charpidou, R. Trigidou, and K. Syrigos. 2014. 'Wedge resection and segmentectomy in patients with stage I non-small cell lung carcinoma', *Oncol Rev*, 8: 234.

Reynolds, J. M., P. Angkasekwinai, and C. Dong. 2010. 'IL-17 family member cytokines: regulation and function in innate immunity', *Cytokine Growth Factor Rev*, 21: 413-23.

Ricciardi, M., M. Zanotto, G. Malpeli, G. Bassi, O. Perbellini, M. Chilosi, F. Bifari, and M. Krampera. 2015. 'Epithelial-to-mesenchymal transition (EMT) induced by inflammatory priming elicits mesenchymal stromal cell-like immune-modulatory properties in cancer cells', *Br J Cancer*, 112: 1067-75.

Rouvier, E., M. F. Luciani, M. G. Mattei, F. Denizot, and P. Golstein. 1993. 'CTLA-8, cloned from an activated T cell, bearing AU-rich messenger RNA instability sequences, and homologous to a herpesvirus saimiri gene', *J Immunol*, 150: 5445-56.

Rudin, C. M., E. Avila-Tang, C. C. Harris, J. G. Herman, F. R. Hirsch, W. Pao, A. G. Schwartz, K. H. Vahakangas, and J. M. Samet. 2009. 'Lung cancer in never smokers: molecular profiles and therapeutic implications', *Clin Cancer Res*, 15: 5646-61.

Ruffini, E., S. Asioli, P. L. Filosso, P. Lyberis, M. C. Bruna, L. Macri, L. Daniele, and A. Oliaro. 2009. 'Clinical significance of tumor-infiltrating lymphocytes in lung neoplasms', *Ann Thorac Surg*, 87: 365-71; discussion 71-2.

Sainio, A., and H. Jarvelainen. 2014. 'Extracellular matrix macromolecules: potential tools and targets in cancer gene therapy', *Mol Cell Ther*, 2: 14.

Salmon, H. W., A. Guha, A. M. Rojiani, and D. W. Siemann. 2012. 'Vascular development in mouse lung metastases', *Am J Cancer Res*, 2: 581-8.

Sanchez-Tillo, E., Y. Liu, O. de Barrios, L. Siles, L. Fanlo, M. Cuatrecasas, D. S. Darling, D. C. Dean, A. Castells, and A. Postigo. 2012. 'EMT-activating transcription factors in cancer: beyond EMT and tumor invasiveness', *Cell Mol Life Sci*, 69: 3429-56.

Sarnaik, A. A., B. Yu, D. Yu, D. Morelli, M. Hall, D. Bogle, L. Yan, S. Targan, J. Solomon, G. Nichol, M. Yellin, and J. S. Weber. 2011. 'Extended dose ipilimumab with a peptide vaccine: immune correlates associated with clinical benefit in patients with resected high-risk stage IIIc/IV melanoma', *Clin Cancer Res*, 17: 896-906.

Savai, R., R. T. Schermuly, S. S. Pullamsetti, M. Schneider, S. Greschus, H. A. Ghofrani, H. Traupe, F. Grimminger, and G. A. Banat. 2007. 'A combination hybrid-based vaccination/adoptive cellular therapy to prevent tumor growth by involvement of T cells', *Cancer Res*, 67: 5443-53.

Schmitt, E., and T. Bopp. 2017. 'Discovery and initial characterization of Th9 cells: the early years', *Semin Immunopathol*, 39: 5-10.

Sekiya, T., and A. Yoshimura. 2016. 'In Vitro Th Differentiation Protocol', *Methods Mol Biol*, 1344: 183-91.

Shames, D. S., and Wistuba, II. 2014. 'The evolving genomic classification of lung cancer', *J Pathol*, 232: 121-33.

Shapley, M., G. Mansell, J. L. Jordan, and K. P. Jordan. 2010. 'Positive predictive values of >/=5% in primary care for cancer: systematic review', *Br J Gen Pract*, 60: e366-77.

Sharp, S. P., D. Avram, S. C. Stain, and E. C. Lee. 2017. 'Local and systemic Th17 immune response associated with advanced stage colon cancer', *J Surg Res*, 208: 180-86.

Shiga, K., M. Hara, T. Nagasaki, T. Sato, H. Takahashi, and H. Takeyama. 2015. 'Cancer-Associated Fibroblasts: Their Characteristics and Their Roles in Tumor Growth', *Cancers (Basel)*, 7: 2443-58.

Smith, S. E., D. B. Hoelzinger, A. L. Dominguez, J. Van Snick, and J. Lustgarten. 2011. 'Signals through 4-1BB inhibit T regulatory cells by blocking IL-9 production enhancing antitumor responses', *Cancer Immunol Immunother*, 60: 1775-87.

Smith-Garvin, J. E., G. A. Koretzky, and M. S. Jordan. 2009. 'T cell activation', *Annu Rev Immunol*, 27: 591-619.

Smolle, E., and M. Pichler. 2019. 'Non-Smoking-Associated Lung Cancer: A distinct Entity in Terms of Tumor Biology, Patient Characteristics and Impact of Hereditary Cancer Predisposition', *Cancers (Basel)*, 11.

Soltermann, A., V. Tischler, S. Arbogast, J. Braun, N. Probst-Hensch, W. Weder, H. Moch, and G. Kristiansen. 2008. 'Prognostic significance of epithelial-mesenchymal and mesenchymal-epithelial transition protein expression in non-small cell lung cancer', *Clin Cancer Res*, 14: 7430-7.

Song, X., and Y. Qian. 2013. 'The activation and regulation of IL-17 receptor mediated signaling', *Cytokine*, 62: 175-82.

Sternlicht, M. D., A. Lochter, C. J. Sympson, B. Huey, J. P. Rougier, J. W. Gray, D. Pinkel, M. J. Bissell, and Z. Werb. 1999. 'The stromal proteinase MMP3/stromelysin-1 promotes mammary carcinogenesis', *Cell*, 98: 137-46.

Stritesky, G. L., N. Yeh, and M. H. Kaplan. 2008. 'IL-23 promotes maintenance but not commitment to the Th17 lineage', *J Immunol*, 181: 5948-55.

Su, Z., Y. Sun, H. Zhu, Y. Liu, X. Lin, H. Shen, J. Chen, W. Xu, and H. Xu. 2014. 'Th17 cell expansion in gastric cancer may contribute to cancer development and metastasis', *Immunol Res*, 58: 118-24.

Sutherland, K. D., and A. Berns. 2010. 'Cell of origin of lung cancer', *Mol Oncol*, 4: 397-403.

Swain, S. L., A. D. Weinberg, M. English, and G. Huston. 1990. 'IL-4 directs the development of Th2-like helper effectors', *J Immunol*, 145: 3796-806.

Takaba, H., and H. Takayanagi. 2017. 'The Mechanisms of T Cell Selection in the Thymus', *Trends Immunol*, 38: 805-16.

Takahama, Y. 2006. 'Journey through the thymus: stromal guides for T-cell development and selection', *Nat Rev Immunol*, 6: 127-35.

Tan, H., S. Wang, and L. Zhao. 2017. 'A tumour-promoting role of Th9 cells in hepatocellular carcinoma through CCL20 and STAT3 pathways', *Clin Exp Pharmacol Physiol*, 44: 213-21.

Tan, T. Z., Q. H. Miow, Y. Miki, T. Noda, S. Mori, R. Y. Huang, and J. P. Thiery. 2014. 'Epithelial-mesenchymal transition spectrum quantification and its efficacy in deciphering survival and drug responses of cancer patients', *EMBO Mol Med*, 6: 1279-93.

Tao, L., G. Huang, H. Song, Y. Chen, and L. Chen. 2017. 'Cancer associated fibroblasts: An essential role in the tumor microenvironment', *Oncol Lett*, 14: 2611-20.

Temann, U. A., Y. Laouar, E. E. Eynon, R. Homer, and R. A. Flavell. 2007. 'IL9 leads to airway inflammation by inducing IL13 expression in airway epithelial cells', *Int Immunol*, 19: 1-10.

Terry, S., P. Savagner, S. Ortiz-Cuaran, L. Mahjoubi, P. Saintigny, J. P. Thiery, and S. Chouaib. 2017. 'New insights into the role of EMT in tumor immune escape', *Mol Oncol*, 11: 824-46.

Thiery, J. P., H. Acloque, R. Y. Huang, and M. A. Nieto. 2009. 'Epithelial-mesenchymal transitions in development and disease', *Cell*, 139: 871-90.

Torre, L. A., R. L. Siegel, and A. Jemal. 2016. 'Lung Cancer Statistics', *Adv Exp Med Biol*, 893: 1-19.

Travis, W. D. 2011. 'Pathology of lung cancer', *Clin Chest Med*, 32: 669-92.

Travis, W. D., E. Brambilla, and G. J. Riely. 2013. 'New pathologic classification of lung cancer: relevance for clinical practice and clinical trials', *J Clin Oncol*, 31: 992-1001.

Varol, C., A. Mildner, and S. Jung. 2015. 'Macrophages: development and tissue specialization', *Annu Rev Immunol*, 33: 643-75.

Veglia, F., and D. I. Gabrilovich. 2017. 'Dendritic cells in cancer: the role revisited', *Curr Opin Immunol*, 45: 43-51.

Vegran, F., L. Apetoh, and F. Ghiringhelli. 2015. 'Th9 cells: a novel CD4 T-cell subset in the immune war against cancer', *Cancer Res*, 75: 475-9.

Vegran, F., H. Berger, R. Boidot, G. Mignot, M. Bruchard, M. Dosset, F. Chalmin, C. Rebe, V. Derangere, B. Ryffel, M. Kato, A. Prevost-Blondel, F. Ghiringhelli, and L. Apetoh. 2014. 'The transcription factor IRF1 dictates the IL-21-dependent anticancer functions of TH9 cells', *Nat Immunol*, 15: 758-66.

Veldhoen, M., R. J. Hocking, C. J. Atkins, R. M. Locksley, and B. Stockinger. 2006. 'TGFbeta in the context of an inflammatory cytokine milieu supports de novo differentiation of IL-17-producing T cells', *Immunity*, 24: 179-89.

Veldhoen, M., C. Uyttenhove, J. van Snick, H. Helmby, A. Westendorf, J. Buer, B. Martin, C. Wilhelm, and B. Stockinger. 2008. 'Transforming growth factor-beta 'reprograms' the differentiation of T helper 2 cells and promotes an interleukin 9-producing subset', *Nat Immunol*, 9: 1341-6.

Wakelee, H., K. Kelly, and M. J. Edelman. 2014. '50 Years of progress in the systemic therapy of non-small cell lung cancer', *Am Soc Clin Oncol Educ Book*: 177-89.

Wang, M., D. Ren, W. Guo, S. Huang, Z. Wang, Q. Li, H. Du, L. Song, and X. Peng. 2016. 'N-cadherin promotes epithelial-mesenchymal transition and cancer stem cell-like traits via ErbB signaling in prostate cancer cells', *Int J Oncol*, 48: 595-606.

Watanabe, N., S. Komatsu, D. Ichikawa, M. Miyamae, T. Ohashi, W. Okajima, T. Kosuga, H. Konishi, A. Shiozaki, H. Fujiwara, K. Okamoto, H. Tsuda, and E. Otsuji. 2016. 'Overexpression of YWHAZ as an independent prognostic factor in adenocarcinoma of the esophago-gastric junction', *Am J Cancer Res*, 6: 2729-36.

Weaver, C. T., R. D. Hatton, P. R. Mangan, and L. E. Harrington. 2007. 'IL-17 family cytokines and the expanding diversity of effector T cell lineages', *Annu Rev Immunol*, 25: 821-52.

Whiteside, T. L. 2008. 'The tumor microenvironment and its role in promoting tumor growth', *Oncogene*, 27: 5904-12.

Wiener, Z., A. Falus, and S. Toth. 2004. 'IL-9 increases the expression of several cytokines in activated mast cells, while the IL-9-induced IL-9 production is inhibited in mast cells of histamine-free transgenic mice', *Cytokine*, 26: 122-30.

Wistuba, II, J. Berry, C. Behrens, A. Maitra, N. Shivapurkar, S. Milchgrub, B. Mackay, J. D. Minna, and A. F. Gazdar. 2000. 'Molecular changes in the bronchial epithelium of patients with small cell lung cancer', *Clin Cancer Res*, 6: 2604-10.

Wistuba, II, and A. F. Gazdar. 2006. 'Lung cancer preneoplasia', *Annu Rev Pathol*, 1: 331-48.

Wolf, D., S. Sopper, A. Pircher, G. Gastl, and A. M. Wolf. 2015. 'Treg(s) in Cancer: Friends or Foe?', *J Cell Physiol*, 230: 2598-605.

Xiao, D., and J. He. 2010. 'Epithelial mesenchymal transition and lung cancer', *J Thorac Dis*, 2: 154-9.

Xie, C., X. Mao, J. Huang, Y. Ding, J. Wu, S. Dong, L. Kong, G. Gao, C. Y. Li, and L. Wei. 2011. 'KOBAS 2.0: a web server for annotation and identification of enriched pathways and diseases', *Nucleic Acids Res*, 39: W316-22.

Yan, J., X. L. Liu, G. Xiao, N. L. Li, Y. N. Deng, L. Z. Han, L. C. Yin, L. J. Ling, and L. X. Liu. 2014. 'Prevalence and clinical relevance of T-helper cells, Th17 and Th1, in hepatitis B virus-related hepatocellular carcinoma', *PLoS One*, 9: e96080.

Yang, L., and Y. Zhang. 2017. 'Tumor-associated macrophages: from basic research to clinical application', *J Hematol Oncol*, 10: 58.

Ye, Z. J., Q. Zhou, W. Yin, M. L. Yuan, W. B. Yang, X. Z. Xiong, J. C. Zhang, and H. Z. Shi. 2012. 'Differentiation and immune regulation of IL-9-producing CD4+ T cells in malignant pleural effusion', *Am J Respir Crit Care Med*, 186: 1168-79.

Yu, Q., X. M. Lou, and Y. He. 2014. 'Prediction of local recurrence in cervical cancer by a Cox model comprised of lymph node status, lymph-vascular space invasion, and intratumoral Th17 cell-infiltration', *Med Oncol*, 31: 795.

Yuan, Y., Y. C. Jiang, C. K. Sun, and Q. M. Chen. 2016. 'Role of the tumor microenvironment in tumor progression and the clinical applications (Review)', *Oncol Rep*, 35: 2499-515.

Zhang, L., J. R. Conejo-Garcia, D. Katsaros, P. A. Gimotty, M. Massobrio, G. Regnani, A. Makrigiannakis, H. Gray, K. Schlienger, M. N. Liebman, S. C. Rubin, and G. Coukos. 2003. 'Intratumoral T cells, recurrence, and survival in epithelial ovarian cancer', *N Engl J Med*, 348: 203-13.

Zhang, N., and M. J. Bevan. 2011. 'CD8(+) T cells: foot soldiers of the immune system', *Immunity*, 35: 161-8.

Zhang, Y., J. W. Kent, Jr., M. Olivier, O. Ali, D. Cerjak, U. Broeckel, R. M. Abdou, T. D. Dyer, A. Comuzzie, J. E. Curran, M. A. Carless, D. L. Rainwater, H. H. Goring, J. Blangero, and A. H. Kissebah. 2013. 'A comprehensive analysis of adiponectin QTLs using SNP association, SNP cis-effects on peripheral blood gene expression and gene expression correlation identified novel metabolic syndrome (MetS) genes with potential role in carcinogenesis and systemic inflammation', *BMC Med Genomics*, 6: 14.

Zhang, Y., Y. Zhang, W. Gu, and B. Sun. 2014. 'TH1/TH2 cell differentiation and molecular signals', *Adv Exp Med Biol*, 841: 15-44.

Zhao, Y., X. Chu, J. Chen, Y. Wang, S. Gao, Y. Jiang, X. Zhu, G. Tan, W. Zhao, H. Yi, H. Xu, X. Ma, Y. Lu, Q. Yi, and S. Wang. 2016. 'Dectin-1-activated dendritic cells trigger potent antitumour immunity through the induction of Th9 cells', *Nat Commun*, 7: 12368.

Zheng, H., X. Liu, J. Zhang, S. J. Rice, M. Wagman, Y. Kong, L. Zhu, J. Zhu, M. Joshi, and C. P. Belani. 2016. 'Expression of PD-1 on CD4+ T cells in peripheral blood associates with poor clinical outcome in non-small cell lung cancer', *Oncotarget*, 7: 56233-40.

Zheng, H., H. Takahashi, Y. Murai, Z. Cui, K. Nomoto, H. Niwa, K. Tsuneyama, and Y. Takano. 2006. 'Expressions of MMP-2, MMP-9 and VEGF are closely linked to

growth, invasion, metastasis and angiogenesis of gastric carcinoma', *Anticancer Res*, 26: 3579-83.

Zigrino, P., I. Kuhn, T. Bauerle, J. Zamek, J. W. Fox, S. Neumann, A. Licht, M. Schorpp-Kistner, P. Angel, and C. Mauch. 2009. 'Stromal expression of MMP-13 is required for melanoma invasion and metastasis', *J Invest Dermatol*, 129: 2686-93.

9. Appendix

Table 13. Human qPCR Primer accession numbers

	Sequence	Accession Number
E-cadherin	FP: 5‘-CCCACCACGTACAAGGGTC-3‘ RP: 5‘-ATGCCATCGTTGTTCACTGGA-3‘	NM_001317184.1
Vimentin	FP: 5‘-GGAAATGGCTCGTCACCTTCGT-3‘ RP: 5‘-GCAGAGAAATCCTGCTCTCCTCG-3‘	NM_003380.5
N-cadherin	FP: 5'-TCAGGCGTCTGTAGAGGCTT-3' RP: 5'-ATGCACATCCTTCGATAAGACTG-3'	NM_001792.5
ZO1	FP: 5’-ACGGTCCTCTGAGCCTGTAA-3’ RP: 5’-CTGCTTTCTGTTGAGAGGCTGG-3’	NM_001355014.1
ZO2	FP: 5’-GCCCCAGGCATGGAAGAGCTG-3’ RP: 5’- CCCACCCGGGAGCACATCAGA-3’	NM_004817.4
ZEB1	FP: 5’-AGGATGACCTGCCAACAGACCA-3’ RP: 5’-TCCTTTCTGTCATCCTCCCAGCA-3’	NM_001323654.1
ZEB2	FP: 5’-AGCCTCTGTAGATGGTCCAGAAGAA-3’ RP: 5’-CACTGTACCATTGTTAATTGCGGTC-3’	NM_014795.4
Smad1	FP: 5’-ACTGCCTCATGTCATTTACTGC-3’ RP:5’-CTATTGGGAGAGTGAGGAAACG-3’	NM_005900.3
Smad3	FP: 5’-CATCGAGCCCCAGAGCAATA-3’ RP: 5’-GTGGTTCATCTGGTGGTCACT-3’	NM_005902.4
Cytokeratin18	FP: 5’-AACAACACCTGCTGTCCGTGT-3’ RP: 5’-TGAAGCTCATGCCCCCAGAAAC-3’	NM_199187.1

Table 14. Antibodies

Epitope	Conjugate	Catalog No.	Manufacturer	Use
α-E-cadherin	-	3195	Cell Signaling, USA	WB, ICC
α-Vimentin	-	5741	Cell Signaling, USA	WB, ICC
α-N-cadherin	-	14215	Cell signaling, USA	WB
α-ZO2	-	2847	Cell signaling, USA	WB
α-β-Actin	-	A2228	SIGMA, USA	WB
α-PCNA	-	sc-7907	Santa cruz, USA	IHC
α-vWf	-	A0082	DAKO, USA	IHC
α-AlexaFluor® 488	-	A11008	Invitrogen, USA	ICC, IHC
α-AlexaFluor® 555	-	A27039	Invitrogen, USA	ICC, IHC
α-CD4	V450	560470	BD, USA	FACS
α-CD44	PE	12-0441-82	Affymetrix, USA	FACS
α-CD62L	AF700	12-0621-82	BD, USA	FACS
α-IFN-γ	PE	12-7311-41	Affymetrix, USA	FACS
α-IL-9	APC	514105	BioLegend, USA	FACS
α-IL-17	FITC	130-103-007	Miltenyi Biotec, Germany	FACS
α-msCD8a	FITC	11-0081-82	Affymetrix, USA	$CD4^+$ T cell isolation
α-msCD11b	FITC	11-0112-82	Affymetrix, USA	$CD4^+$ T cell isolation
α-msCD11c	FITC	14-0114-82	Affymetrix, USA	$CD4^+$ T cell isolation
α-msB220	FITC	553929	BD, USA	$CD4^+$ T cell isolation
α-msCD49b	FITC	14-5971-85	Affymetrix, USA	$CD4^+$ T cell isolation
α-msTer119	FITC	13-5921-82	Affymetrix, USA	$CD4^+$ T cell isolation
α-Cytokeratin	Opal 520	MA1-26237	DAKO, USA	Opal staining
α-PU.1	Opal 540	ab76543	Abcam, USA	Opal staining
α-IL-9	Opal 570	ab181397	Abcam, USA	Opal staining
α-STAT3	Opal 690	12640S	Cell Signaling, USA	Opal staining
α-IL-17	Opal 650	ab79056	Abcam, USA	Opal staining
α-CD4	Opal 620	ab133616	Abcam, USA	Opal staining

Table 15. Buffers for cell biology

Buffer	Composition
BSS	9.9 g/l Hank's Salt, 1.425 g/l $NaHCO_3$, 10mM HEPES in H_2O dest. pH 7.2
Coating buffer	50mM Tris-Base (pH 9.5) in H_2O dest.
MACS buffer	0.5 % BSA [w/v], 2mM EDTA (pH 8.0) in PBS
Saponin buffer	0.3 % Saponin [w/v], 2%FCS [v/v] in PBS

10. Statement of authenticity

„Hiermit erkläre ich, dass ich die vorliegende Arbeit selbständig und ohne unzulässige Hilfe oder Benutzung anderer als der angegebenen Hilfsmittel angefertigt habe. Alle Textstellen, die wörtlich oder sinngemäß aus veröffentlichten oder nichtveröffentlichten Schriften entnommen sind, und alle Angaben, die auf mündlichen Auskünften beruhen, sind als solche kenntlich gemacht. Bei den von mir durchgeführten und in der Dissertation erwähnten Untersuchungen habe ich die Grundsätze guter wissenschaftlicher Praxis, wie sie in der „Satzung der Justus- Liebig-Universität Gießen zur Sicherung guter wissenschaftlicher Praxis“ niedergelegt sind, eingehalten sowie ethische, datenschutzrechtliche und tierschutzrechtliche Grundsätze befolgt. Ich versichere, dass Dritte von mir weder unmittelbar noch mittelbar geldwerte Leistungen für Arbeiten erhalten haben, die im Zusammenhang mit dem Inhalt der vorgelegten Dissertation stehen, oder habe diese nachstehend spezifiziert. Die vorgelegte Arbeit wurde weder im Inland noch im Ausland in gleicher oder ähnlicher Form einer anderen Prüfungsbehörde zum Zweck einer Promotion oder eines anderen Prüfungsverfahrens vorgelegt. Alles aus anderen Quellen und von anderen Personen übernommene Material, das in der Arbeit verwendet wurde oder auf das direkt Bezug genommen wird, wurde als solches kenntlich gemacht. Insbesondere wurden alle Personen genannt, die direkt und indirekt an der Entstehung der vorliegenden Arbeit beteiligt waren. Mit der Überprüfung meiner Arbeit durch eine Plagiatserkennungssoftware bzw. ein internetbasiertes Softwareprogramm erkläre ich mich einverstanden.“

Ort, Datum _____ Unterschrift _____

11. Acknowledgments

I would like to express my gratitude to PD Dr. Rajkumar Savai and Dr. Soni Pullamsetti for the opportunity to perform my studies in their lab and for the constant support throughout my time as a PhD student. I am also in great debt to Prof. Werner Seeger, who as head of our department, has offered continuous feedback in every aspect of my project during my time at the Max Planck Institute.

I would also like to thank the IMPRS Research School and its coordinators Dorothea Linn and Bilge Reischauer, this program allowed me to connect with fellow students and complete the academic part of my PhD. I am extremely thankful to my colleagues in both the Pullamsetti and Savai labs, who have been integral in helping me reach this goal, specially Dr. Swati Dabral, Dijana Iloska, Natascha Wilker and Dr. Elisabetta Gamen.

I would also like to thank, Dr. Anja Schmall, who was responsible for my training and the initial stages of my project. Likewise, essential to the development of the Opal staining shown in my work was my colleague Xiang Zheng, who was gracious to assist and further help with standardizing the method and processing the massive amounts of data that are obtained.

Through Giessens Biobank and the gracious help from Andrea Mohr we were able to obtain primary tumor cells and human lymphocytes, both vital for the development of this work. Likewise, I owe a great deal to Prof. Dr. Magdalena Huber, for both material and intellectual contributions to my project. Colleagues from her workgroup, Dr. Lucia Campos, Dr. Hartmann Raifer, Christina Lückel, Dennis Vogel, Felix Picard and Anna Guralki have contributed and been a great support to this work.

Without the work from the RNAseq facility available in our institute and the close contact with Dr. Stefan Gunther, we would not have been able to elucidate the mechanisms at play in the cancer-immune cell interaction. Additionally, the great technical support from Yanina Knepper and Vanessa Golchert was essential to carry out all the animal experiments in this project.

Last but not least, I would like to thank my parents for their patience and support through this time and my sister for her constant encouragement and acceptance. To my chosen family specially, Dr. Anamaria Radu, Piotr Sienkiewicz, Dr. Ana Ledezma, Dr. Karla Rubio, Fernando Viamonte, Bibiana Sucre and Franziska Strecker for always being there, motivating to move forward and their unwavering support.